PhD Thesis

Development of novel sulfonium containing drug carriers with inherent antimicrobial activities to combat drug resistance

A dissertation submitted to the

Indian Institute of Technology Guwahati

as partial fulfilment for the degree of

Doctor of Philosophy in Centre for the Environment

by

Anjali Patel

Roll No: 186152103

Centre for the Environment

Indian Institute of Technology Guwahati

Guwahati 781039, Assam India

TO

MY BELOVED FAMILY

Declaration

16th August, 2023

I hereby declare that the thesis entitled "**Development of novel sulfonium containing drug carriers with inherent antimicrobial activities to combat drug resistance**" is upshots of research that was carried out by me under the supervision of Prof. Debasis Manna, Centre for the Environment, Indian Institute of Technology Guwahati. This thesis has been submitted by me to the Centre for the Environment, Indian Institute of Technology Guwahati, for the award of the degree of Doctor of Philosophy. In keeping with the general practice of reporting scientific observations, due acknowledgments have been made wherever the work described is based on the findings of other investigators.

I further declare that this work has not been submitted anywhere else for any degree, diploma, associateship or membership etc., of any Institute or University to the best of my knowledge.

(Anjali Patel)

भारतीय प्रौद्योगिकी संस्थान गुवाहाटी

Indian Institute of Technology Guwahati

Prof. Debasis Manna

Centre for the Environment

Phone: +91-0361-258-2325

Fax: +91-0361-258-2349

E-mail: dmanna@iitg.ac.in

18th August, 2023

TO WHOM IT MAY CONCERN

This is to certify that the thesis entitled "**Development of novel sulfonium containing drug carriers with inherent antimicrobial activities to combat drug resistance**" is being submitted by Ms. Anjali Patel (Roll No. 186152103) for the award of the PhD degree in Centre for the Environment to the Indian Institute of Technology Guwahati, is a genuinely her own research work which was carried out by her. The information and data reported by her are completely her original findings. She has meticulously carried out the investigations and also followed the guidelines of my laboratory. Neither this thesis nor any part of it has been submitted for the award of any degree/diploma to anywhere before.

(Prof. Debasis Manna)

भारतीय प्रौद्योगिकी संस्थान गुवाहाटी
Indian Institute of Technology Guwahati

Contents

ACKNOWLEDGEMENTS

This dissertation has been accomplished by the endless support and encouragement of numerous well-wishers' to whom I will be grateful for the rest of my life. Here by I wish to extend few words of acknowledge to each of them for helping me to reach this milestone. Prior to all, I would like to convey my sincere gratefulness to my supervising mentor, Prof. Debasis Manna, who introduced me to the splendid world of research. Your constant guidance and encouragement have always been an inspiration to look forward and do better in research. I am truly honoured and blessed to have been a part of his research group. In addition to my research carrier your thoughtful ideas and disciplined routine of life have paved the way of being a better version of me. Thank you, Sir, for being my Mentor. My grateful appreciation also goes to my Co-supervisor Prof. S. Senthil Kumar (Department of Bioscience and Bioengineering, IIT Guwahati) who has always extended his helping hand to provide the facilities required for my research. Sir I am truly honoured to have you as my co-supervisor.

My sincere and heartfelt thanks to my collaborators, Dr. Sachin Kumar (Dept. of BSBE, IIT Guwahati, India), Dr. Surajit Bhattacharjee (Dept. of molecular biology, University of Tripura, India), for their constructive support in my research. I would also like to thank my doctoral committee members Prof. Sanjucta Patra, Prof. Animes Kr. Golder, and Prof. Chandan Das, for their valuable suggestions and consistent evaluation of my research works. I would like to express my gratitude to all the faculty and staff members of the Centre for the Environment for their continuous support. Also, I am immensely thankful to the Department of Chemistry, centre for the Environment and CIF (IIT Guwahati) for allowing me to use the sophisticated instrument facility. A special mention in this note of acknowledgment will certainly be of IIT Guwahati for providing me with the financial support.

I would also like to acknowledge all my past and present lab members, including Dr. Subhankar Panda, Dr. Ashalata Roy, Dr. Abhishek Saha, Dr. Nirmalya Pradhan, Dr. Nasim Akhtar, Dr. Subhasis Dey, Dr. Oindrila Biswas, Mr. Sribash Das, Ms. Priyanka Mazumder, Mr. Gunanka Hazarika, Mr. Biswa Mohan Prusty, Ms. Soumya Srimayee, Ms. Nikumoni Das and Mr. Mohit Kumar, Mr. Mrinal Kar, Ms. Rama Karn for providing me a healthy and eruditely atmosphere in the lab. I acknowledge all my colleagues and friends for their support and cheering me up in my down time.

Last but not least, my PhD endeavours would not have been accomplished without acknowledging the members of my life, my dearest parents and grandparents. I dedicate this page to them whose continuous sustenance and sunlight of love have been a blessing. My grandparents Mr. R.B. Chaudhary and Late Mrs. Ganga Chaudhary and my lovely parents Mr. Dayanand Chaudhary and Mrs. Nirmala Chaudhary who have shaped my childhood days with their unconditional love and their precious suggestions of life, have made me the way I am. Your tremendous support and care have been a backbone of my edification. My grateful appreciation also goes to my siblings Ms. Deepa Patel, Mr. Hemant Chaudhary and other family members including uncle, aunty, cousins and others for their emotional support and encouragement. Their endless love and blessings boost me up to cross the hurdles of my career. Thank you all for being a memorable part of my life.

Anjali Patel

ABSTRACT

This Thesis title **"Development of novel sulfonium containing drug carriers with inherent antimicrobial activities to combat drug resistance"** deals with the study of sulfonium containing liposome and polymers which contains membrane directed bactericidal activity and hence it can counteract different drug resistance mechanism of the drug resistance due to efflux transporter, reduced number of porins, metabolic drug inactivation and hence it can rejuvenate the activity of the clinically proven antibiotics against drug resistant bacterial strains.

Chapter 1 elaborates the history of antibiotic development and its resistance mechanism in different bacterial strains followed by the strategy to cope up with the drug resistant bacterial superbugs. Here it also elaborates the rationale behind designing the antimicrobial drug carrier with bactericidal activity

Chapter 2 deals with the development of sulfonium containing liposome with antimicrobial and antibiofilm activity against gram-negative and gram-positive bacterial strains and after encapsulation it shows synergistic activity with very less toxicity against host cells.

Chapter 3 is pact with the characterization and drug encapsulation study of sulfonium and lauryl amine conjugated albumin protein. This antibacterial nano aggregate is entrenched with the antibiofilm and synergistic efficacy test after encapsulation of ciprofloxacin drug in it. This nano aggregate reveals the antibacterial and antibiofilm activity in mice model by reducing the number of colony forming unites in liver and spleen.

Chapter 4 elaborates the design of stimuli responsive sulfonium cross linked hyaluronic acid hydrogel with self-healing and drug entrapment property. antibacterial and antibiofilm activity against drug resistant bacterial strains. This study also corroborates the wound healing property of the hydrogel.

List of abbreviation

ADSc	Antibiotics-delivery systems
Amox	Amoxicillin
AMPs	Antimicrobial peptides
ATCC	American type cell culture
BHI	Brain heart Infusion
BSA	Bovine serum albumin
CAC	Critical aggregation concentration
CAM	Cationic amphiphile
CD	Circular dichroism
CD-44	Cluster of differentiation-44
$CDCl_3$	Deuterated chloroform
Cefta	Ceftazidime
CF	Cystic fibrosis
cFDA_SE	Carboxyfluorescein diacetate succinimidyl ester
CFSE	Carboxyfluorescein succinimidyl ester
CFU	Colony forming unit
CiproF	Ciprofloxacin
CV	Cristal violet
DCM	Dichloromethane
DIPEA	N,N -Diisopropylethylamine
$DiSC_3(5)$	3,3-Dipropylthiadicarbocyanine iodide
DLS	Dynamic light scattering
DMEM	Dulbecco's Modified Eagle Medium
DMF	Dimethylformamide
DMSO	Dimethyl sulfoxide
DMTMM	4-(4,6-dimethoxy-1,3,5-triazin-2-yl)-4-methyl-morpholinium chloride
DNA	Deoxyribonucleic acid
E. coli	*Escherichia coli*
EDC	1-Ethyl-3- (3-dimethylaminopropyl)carbodiimide
ESI	Electrospray ionization
EtOAc	Ethyl acetate
FDA	Food and Drug Administration
FESEM	Field emission scanning electron microscope
FETEM	Field emission transmission electron microscopy
FIC	fractional inhibitory concentration
FTIR	Fourier-transform infrared
GR-MRSA	Gentamycin resistant-methicillin resistant *Staphylococcus aureus*
HA	Hyaluronic acid
HaCat	Human keratinocyte line
HCl	Hydrochloric acid
HeLa	Henrietta Lacks cell line

HEPES	4-(2-hydroxyethyl)-1-piperazineethanesulfonic acid
HOBT	Hydroxybenzotriazole
HPLC	High-performance liquid chromatography
KCl	Potassium chloride
KH_2PO_4	Monopotassium phosphate
K. *pneumonia*	*Klebsiella pneumonia*
LB	Luria-Bertani
LPS	Lipopolysaccharide
MALDI-TOF	Matrix Assisted Laser Desorption/Ionization- Time of flying
MBC	Minimum bactericidal concentration
MDa	Mega Dalton
MDR1	Multiple Drug Resistance1
MeOH	Methanol
MIC	Minimum inhibitory concentration
MS	Mass spectrometry
MTCC	Microbial type cell culture
MTT	3-(4,5-Dimethylthiazol-2-yl)-2,5-Diphenyltetrazolium Bromide
Na_2HPO_4	Disodium phosphate
NaH_2PO_4	Sodium dihydrogen phosphate
NaCl	Sodium Chloride
NADH	Nicotinamide Adenine Dinucleotide Hydrogen
NAG	N-acetyl glucosamine
NAM	N-acetyl muramic acid
NMR	Nuclear magnetic resonance
NSAID	Non-steroidal anti-inflammatory drugs
OD	Optical density
P. aeruginosa	*Pseudomonas aeruginosa*
PBMC	peripheral blood mononuclear cell
PBS	Phosphate-buffered saline
PI	Propidium iodide
PNPs	Protein nano particles
RBC	Red blood cell
RNA	Ribonucleic acid
ROS	Reactive oxygen species
RPMI	Roswell Park Memorial Institute
RT	Room temperature
S. aureus	*Staphylococcus aureus*
SIC	Sub inhibitory concentration
TA	Teichoic acid
Tet	Tetracycline
TFA	Trifluoroacetic acid
TLC	Thin layer chromatography
TTC	2,3,5-triphenyltetrazolium chloride

Tx-100	TritonX-100
UTI	Urinary tract infection
UV-VIS	Ultraviolet-visible
Van	Vancomycin
VRE	Vancomycin resistant *Enterococci*
VSE	Vancomycin sensitive *Enterococci*
WHO	World Health Organisation

For symbols/units

α	Alpha
Å	Angstrom
atm	Atmosphere
β	Beta
C	Celsius
°	Degree
δ	Delta
Hz	Hertz
m	Meta
µg	Micro gram
µM	Micro mole
mL	Millilitre
mV	Mili Volt
min	Minute
nM	Nano mole
o	Ortho
p	Para
%	Percentage
s	Second

Chapter 1

Introduction

Antimicrobial drug resistance has intimidated the success of prevention and treatment of infectious diseases and other ailments such as cancer therapy.[1, 2] Various medical procedures such as major surgery and organ implant are also facing uncertain outcomes due to bacterial infection and antibacterial drug resistance.[3] A combinatorial strategy could also be beneficial to fight against bacteria as the synergistic effect likely to upsurge superior bactericidal effect, reduce host-specific toxicity, and operational killing dose. The therapeutic efficiency of this antibacterial strategy depends on the ability of the carrier to infringement the intrinsic resilience of the bacterial cells and in reestablishing the susceptibility to the antibacterial agent. Drugs with membrane-targeted activity have an important role in antibacterial activity and comparatively can better counteract the bacterial resistance system. The membrane-targeted antibacterial drugs provide the extra benefit without developing resistance as they can act effectively towards the dormant or spore form of the bacteria and biofilm-forming strain because of conserved membrane composition in all growth forms of the bacterial cell and distinct mechanism of action that implicates less specific membrane permeabilization.

In this regard, small molecule-based membrane-active synthetic amphiphilic compounds are considered as potential antibacterial agents that hold the prospect of success of the combinatorial antimicrobial therapy. Amphiphilic compounds with cationic moiety convey membrane-oriented activity because of the presence of negatively charged lipopolysaccharide (LPS) and teichoic acid (TA) in gram-negative and gram-positive bacteria, respectively.[4-6] Membrane directed antibiotic render bactericidal activity which can neutralize the various drug resistance mechanisms of the bacterial cells. Recent studies revealed that the sulfonium-linked vancomycin analogue had enhanced antibacterial activity against vancomycin-resistant bacteria both under *in vitro* and *in vivo* conditions.[7] The amphiphilicity and the presence of cationic sulfonium moieties would also allow the sulfonium-based lipids to fuse with the outer membrane of the bacteria cells and release the encapsulated antibiotics.[8]

Herein, we report the synthesis and mechanism of the antibacterial activity of sulfonium-based compounds. The role of cationic charge and hydrocarbon chain length in antimicrobial activity was investigated by their structural modification against both gram-positive and gram-negative strains of bacteria. Sulfonium compounds have been

conjugated with biocompatible polymers to harbour their specific properties and biocompatibility. These polymers were used to encapsulate or trap the other antibiotic in it with sustained release profile. The encapsulation reduces the multiple dosing and renders the synergistic efficacy.

Aim of the thesis

Currently increasing cases of antimicrobial drug resistance and higher mortality rate persuaded us to develop the new antimicrobial agents which can counteract the drug resistance strategy of the bacterial strains. The aim of the thesis work is to focus on developing such antimicrobial drugs with membrane disrupting property. Membrane disruption causes faster bactericidal activity and also it does not interact with the bacterial cell metabolism and hence does not allow the bacterial cell to develop the resistance. Furthermore, we also aim to develop a drug carrier with inherent antimicrobial activity which can rejuvenate the activity of the clinically approved drugs. Thesis describes the develops the sulfonium based antimicrobial liposomes and biopolymers for improved biocompatibility.

Chapter 2 corroborates with the design and development of sulfonium containing liposome with pyridinium or triazole head group with structure activity relationship test

Chapter 3 deals with the conjugation of sulfonium and hydrophobic chain molecules with biopolymers to enhance its biocompatibility and drug encapsulation efficacy

Chapter 4 elaborates the preparation of sulfonium containing hydrogel for antibacterial and wound healing activity

---

Chapter 2

Sulfonium-based liposome-encapsulated antibiotics deliver a synergistic antibacterial activity

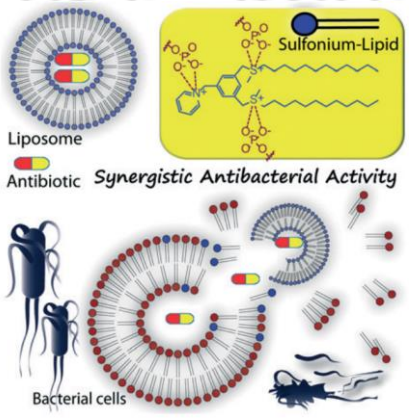

Figure 2.1 Development of sulfonium liposome and its antimicrobial activity

Herein, this study describes the synthesis and mechanism of the antibacterial activity of sulfonium-based amphiphilic compounds. In addition, antibiotics were encapsulated in the potent liposomal compound and antibacterial efficacies of the composite were also investigated. The composite showed moderate loading of water-soluble antibiotics and sustained release profile. Overall, our studies propose that electrostatic interaction of cationic liposomes with the bacterial membrane allows its disassembly and insertion of the amphiphilic compound to the bacterial membrane, resulting in the concomitant release of antibiotics at the target site to achieve synergistic antibacterial activities.

2.1 Design and synthesis of compounds

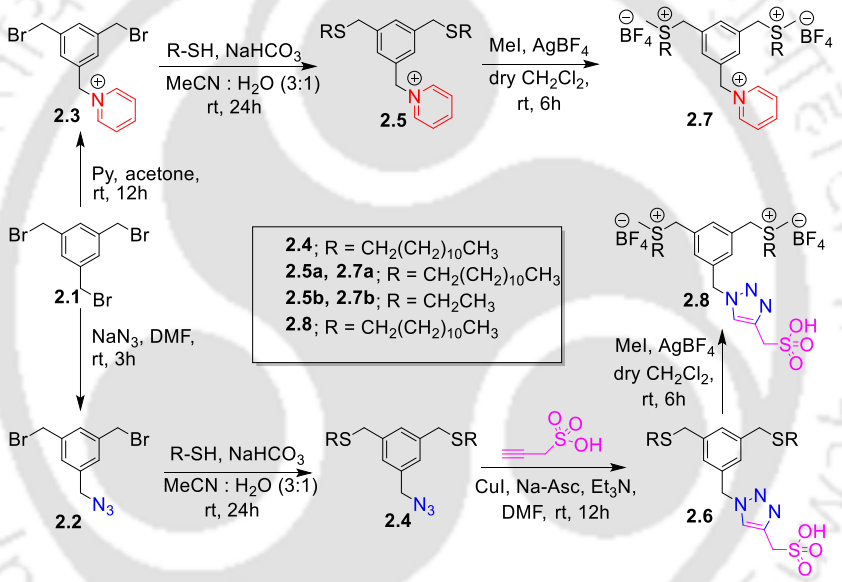

Scheme 2.1. Synthetic routes to the sulfonium-based compounds.

2.2 Aggregation behavior in aqueous solution — To investigate the behavior of these amphiphilic compounds under an aqueous environment, the compounds were dissolved in phosphate-buffered saline (PBS).[9] The field-emission transmission electron microscope (FE-TEM) analysis showed that compound **2.7a** form spherical aggregates in an aqueous medium (Figure 1B). The dynamic light scattering (DLS) study showed that the size of the spherical aggregates varies between 270-340 nm at different pH of the respective buffers at 25 ˚C (Figure 1C, 1D and S6). The zeta-potential measurements showed that the overall surface charge of the spherical aggregates was positive.

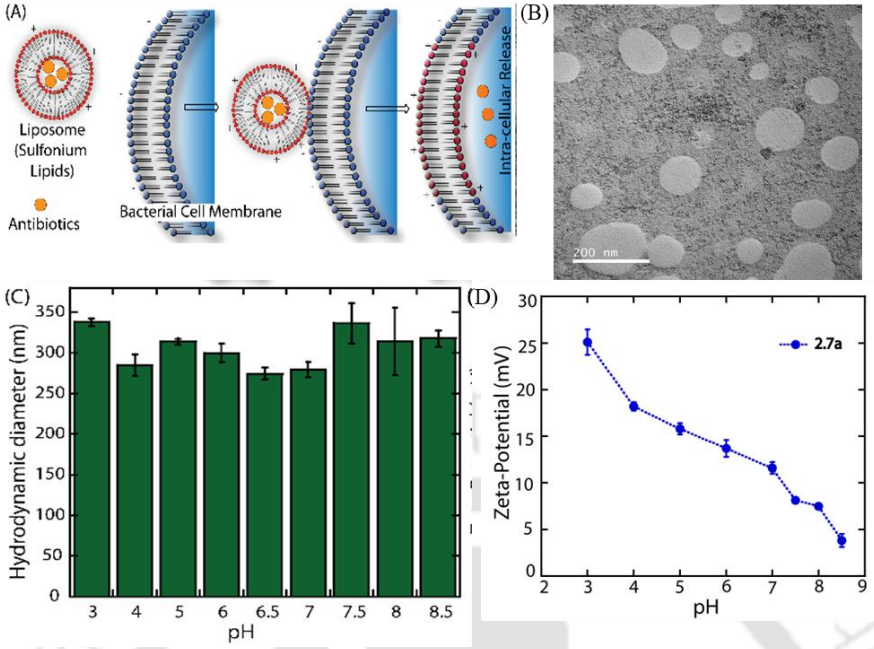

Figure 2.2. Cartoon diagram demonstrating the probable pathway for the bactericidal effect of antibiotics encapsulated liposomes of compound **2.7a** (A). Representative TEM image of the soluble aggregates generated from the 100% compound **2.7a** (B). Variation of the hydrodynamic diameter of the soluble aggregates generated from the 100% compound **2.7a** at different pH was measured by DLS analysis **(C)**. The surface potential of the soluble aggregates generated from the 100% compound **2.7a** at different pH (D).

2.3 Antibacterial activities of the compounds — The sulfonium-based compounds showed antibacterial activity against both gram-positive and gram-negative bacteria.[9] The minimum inhibitory concentrations (MIC) of the compounds were calculated against gram-negative bacteria such as *Escherichia coli* MTCC 1687 and *Pseudomonas aeruginosa* MTCC 2488 and gram-positive bacteria such as *Staphylococcus aureus* MTCC 96 and methicillin-resistant *Staphylococcus aureus* (MRSA) by micro broth dilution method.[10] Interestingly, the antibacterial activity of these sulfonium lipids **2.7a** and **2.8** are similar to other substances, especially to some widely used antiseptics.

Table 2.1. Antibacterial activities of the synthesized compounds.

Compound			MIC (μM)/ MBC (μM)				HC_{50} (μM)
	n	R	*E. coli*	*P. aeruginosa*	*S. aureus*	*S. aureus* (MRSA)	
2.4	11	$-N_3$	>100	>100	>100	>100	-

2.5a	11	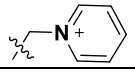	>100	>100	>100	>100	-
2.5b	2	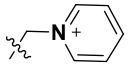	>100	>100	>100	>100	-
2.7a	11	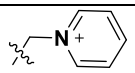	7.5 ± 1 / 10 ± 1	12 ± 0.5 / 24 ± 1	6.3 ± 1 / 12.5 ± 1	6.3 ± 1 / 12.5 ± 1.5	29
2.7b	2	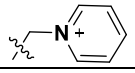	>100	>100	>100	>100	-
2.8	11	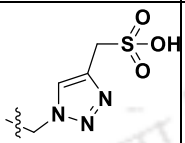	12 ± 1 / 20 ± 1	25 ± 1 / 50 ± 1	10 ± 0.5 / 12.5 ± 1	25 ± 1 / >100	35

The mechanism of bactericidal activity was studied by propidium iodide (PI) uptake assay.[11, 12] The increase in fluorescence intensity of PI revealed that the antibacterial activity of compound **2.7a** is membrane directed and time-dependent, suggesting that the number of dead cells increases with time (Figure 3A). Further mechanistic studies were performed by membrane depolarization assay using $DiSC_3(5)$ dye. Fluorescence-based live and dead cell imaging study by staining the drug-treated cells with PI and 5(6)-carboxyfluorescein diacetate *N*-succinimidyl ester (cFDA-SE) was also done to investigate the bactericidal activity of the compound (Figure 2.3C).

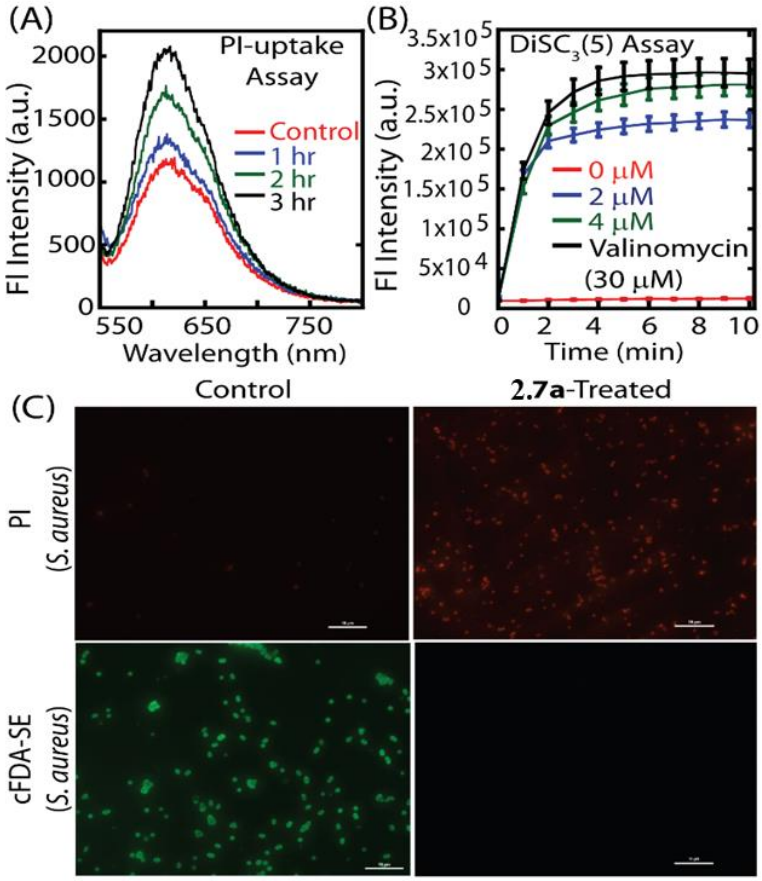

Figure 2.3. Fluorescence-based PI-uptake assay of compound **2.7a** using *S. aureus* (MRSA) cells (A). Compound **2.7a**-treated membrane depolarization assay using $DiSC_3(5)$ dye on *S. aureus* (MRSA) cells (B). Representative fluorescence microscopic images of untreated and compound **2.7a**-treated bacterial cells (C). The scale bar for the images is 10 μm.

2.4 Antibiotics encapsulation and antibacterial efficacy —Antibiotics and other drugs, when encapsulated in liposomes, are more effective and protected from the adverse environment of the cell. Compound **2.7a** showed satisfactory loading ability for tetracycline (18%) and amoxicillin (28%) at pH 7.4, Fluorescence measurements of these antibiotics showed sustained release profiles with 40% and 60% of tetracycline and amoxicillin, respectively, which were released after 60 hours of incubation at 37 °C (Figure 2.4B).

Table 2.2. Antibacterial activities of the commercial antibiotics and antibiotic encapsulated sulfonium based amphiphilic compound.

Antibiotic	Bacterial train	MIC (μg/mL)	MIC (**2.7a**@antibiotic) (μg/mL)
Tetracycline	S. *aureus*	1.87	0.31
	E. *coli*	3.75	0.87
Amoxicillin	S. *aureus*	2.50	0.44
	E. *coli*	4.0	0.62

2.5 Host cell cytocompatibility test

An antimicrobial agent can be used for further bio-application only when it is biocompatible and non-toxic to human cells. In this regard, the cytocompatibility of synthesized potent amphiphiles and antibiotic-loaded amphiphiles were verified against HeLa (human cervical cancer) and HaCaT (human keratinocyte) cells. To ensure the compatibility of the sulfonium-based amphiphiles against red blood cells, hemolytic activity was performed.

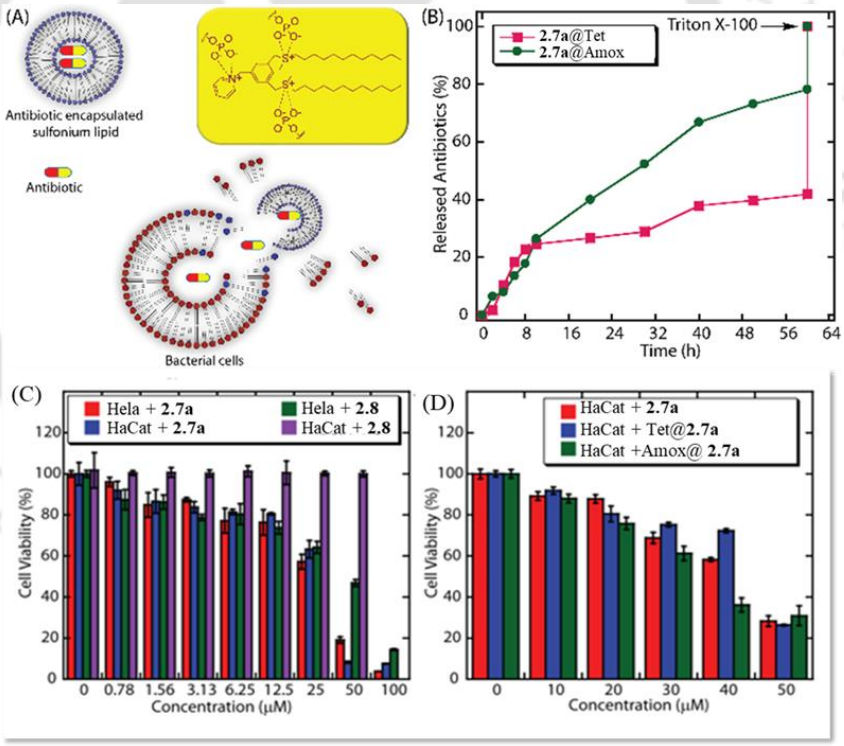

Figure 2.4. Cartoon diagram demonstrating the antibiotic release pathways from the liposomes of compound **2.7a** (A). The antibiotics (tetracycline and amoxicillin) release profile of compound **2.7a** at pH 7.4 (B) MTT test of the HeLa and HaCaT cells in the presence of compounds **2.7a** and **2.8** (C). Concentration-dependent viabilities of the HaCaT cells in the presence of compounds **2.7a** and antibiotics encapsulated compound **2.7a** (D).

Chapter 3

Onium and alkyl amine decorated protein nanoparticles as antimicrobial agents and carriers of antibiotics to promote synergistic antibacterial and antibiofilm activities

In this study we developed sulfonium and lauryl amine tethered BSA-based nanoparticles and investigated their inherent antibacterial properties and antibiotic delivery aptitude. The sulfonium and lauryl amine conjugated BSA protein nanoparticles (PNPs) showed a synergistic effect when clinically proven antibiotics were encapsulated, fulfilling one goal of antibiotic stewardship: to reduce the effective dose of antibiotics and their exposure to other bacterial sp.

3.1 Synthesis and characterization of R-BSA-S nano aggregates and its characterization

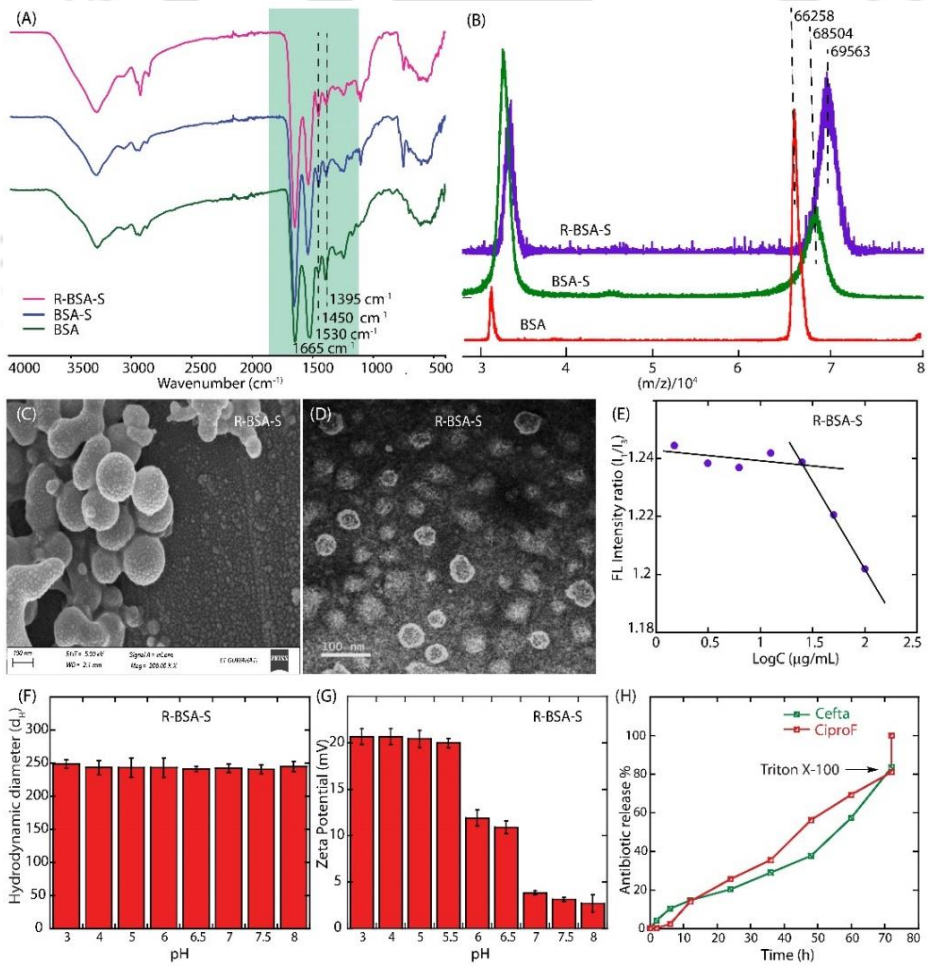

Figure 3.1. Characterization of BSA-based PNPs. Representative FTIR (A) and MALDI-TOF (B) spectra of BSA, BSA-S, and R-BSA-S. Representative FESEM (C) and FETEM (D) images of R-BSA-S. CAC measurements of R-BSA-S (E). DLS (F) and surface

potential (G) of R-BSA-S across different pH. The antibiotics release profile of R-BSA-S (H).

The antibiotics loading efficacy of R-BSA-S was investigated using commercial antibiotics, CiproF, and Cefta.

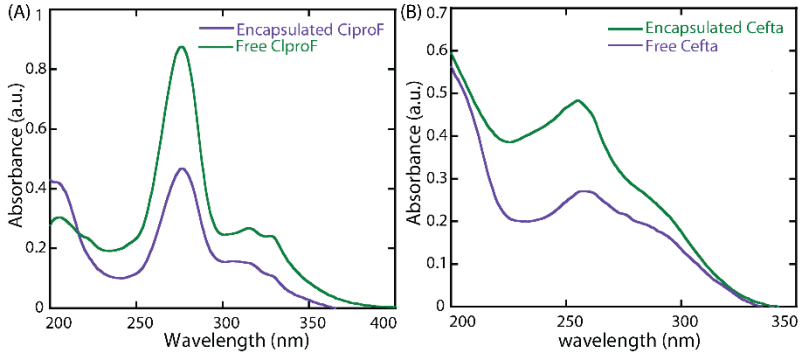

Figure 3.2. Antibiotics loading efficacy of R-BSA-S (A and B)

3.2 Biocidal activities of modified BSA

Table 3.1. Antibacterial activities of the modified BSA.

Bacterial strains MIC (µg/mL)				
Antimicrobial agents	***S. aureus***	**GR-MRSA**	***E. coli***	***P. aeruginosa***
BSA	>100	>100	>100	>100
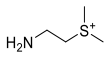	>100	>100	>100	>100
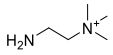	>100	>100	>100	>100
Lauryl amine	>100	>100	>100	>100
R-BSA	>100	>100	>100	>100
R-BSA-S	15 ± 2	20 ± 3	24 ± 1	30 ± 4
R-BSA-N	37.5 ± 2.5	40 ± 4	42 ± 3	>45
CiproF	0.019 ± 0.001	0.15 ± 0.02	0.058 ± 0.002	0.156 ± 0.071
Cefta	1.25 ± 0.31	125	1 ± 0.12	2.5 ± 0.31

CiproF@R-BSA-S[a]	0.004 ± 0.001	0.12 ± 0.04	0.007 ± 0.002	0.018 ± 0.007
Cefta@R-BSA-S[a]	0.156 ± 0.01	15 ± 2	0.125 ± 0.07	0.625 ± 0.11

[a]MIC values were calculated based on the concentration of the encapsulated antibiotic (Cipro and Cefta).

3.3 Antibiofilm activity of R-BSA-S

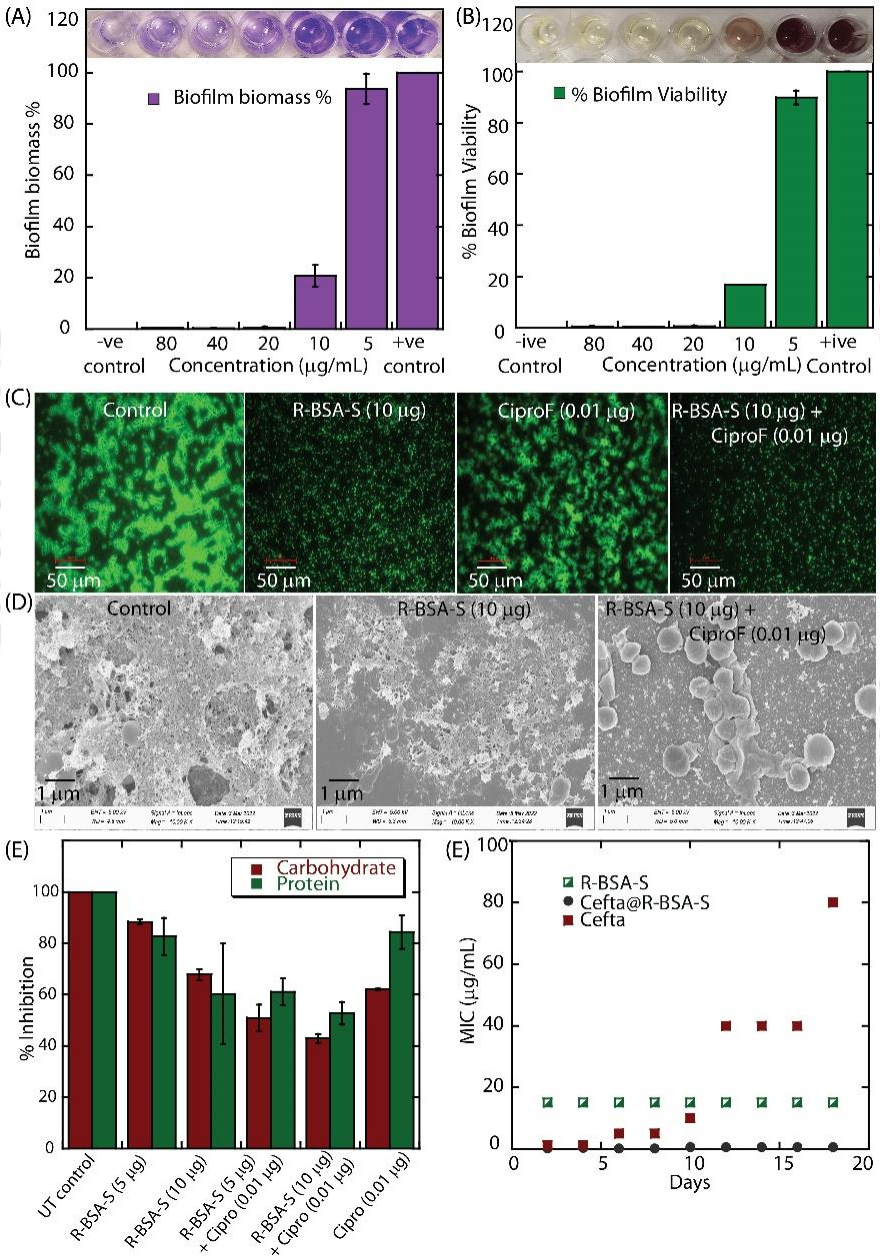

Figure 3.3. Antibiofilm activity of R-BSA-S alone and in combination with CiproF. Biomass (A) and viability (B) of GR-MRSA biofilm in the presence of different

concentrations of R-BSA-S using crystal violet and TTC dye, respectively. Effect of R-BSA-S (10 µg/mL) alone and in combination with CiproF (0.01 µg/mL) on the MRSA biofilm formation. Acridine orange is used as a dye, and the attachments of MRSA biofilm live cells on the glass surface are visualized under a fluorescence microscope (C). FESEM images of MRSA biofilm treated with R-BSA-S (10 µg/mL) and in combination with CiproF (0.01 µg/mL) (D). Estimation of polysaccharide (EPS) and total protein from MRSA biofilm. The samples were treated with R-BSA-S (5 µg/mL and 10 µg/mL) alone and in combination with CiproF (0.01 µg/mL) (E). Resistance studies against *S. aureus* cells (F).

Table 3.2: Fractional Inhibitory concentration (FIC) index

Formulation	Bacterial Strain	MIC (µg/mL)	FIC Index
CiproF@R-BSA-S	*S. aureus*	0.004 ± 0.001	0.21
	GR-MRSA	0.12 ± 0.04	0.3
	E. coli	0.007 ± 0.002	0.12
	P. aeruginosa	0.018 ± 0.007	0.12
Cefta@R-BSA-S	*S. aureus*	0.156 ± 0.01	0.2
	GR-MRSA	15 ± 2	ND
	E. coli	0.125 ± 0.07	0.16
	P. aeruginosa	0.625 ± 0.11	0.41

ND- Not determined.

3.4 Mechanistic studies

The antimicrobial activity of membrane-directed cationic amphiphilic compounds have been reported due to their electrostatic interaction with the negatively charged surface studded with lipopolysaccharide (Gram-negative bacteria) and teichoic acid (Gram-positive bacteria).[13-15]

The fluorescence-based live and dead cell imaging assay using PI and 5(6)-carboxyfluorescein diacetate *N*-succinimidyl ester (cFDA-SE) revealed that the R-BSA-S-

treated *S. aureus* cells lacked carboxyfluorescein succinimidyl ester (CFSE) fluorescence, which suggested the inactivity of bacterial metabolism due to superior membrane damage, which resulted in cell death (Figure 3.6C). The esterase-mediated conversion of cFDA-SE to CFSE only shows a fluorescence signal, which is an indicator of bacterial cell viability.

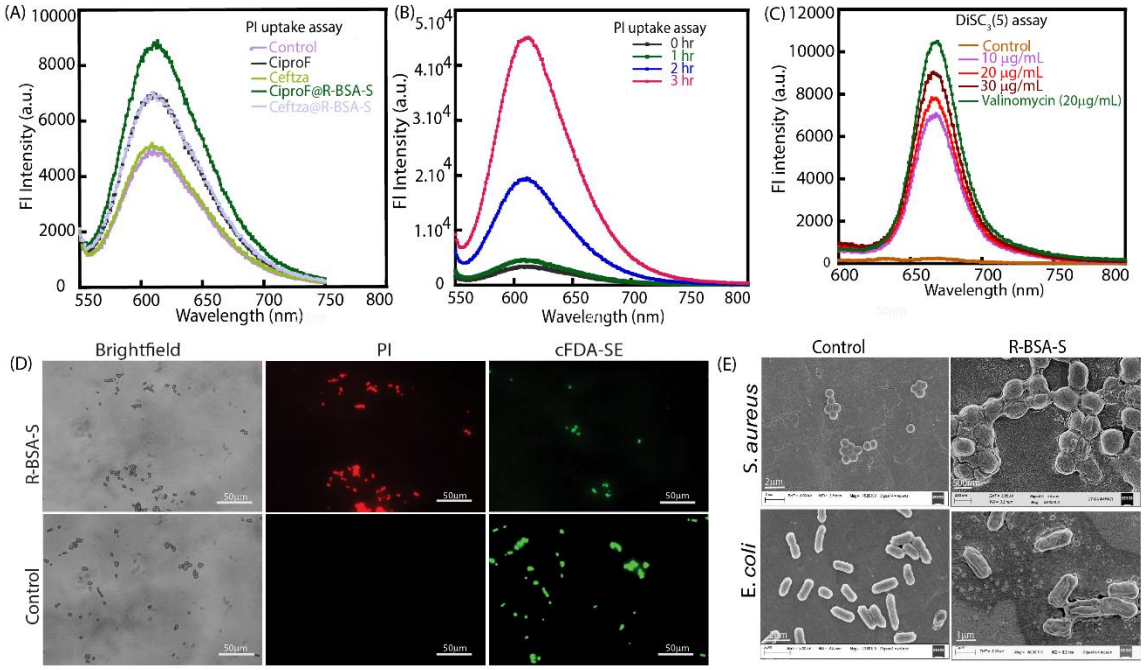

Figure 3.4. PI-uptake assay after treatment of *S. aureus* with CiproF, Ceftza, CiproF@R-BSA-S, and Ceftza@R-BSA-S (A). PI-uptake assay after treatment of *S. aureus* with CiproF@R-BSA-S at different time intervals (B). Representative fluorescence microscopic images of R-BSA-S and untreated *S. aureus* (C). The scale bar for the images is 50 µm. $DiSC_3(5)$–based membrane depolarization assay using *S. aureus* (D). Representative FESEM images of untreated and R-BSA-S treated bacterial cells (E)

3.5 Hemolytic assessment and in vivo antimicrobial activity

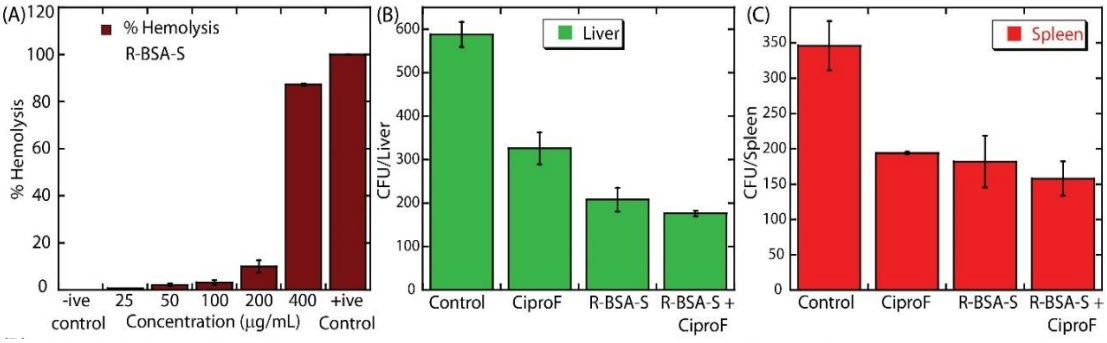

Figure 3.5. The extent of hemolysis in the presence of different concentrations of R-BSA-S and R-BSA-N (A). Effect of R-BSA-S alone or in combination with ciproF on a mouse model of catheter-associated infection. Estimation of bacterial load in mouse (*S. aureus* in vivo biofilm model) liver (B) and spleen (C) determined through CFU count on an agar plate.

Chapter 4

Sulfonium-cross-linked Hyaluronic acid-based Self-healing Hydrogel: Stimuli-responsive Drug Carrier with Inherent Antibacterial Activity to Counteract Antibiotic-Resistant Bacteria

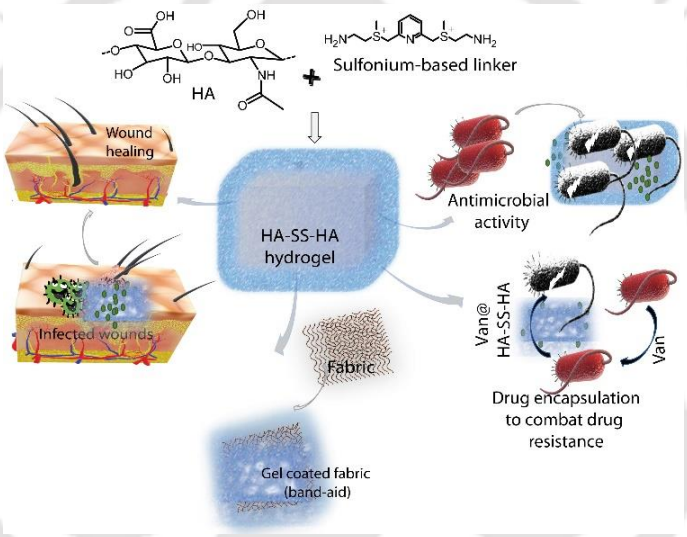

Figure 4.1 Sulfonium linked hydrogel preparation and its application as an antimicrobial agent to combat drug resistance and faster wound healing

Inspired by the success of sulfonium-based amphiphiles, we synthesized (pyridine-2,6-diylbis(methylene))bis((2-aminoethyl)(methyl)sulfonium) as a linker molecule with two sulfonium and one pyridine group that can be conjugated from both sides with –COOH group of the HA. Cross-linking of HA with this pyridine-containing sulfonium linker (HA-SS-HA) provided antimicrobial activity and riveted it with the porous structure to trap the antibiotics. The HA-SS-HA showed moderate antibacterial activity; however, the antibiotics encapsulated HA-SS-HA (antibiotics@HA-SS-HA) showed excellent antibacterial activity against antibiotic-susceptible and antibiotic-resistant bacterial strains. HA is sensitive to the hyaluronidase enzyme, which is also secreted by bacterial cells in its extracellular space. Hence, we used hyaluronidase as stimuli to regulate the release of

antibiotics from the antibiotics@HA-SS-HA in a controlled manner. Coating of this gel onto fabrics showed a Band-Aid-like use of HA-SS-HA and antibiotics@HA-SS-HA.

4.1 Synthesis and characterization of HA-SS-HA hydrogel and its characterization

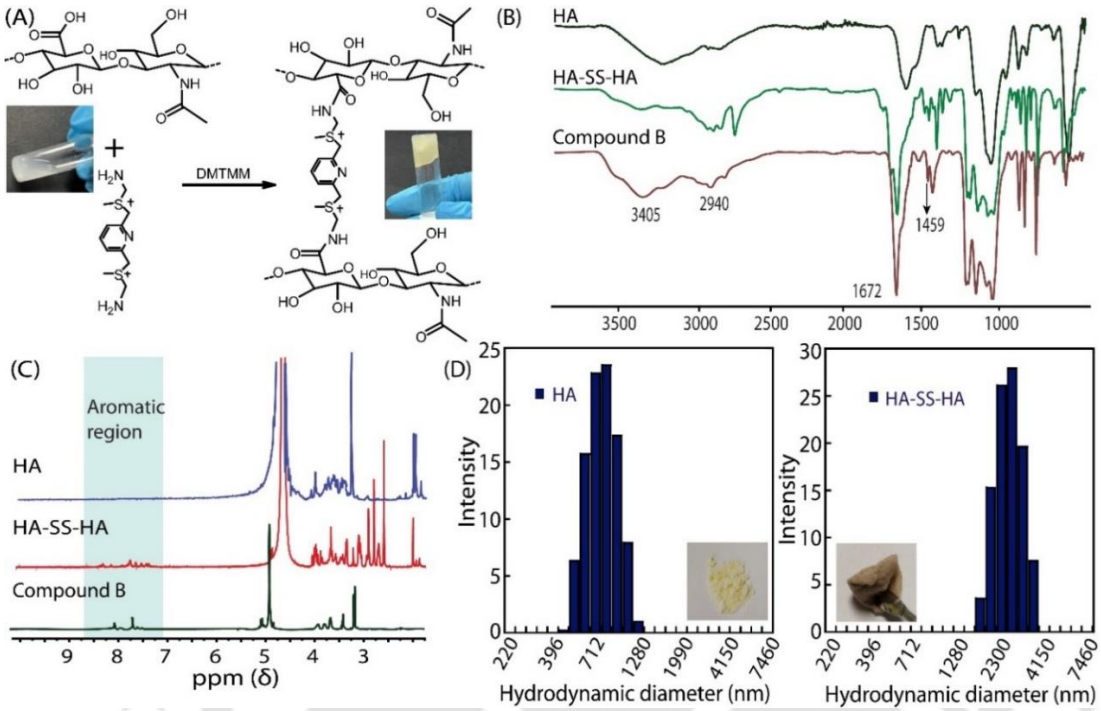

Figure 4.2. Synthetic route to HA-SS-HA biopolymer (A). FTIR spectra of HA, HA-SS-HA, and compound B (B). ^{1}H NMR spectra of HA, HA-SS-HA, and compound B (C). Average hydrodynamic diameter (nm) of HA and HA-SS-HA biopolymer (D).

4.2 Physical and morphological characterization —

The dry cross-linked HA-SS-HA polymer had a porous structure, which inspired us to investigate its gelation property. The rheological properties of the hydrogel were recorded to analyze the viscoelastic property of the HA-SS-HA gel and it was followed by the study of of self-healing and adhesive property

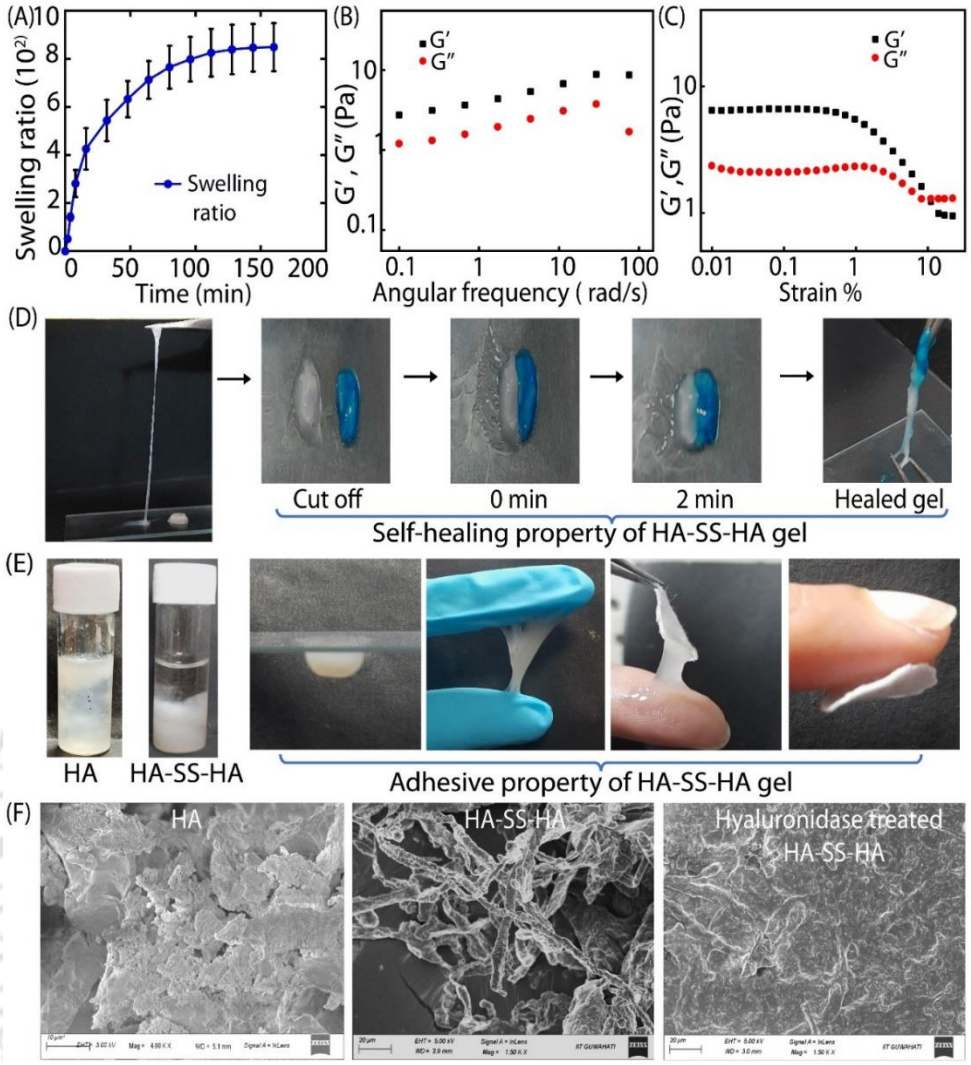

Figure 4.3. Water uptake-dependent swelling property of HA-SS-HA hydrogel (A). Dynamic storage moduli (G') and Loss moduli (G") of HA-SS-HA hydrogel at a variable angular frequency (B) and strain (C). Representative images demonstrating the elastic and self-healing properties of the HA-SS-HA hydrogel (D). Representative images demonstrate the adhesive property of HA-SS-HA hydrogel (E). Morphological analysis of HA, HA-SS-HA, and Hyaluronidase treated HA-SS-HA (F).

4.3 Antimicrobial activity of the modified hyaluronic acid -We tested the antibacterial efficacy of the HA-SS-HA hydrogel against both Gram-negative and Gram-positive bacterial cells. The Gram-positive bacteria such as *S. aureus*, GR-MRSA, vancomycin-sensitive *Enterococci sp.* (VSE), and vancomycin-resistant *Enterococci* (VRE1, VRE4, and VRE5) and Gram-negative bacteria such as *E. coli* and *P. aeruginosa* were used for antibacterial studies.

Table 4.1. In vitro activities of the HA-SS-HA and antibiotics encapsulated HA-SS-HA hydrogels against various bacterial strains

Bacterial strains	Minimum Inhibitory Concentration (MIC) µg/mL							
	HA	HA-SS-HA	Van	Amox	Tet	Van@HA-SS-HA	Amox@HA-SS-HA	Tet@HA-SS-HA
S. aureus	>250	31.21 ± 7.52	1.56 ± 0.78	2.54 ± 0.62	1.86 ± 0.61	1.11 ± 0.20	0.22 ± 0.06	0.91 ± 0.21
GR-MRSA	>250	125 ± 15	3.92 ± 0.91	20 ± 5	168 ± 42	2.00 ± 0.41	3.71 ± 0.92	1.82 ± 0.45
VSE	>250	31.25 ± 7.51	3.12 ± 0.72	1.92 ± 0.51	3.92 ± 0.91	2.33 ± 0.45	0.45 ± 0.11	1.82 ± 0.45
VRE1	>250	31.25 ± 7.51	>125	31.25 ± 7.53	15.62 ± 3.02	1.51 ± 0.41	7.51 ± 1.81	0.91 ± 0.21
VRE4	>250	31.25 ± 7.51	>125	31.25 ± 7.52	15.62 ± 3.01	2.52 ± 1.21	3.72 ± 0.92	1.82 ± 0.45
VRE5	>250	31.25 ± 7.51	>125	62.52 ± 15	15.62 ± 3.05	1.92 ± 0.51	3.71 ± 0.91	7.52 ± 1.81
E. coli	>250	62.52 ± 15.01	125 ± 15	4.51 ± 1.12	3.77 ± 0.92	3.52 ± 0.87	0.94 ± 0.23	1.89 ± 0.46
P. aeruginosa	>250	31.21 ± 7.53	125 ± 15	3.37 ± 0.92	6.67 ± 1.61	3.52 ± 0.87	1.92 ± 0.42	3.91 ± 0.91

Van = vancomycin; Amox = amoxicillin; Tet = tetracycline. The MIC values were calculated using the weight of the HA-SS-HA polymer. VRE1, VRE4, and VRE5 are different clinical isolates. For antibiotic@HA-SS-HA, the MIC values were calculated based on the encapsulated concentration of antibiotics. All measurements were performed in triplicate.

4.4 Antibiotic encapsulation and release efficacy of the modified hyaluronic acid

Different classes of antibiotics, such as β-lactam (amoxicillin), polyketide (tetracycline), and arsenal (vancomycin) antibiotics, were entrapped within the hydrogel. The antibiotic encapsulation efficacy of the hydrogel was investigated from the loading and release profiles of the respective antibiotics. The spectrophotometric method revealed that the antibiotic loading efficacy was around 48% for HA-SS-HA gel. Here, we monitored the representative antibiotic release profile of vancomycin-encapsulated HA-SS-HA (vancomycin@HA-SS-HA).

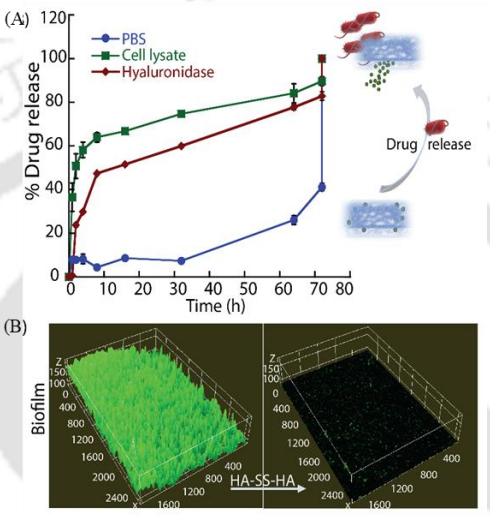

Figure 4.4. The drug release profile of Van@HA-SS-HA at different time intervals in the presence of bacterial cell lysate and hyaluronidase enzyme (A). Biofilm eradication activity of HA-SS-HA hydrogel (B).

4.5 Mechanistic studies for antibacterial activities

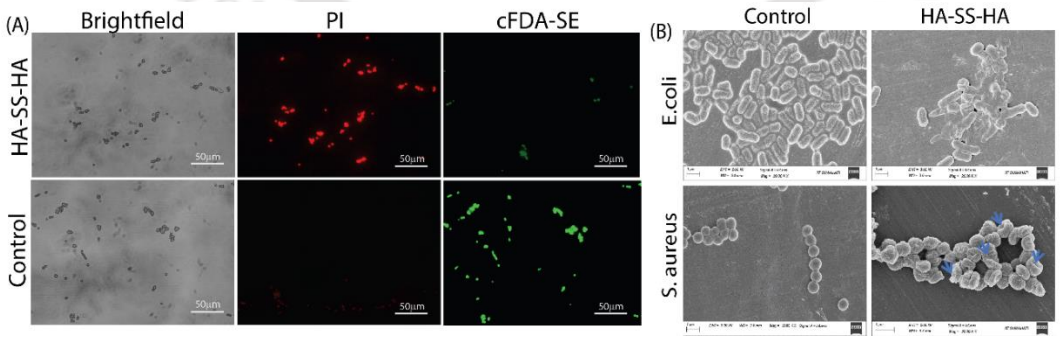

Figure 4.5. Live dead (cFDA-SE and PI stained) cell imaging of control and HA-SS-HA treated *S. aureus* cells shows membrane-directed antimicrobial activity (A). Morphological analysis of HA-SS-HA treated *E. coli* and *S. aureus* cells by FESEM (B).

4.6 Resistance and in vivo wound healing activity test

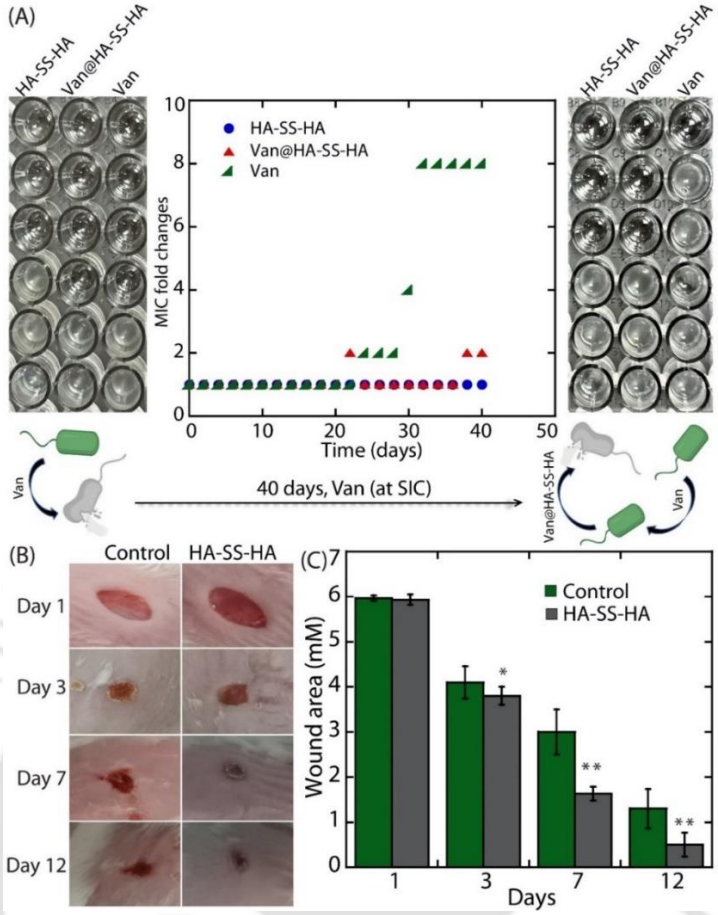

Figure 4.6. Resistance study of the HA-SS-HA, Van@HA-SS-HA, and Van. Representative plate images depict the changes in the growth pattern at 0 and after 40 days (A). The plot demonstrates the changes in MIC values within 0-40 days. SIC = Sub-inhibitory concentration. Promotion of wound healing in a BALB/c mouse model by HA-SS-HA hydrogel (C).

4.7 Application of HA-SS-HA hydrogel

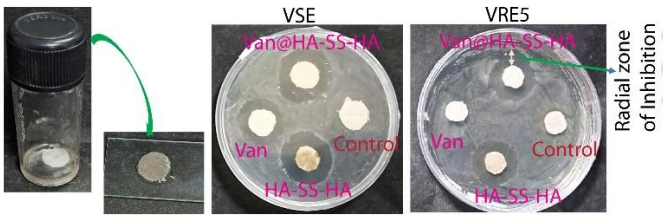

Figure 4.7. Plate images to reveal the antimicrobial efficacy of the Van, Van@HA-SS-HA, and HA-SS-HA against VSE and VRE by zone inhibition method.

5 Conclusion

Thesis commences with (**Chapter 1**) laconic information about the role of antibiotic and its development. It explains the requirement to develop new antimicrobial drug due to drug

resistant superbugs. Here we concluded that due to simple and smart genetic machinery of bacterial cell they can adopt themselves in harsh environment and can cop up with the antibiotics too. Hence development of new antibacterial agent is highly required and for this we concluded that drug with membrane directed activity can withstand the drug resistance strategy of the bacterial cell. Cationic amphiphilic molecules (eg. Sulfonium) are supposed to meet these criteria because they can provide electrostatic interaction with the negatively charged bacterial membrane as well as they can form nanoaggregate to encapsulate the drug and enhance their activity. Research work about sulfonium compounds enunciates that it is the rising epitome of potent antimicrobial agents to combat the resistance mechanism of the bacterial strains. In our prior study (**Chapter 2**) bactericidal amphiphilic **2.7a** compound was proved to be effective against drug sensitive and drug resistant bacterial strains with lower MIC value and antibiofilm activity. It had the tendency to form liposomes which can be used to encapsulate the other drug molecules approved by the drug encapsulation and release behavior study followed by its synergistic antibacterial activity test. This finding suggests that sulfonium amphiphilic compounds have the buoyancy to become a perspective antimicrobial agent to treat the drug resistant infections. The liposome forming aptitude acclaims that it can be used as aerosol agent for the patients suffering from lung infections including pneumonia, cystic fibrosis, bronchitis, asthma etc. With a purpose to make sulfonium compound more biocompatible and efficient drug carrier we conjugated long hydrocarbon chain and small sulfonium molecule to a biopolymer namely albumin that is a natural drug transporter in blood (**Chapter 3**). This was successfully used to encapsulate clinically proven antibiotics with synergistic efficacy. Membrane directed bactericidal activity of the R-BSA-S had the ability to counteract the resistance mechanism of the bacterial strains. Compound was tested under in vivo condition for its antimicrobial activity in mice model where it had number of bacterial colony reduction. Furthermore, similar sulfonium linker molecule was designed and used to cross link a polysaccharide molecule with inherent wound healing property (**Chapter 4**). Fibrous and porous polymer was utilized to incorporate vancomycin antibiotic to rejuvenate its activity against VRE bacterial strains. With wound healing property it was applied on to fabrics to prepare Band-Aid like material for wound dressing and it was tested for its antimicrobial activity against drug resistant bacterial strains.

6 Future prospects

Antimicrobial drug resistance has become one of the major 10 global health issues and parallel to this hospital is running out of effective antibiotics to fight back the infectious diseases caused by bacteria pushing us back to the pre antibiotic era. It has been reported that antibiotic drugs which can act on multiplying and non-multiplying bacteria both have better potency to be used against drug resistant bacterial strains. In this regard membrane directed agents are of good values which are effective against all growth form. Our reported sulfonium molecules had this tendency with bactericidal activity which makes them suitable agents for future uses. All these research work presented in this report elaborated the development of both membranes targeted antimicrobial agent and drug carrier molecule in one chemical composite. All these developed compounds had the potency against drug resistant and drug sensitive bacterial strains which paves the way for further research as they have the potency to provide new hope against infectious superbugs.

References-

1. Papanicolas, L. E.; Gordon, D. L.; Wesselingh, S. L.; Rogers, G. B. J. T. i. m., Not just antibiotics: is cancer chemotherapy driving antimicrobial resistance? *Front. Chem.***2018,** *26* (5), 393-400.

2. Sedighi, M.; Zahedi Bialvaei, A.; Hamblin, M. R.; Ohadi, E.; Asadi, A.; Halajzadeh, M.; Lohrasbi, V.; Mohammadzadeh, N.; Amiriani, T.; Krutova, M. J. C. m., Therapeutic bacteria to combat cancer; current advances, challenges, and opportunities. *Cancer Med* **2019,** *8* (6), 3167-3181.

3. Schwartz, D. J.; Rebeck, O. N.; Dantas, G. J. C. r. i. c. l. s., Complex interactions between the microbiome and cancer immune therapy. *Crit Rev Clin Lab Sci* **2019,** *56* (8), 567-585.

4. Gilbert, P.; Moore, L. J. J. o. a. m., Cationic antiseptics: diversity of action under a common epithet. *J Appl Microbiol* **2005,** *99* (4), 703-715.

5. Moore, L. E.; Ledder, R. G.; Gilbert, P.; McBain, A. J. J. A.; microbiology, e., In vitro study of the effect of cationic biocides on bacterial population dynamics and susceptibility. *Appl Environ Microbiol* **2008,** *74* (15), 4825-4834.

6. Dey, P.; Mukherjee, S.; Das, G.; Ramesh, A. J. J. o. M. C. B., Micellar chemotherapeutic platform based on a bifunctional salicaldehyde amphiphile delivers a “combo-effect” for heightened killing of MRSA. *J Mater Chem B* **2018,** *6* (14), 2116-2125.

7. Guan, D.; Chen, F.; Qiu, Y.; Jiang, B.; Gong, L.; Lan, L.; Huang, W. J. A. C., Sulfonium, an Underestimated Moiety for Structural Modification, Alters the Antibacterial Profile of Vancomycin Against Multidrug-Resistant Bacteria. *Angew. Chem.* **2019,** *131* (20), 6750-6754.

8. Wang, D.-Y.; Van der Mei, H. C.; Ren, Y.; Busscher, H. J.; Shi, L. J. F. i. c., Lipid-based antimicrobial delivery-systems for the treatment of bacterial infections. *Front. Chem.* **2020,** *7*, 872.

9. Dey, S.; Patel, A.; Raina, K.; Pradhan, N.; Biswas, O.; Thummer, R. P.; Manna, D. J. C. C., A stimuli-responsive anticancer drug delivery system with inherent antibacterial activities. *Chem Commun* **2020,** *56* (11), 1661-1664.
10. Balouiri, M.; Sadiki, M.; Ibnsouda, S. K. J. J. o. p. a., Methods for in vitro evaluating antimicrobial activity: A review. *J. Pharm. Anal.* **2016,** *6* (2), 71-79.

11. Yasir, M.; Dutta, D.; Willcox, M. D. J. S. r., Comparative mode of action of the antimicrobial peptide melimine and its derivative Mel4 against Pseudomonas aeruginosa. *Sci. Rep.* **2019,** *9* (1), 7063.

12. Kannan, R.; Prabakaran, P.; Basu, R.; Pindi, C.; Senapati, S.; Muthuvijayan, V.; Prasad, E. J. A. A. B. M., Mechanistic study on the antibacterial activity of self-assembled poly (aryl ether)-based amphiphilic dendrimers. *ACS Appl. Bio Mater.* **2019,** *2* (8), 3212-3224.

13. Patel, A.; Dey, S.; Shokeen, K.; Karpiński, T. M.; Sivaprakasam, S.; Kumar, S.; Manna, D. J. R. M. C., Sulfonium-based liposome-encapsulated antibiotics deliver a synergistic antibacterial activity. *med. chem.* **2021,** *12* (6), 1005-1015.

14. Hoque, J.; Konai, M. M.; Gonuguntla, S.; Manjunath, G. B.; Samaddar, S.; Yarlagadda, V.; Haldar, J. J. J. o. m. c., Membrane active small molecules show selective broad spectrum antibacterial activity with no detectable resistance and eradicate biofilms. *J. Med. Chem.* **2015,** *58* (14), 5486-5500.

15. Zhou, M.; Zheng, M.; Cai, J. J. A. a. m.; interfaces, Small molecules with membrane-active antibacterial activity. *ACS Appl. Mater. Interfaces* **2020,** *12* (19), 21292-21299.

CHAPTER 1

INTRODUCTION OF ANTIBIOTICS AND ITS RESISTANCE IN BACTERIA

1.1 Introduction

Thousands of years ago, humans were surrounded by an enormous number of microbial flora, and a few of these were commensal to them. The efficient human immune system has the tendency to respond to and neutralize bacterial attacks in their tissues. Over time, genetic mutations accelerated in some microbes, and they evolved to cope with the innate immune system of hosts. Their pathogenic nature overburdened human health and started engulfing millions of lives, slowly becoming epidemic forms.[1,2] The suffering of human beings was followed by the impulse to discover the root cause and cure of the infections. Towards this approach, some of the earliest civilizations started using plant and mold extracts for a curative effect. The onset of 20th-century development in science and technology paved the way for drug research, providing the first arsenic-based antibacterial prodrug, salvarsan, developed by Paul Ehrlich. It was introduced in 1910 to treat infections, specifically syphilis.[3] The journey of natural antibiotics started in 1928 when Alexander Fleming discovered the first antibacterial agent from a fungus, later named penicillin. After clinical trials, penicillin was conceded to be prescribed for humans. Later in 1945, Dorothy Hodgkin solved the β-lactam structure of penicillin, which facilitated the development of semisynthetic antibiotics, namely ampicillin, methicillin, cephalosporin, carbapenem, and others.[4] Furthermore, the antimicrobial drug screening strategy led by Paul Ehrlich became the foundation to search for new drugs in the pharmaceutical industry. The commencement of vigorous antibiotic discovery started and resulted in the development of sulfa drugs, namely sulfonamidochrysoidine. The decade of 1950 to 1960 became a golden era of antibiotics, as most antibacterial drugs were discovered in this period, followed by a decline in the discovery of new drugs.[5] Since then, these antibacterial agents have played a pivotal role in counteracting infectious diseases, including urinary tract infections, respiratory tract infections (such as whooping cough, pneumonia, and others), skin infections, and many others.[6-8] Additionally, the uses of antibiotics have been decisive for the success of many medical procedures, including cancer treatment, organ transplantation, surgery, and others. Antibiotics are usually taken orally, but in more severe cases, particularly deep-seated systemic infections, antibiotics can be given intravenously or by injection.[9] These drugs can be either bacteriostatic or bactericidal in their interactions with target bacteria. Bacteriostatic drugs cause reversible inhibition of growth, with bacterial growth restarting after the elimination of the drug. In contrast, bactericidal drugs kill their target bacteria. The decision of whether to use a bacteriostatic or bactericidal drug depends on the type of

infection and the immune status of the patient. In a patient with strong immune defenses, both bacteriostatic and bactericidal drugs can be effective in achieving clinical cure. However, when a patient is immunocompromised, a bactericidal drug is essential for the successful treatment of infections.[10, 11]

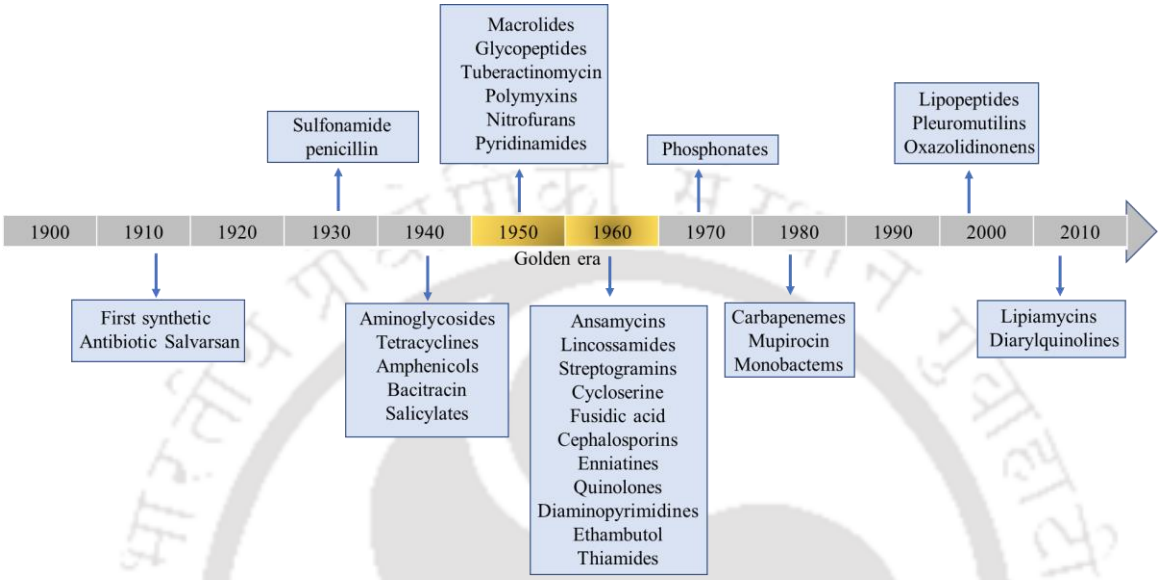

Figure 1.1 List of antibiotics at an evolutionary scale.[5]

Regardless of the immune status of the patient, life-threatening infections such as acute endocarditis require the use of a bactericidal drug. Microbes differ from animals and humans in terms of hierarchy, cell architecture, and metabolism. These differences help researchers construct a drug design that should fulfil safety and selectivity criteria to minimize side effects. A plethora of chemical molecules are known to kill bacterial cells, but very few have the propensity to kill bacterial cells without harming the host. Accordingly, a drug needs to have a defined target. Hence, antibiotics have been classified based on the mode of action and the effect they have on microorganisms.

Mode of action

Antibiotics have various modes of action based on their targets; they have been classified as

- ❖ Inhibition of cell wall synthesis, *e.g.,* penicillin
- ❖ Inhibition of protein synthesis, *e.g.,* chloramphenicol
- ❖ Interfering genetic material synthesis, *e.g.,* metronidazole

- ❖ Interfering the cellular metabolism, *e.g.,* sulfa drugs
- ❖ Leakage of cell contents by damaging the bacterial membrane, *e.g.,* amphotericin

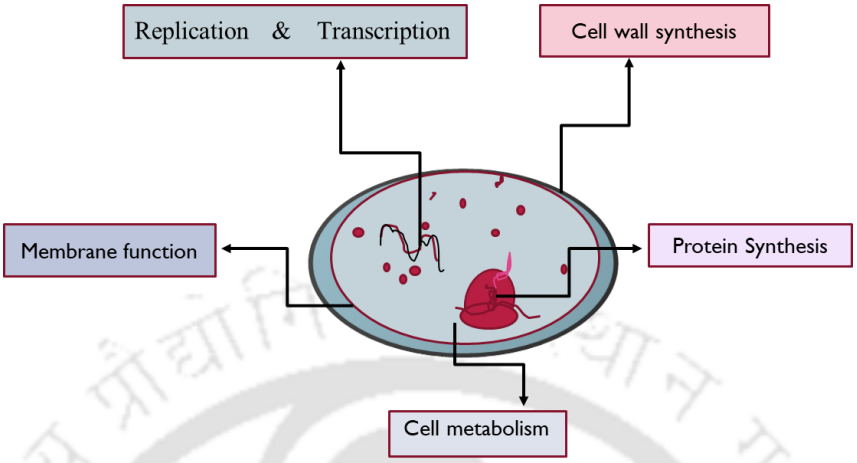

Figure 1.2 Pictorial diagram to show the antibiotic mode of action

1.2.1 Inhibition of cell wall synthesis

Cell wall biosynthesis and cell division are integral to bacterial cell survival. Since mammalian cells are devoid of cell walls, this antibiotic target is safe and selective. The bacterial cell wall is a rigid structure studded with a polypeptide backbone of N-acetylglucosamine (NAG) and N-acetylmuramic acid (NAM), cross-linked by a pentapeptide made up of D and L forms of amino acids. Based on the type of cell wall components, bacterial strains have been classified into Gram-positive and Gram-negative. The presence of an additional outer layer of lipopolysaccharide in Gram-negative bacteria differentiates them from Gram-positive bacteria.[12] The outer membrane restricts the entry of small drug molecules, and hence the presence of the outer membrane in Gram-negative bacteria provides resistance to some antibiotics or needs a higher dose of the drug to treat the infection. There are teichoic acids in the Gram-positive bacterial cell wall but not in the Gram-negative bacterial cell wall, and lipopolysaccharide and lipid concentrations in the Gram-positive cell wall are lower than in the Gram-negative cell wall.[13] A drug molecule that can inhibit bacterial cell wall synthesis provides selective bactericidal activity, and this is the mechanism opted for by the first natural antibiotic, penicillin.[14-16] Penicillin inhibits cell wall formation by inhibiting the transpeptidation reaction. Examples of cell wall synthesis inhibiting drug molecules are β-lactam derivatives, fosfomycin, glycopeptides, moenomycin, mannopeptimycin, lantibiotics, defensin, bacitracin, and others. [17]

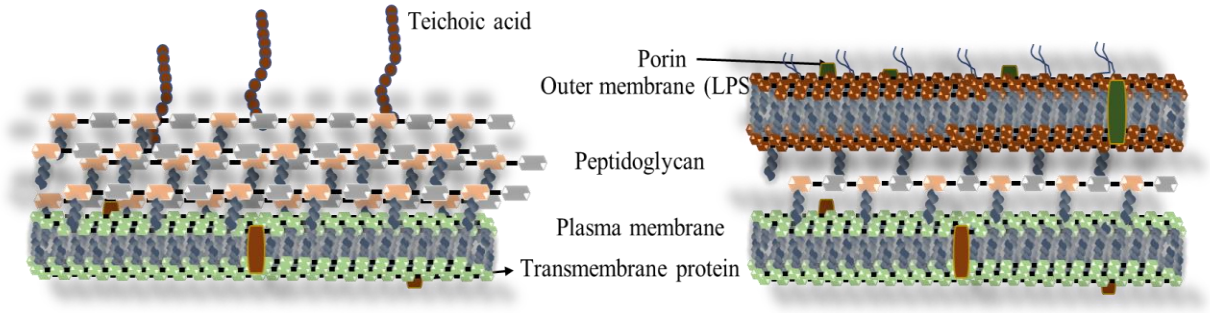

Figure 2– Animation diagram showing differences in Gram-negative and Gram-positive cell wall architecture

1.2.2 Inhibition of protein synthesis

Protein translation in bacterial cells is different from that in eukaryotic cells with regard to the ribosomal subunit and its progression. Protein synthesis inhibitor molecule interferes either with tRNA by mimicking its amino acid form or with the ribosomal assembly process.[18-20] Antibiotics following this mechanism are known to provide bacteriostatic activity. Antibiotics such as tetracycline, erythromycin, fusidic acid, lincomycin, erythromycin, and others act as inhibitors of bacterial protein synthesis. [21]

1.2.3 Interfering of genetic material synthesis

Interference in the replication and transcription processes of bacterial cell metabolism by an antibacterial molecule is one of the successful strategies to combat microbial infection.[22] These drug molecules inhibit bacterial growth by impeding the RNA transcription or protein translation pathways. DNA replication is indirectly inhibited by targeting the DNA gyrases.[23-25] Rifamycin, sorangicin, streptolydigin, safinamide, tagititoxin, squaramides, and others are some of the examples that interrupt the genetic material synthesis.

1.2.4 Inhibition of bacterial cell metabolism

Antibacterial agents targeting the metabolic system of the bacterium generally target the amino acid and nucleic acid synthetic pathways. The bacterial metabolic system can synthesize all the common 20 amino acids, and *Homo sapiens* can synthesize only 11 amino acids. Hence, nine amino acid synthetic processes are unique in bacterial metabolism, and these pathways can be targeted by antibiotics to kill the bacterium selectively. A coenzyme, namely tetrahydro-folic acid (TH4) is a key enzyme that plays a pivotal role in amino acid

and nucleic acid synthesis in bacteria. Sulfonamides, trimethoprim, Isonicotinic acid hydrazide, are some of the known exmpales of bacterial cell metabolic inhibitors and are used to treat the bacterial infections.

1.2.5 Leakage of cell contents by damaging the bacterial membrane

The bacterial cell membrane is an impressive and effective target for an antimicrobial compound. It provides bactericidal activity, while the membrane-oriented activity of the drug molecule allows the bacterial cells to develop resistance. This is possible for several reasons, including: (1) membrane-oriented drug molecules act as chemosensitizers, which can potentiate the activity of other antibiotics, (2) membrane is a target that is preserved in all growth forms of bacterial strains and growth stages (3) multiple modes of action (4) shows activity against dormant or metabolically inactive and biofilm forms of bacteria ~~also~~ and (5) suitable pharmacokinetics regarding nonspecific binding to human serum proteins, and high tissue penetration.[26] These drugs show selectivity based on the differences in surface potential and bacterial membrane lipid profile against mammalian membrane components.[27] Membrane composition of the Gram-negative and Gram-positive bacterial strains renders more negative charge onto the membrane.[28] Membrane damaging antibacterial compounds include amphiphilic compounds such as daptomycin, amphotericin B, polymyxin B, and others. [29, 30]

1.3 Drug resistance

Antibiotic resistance is a case where the bacterial metabolic system develops the mechanism to counteract the mechanism of action of antibiotics, which they use against them. In this scenario, a higher dose of the drug is required to treat the infections, or the disease becomes dreadful to treat, increasing the mortality and morbidity rates. The majority of antimicrobial drugs that were discovered in the 19th century are facing the challenge of drug resistance in a plethora of bacterial strains. The aftermath of drug resistance is that the drug market is running with a shortage of potent antimicrobial compounds when so many are available. Drug resistance has increased the mortality rate at a critical rate which demands more emphasis on drug resistance mechanisms and methods to combat this problem. Drug-resistant infections are causing about 7 lakh lethality each year globally, according to an estimate, which reflects the severity of the problem. The World Health Organization (WHO) has listed the ten most alarming bacteria families,

further divided into critical, high, and medium categories. [25] Most dangerous bacterial strains are of *Pseudomonas aeruginosa (P. aeruginosa)*, *Enterobacteriaceae*, and *Acinetobacter baumannii,* and these Gram-negative bacteria reside in the gut and cause pneumonia and blood infection. The second most life-threatening infectious bacteria are Methicillin-resistant *Staphylococcus aureus* (MRSA) *and Enterococcus faecium*.

1.3.1. Types of drug resistance

Antibiotic drug resistance can be classified in to intrinsic, acquired, and adaptive.

1.3.1.1 Intrinsic resistance

Intrinsic resistance is the resistance exhibited due to the inherent properties of the bacterium. Examples of intrinsic resistance include the glycopeptide resistance exhibited by Gram-negative bacteria due to the limited permeability of the outer membrane present in the Gram-negative bacterial cell envelope.[31]

1.3.1.2 Acquired resistance

Acquired resistance is the resistance exhibited when a previously sensitive bacterium acquires a resistance strategy by either mutating its genomic material or acquiring new genetic material from an external source by horizontal gene transfer. Horizontal gene transfer can occur through three main mechanisms- transformation, transduction, and conjugation.[31]

1.3.1.3 Adaptive resistance

Adaptive resistance is defined as the resistance to one or more antibiotics induced by a specific environmental condition (e.g., stress, growth state, pH, concentrations of ions, nutrient conditions, and sub-inhibitory levels of antibiotics). In contrast to intrinsic and acquired resistance, adaptive resistance is transient. Adaptive resistance allows bacteria to respond more rapidly to antibiotic challenges and generally reverts once the inducing signal is removed. Drug resistance starts with a gene mutation or gene transfer from a drug-resistant to a drug-sensitive strain of bacteria, which follows a number of mechanisms to thwart the effect of the drug. This mechanism includes enzyme inactivation and modification, modification of the target sites, reduced antibiotic accumulation efflux, and reduced permeability.

1.3.2 Drug resistance mechanism

The molecular mechanism of their resistance should be explored to tackle the antibacterial drug resistance by infectious agents. Henceforth following are a few identified important drug resistance mechanisms and their impact.

1.3.2.1. Antibiotics inactivation

β-Lactamases are the best example of antibiotic resistance mediated by the inactivation of the antibiotic molecule. More than 7,000 β-lactamases have been recorded up to date produced by diverse bacteria and are considered to be the most common resistance mechanism leading to β-lactam resistance among Gram-negative bacteria. The resistance mechanism occurs because of β-Lactamase enzymes, which destroy and inactivate β-Lactam antibiotics such as penicillin. These enzymes destroy the amide bond of the β-lactam ring, essentially rendering the antimicrobial activity of the drug ineffective.[32-34]

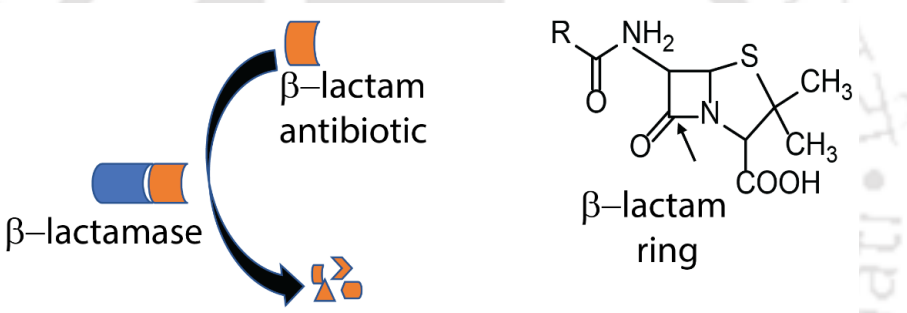

Figure 1.3. Schematic of β-lactamase enzyme degrading penicillin, which contains β-lactam ring (an example of bacterial enzyme directed inactivation of antibiotic)

Another type of resistance in the β-lactam class is carbapenem resistance which occurs in some Gram-negative bacterial strains due to enzyme-mediated degradation. Carbapenem antibiotics are a class of drugs considered the last resort antibiotics to treat the infection. Carbapenem-resistant bacterial strains are generally pan-drug-resistant. This type of resistance is also of great concern because it spreads in other bacterial strains due to gene transfer by a horizontal gene transfer mechanism. [35]

1.3.2.2. Antibiotic modification

Enzymatic modification of antibiotics is also a common mechanism of drug resistance, where aminoglycoside antibiotics are enzymatically modified either by adenylation, acetylation, or phosphorylation.[36] Enzymatic acetylation has been reported in

chloramphenicol and phosphorylation in kanamycin A antibiotics.[37] An epitome of this is erythromycin ribosomal methylation, which occurs due to the erm gene that delivers resistance against macrolide antibiotics such as erythromycin. The translated enzyme from this gene causes the partial methylation of the ribosome, which is targeted by erythromycin. Due to methylation, ribosomes cannot bind erythromycin, denoting that bacterial growth becomes ineffective even in antibiotics. Another good example is the phosphorylation of kanamycin by a kinase enzyme because this drug can no longer hinder the activity of ribosomes.[38]

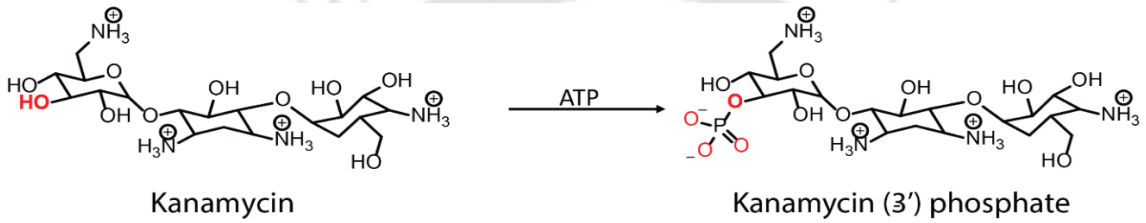

Figure 1.4. Enzymatic phosphorylation of Kanamycin A

1.3.2.3. Decreased permeability of the bacterial outer membrane

Some Gram-negative bacteria are resistant to the drug because of their outer membrane architecture, which has very little permeability. The bacterial outer membrane contains porins that allow small hydrophilic molecules to enter and also provide an entry site for water-soluble antibiotics (tetracycline, chloramphenicol, β-lactams). A mutation in the gene coding porin may cause reduced permeability or loss of porin from the outer membrane.[38-40]

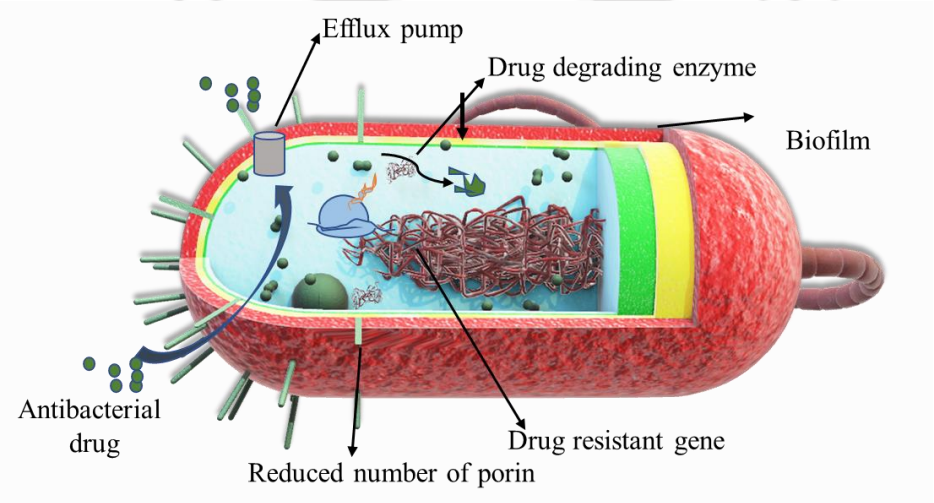

Figure 1.5 Diagram showing the drug resistance strategy adopted by bacterial cells

1.3.2.4. Efflux pumps

Efflux pumps are energy-dependent complex bacterial systems present in the cytoplasmic membrane and can efflux toxic molecules out of the cell. The first efflux pump expelling tetracycline out of the bacterial cell was described in *Escherichia coli* (*E. coli)* in 1980. Since then, numerous efflux systems involved in antibiotic resistance have been identified in Gram-positive and Gram-negative bacterial strains.[41] Most efflux systems have a broad range of substrates and hence can transport multiple unrelated substances or drug molecules, resulting in multi-drug resistance.[39]

1.3.2.5. Biofilm formation

One of the mechanisms of resistance used by bacteria is biofilm formation, which is also a mechanism of virulence. Studies have been done to analyse the possible relationship between antimicrobial resistance and biofilm formation among Gram-negative and Gram-positive bacterial species isolates.[42] Several relationships were found between the ability to form biofilm and antimicrobial resistance. Indeed, gentamicin and ceftazidime resistance were related to biofilm formation in *E. coli*, piperacillin/tazobactam, colistin in *K. pneumoniae*, and ciprofloxacin in *P. aeruginosa*. The biofilm-related resistance has been reported most commonly in case of periodontal disease. Cystic fibrosis (CF) patients also suffer from the robust biofilm-forming bacteria *P. aeruginosa* and *S. aureus*.[43]

1.4. Strategy and proposed criteria to address drug resistance

To protect a drug from being ineffective against the drug-resistant bacterium or to combat resistance-related infections, a few criteria should be followed, which include (1) appropriate therapeutic use of antibiotics in human and veterinary (2) prevention of drug-resistant infections, (3) More emphasis on the development of new drugs. Moreover, societal changes should occur to prevent drug resistance not only in the medical field but at a global level. At the research level, there are several criteria in process to combat the drug resistance. These are development of new drugs with different targets, design of drug carriers and membrane targeted drugs and others.

1.4.1. Developing new drugs

The increased number of resistant bacterial strains demands the development of new drugs in parallel. After carefully studying resistance mechanisms, new drug formulas are being designed. Some biologically studied molecules that can counteract the resistance are quorum-sensing inhibitors, bacteriophages, biosurfactants or amphiphiles, and enzyme-substrate analogs.[44] An increasing number of studies have been focused on advancing synthetic compounds that could supersede the development of antimicrobial resistance by microbes. In this regard, the first priority has been synthesizing molecules that destabilizes and disrupts the membrane integrity of the Gram-negative and Gram-positive bacteria.[26] Pethe and co-workers presented a paper about the antimicrobial activity of glycosylated cationic poly(β-peptide), PAS8-*b*-PDM12. These compounds have the property to reverse the antimicrobial resistance by disrupting the bacterial outer membrane, which further enhances the drug uptake activity. The cationic polymer does not perturb the mammalian cell membrane, which is simply because of the differences in the membrane composition of the prokaryotic and eukaryotic cell. PAS8-*b*-PDM12 destabilizes the membrane at a very low concentration, that was visualized by cryo- transmission electron microscopy. A combination treatment was examined with the antibiotic rifampicin and PAS8-*b*-PDM12, which resulted in a synergistic effect.[45, 46] Combinations of membrane directed amphiphiles and known antibiotics are of good approach because the membrane disruption can allow the entry of antibiotics and help to exhibit synergistic activity. Antimicrobial polymers and amphiphiles have also been tested in this aspect to counteract the resistance mechanism. These polymers or amphiphiles show inherent antimicrobial activity and augment the activity of antibiotics if combined with it.[47, 48] Imidazole, benzimidazole, benzalkonium salt, guanidine derivatives, and others have also proven to be successful antimicrobial drugs.[49-51] Mi Zhau and co-workers have reported the membrane active hydantoin based molecule, dimeric lysine *N*-alkyl amide derivatives, and these were effective against MRSA, vancomycin-resistant *Enterococcus* strain of bacteria.[52]

1.4.2. Reactive oxygen species (ROS) generating molecules

The ROS-generating molecules are another very interesting alternative approach against drug resistance that does not deal with resistance mechanisms but kills the bacteria. Till now, no resistance mechanism has been reported against ROS-generated antimicrobial activity in bacterial strains. ROS is a collective term for all the highly reactive oxygen species, including superoxide radical ($^{\cdot}O_2^-$), hydroxyl radical ($HO^{\cdot}$), singlet oxygen ($^1O_2$),

and hydrogen peroxide (H_2O_2). Generally, the biological system generates these free radicals during metabolism that are neutralized by the redox system of the cell. So far, there have been many interesting reports on the use of ROS to kill microbes. Photodynamic therapy is a very good and successful remedy that has been established and cast off at the industrial level for sterilization. [53-56]

1.4.3. Antimicrobial peptides

Antimicrobial peptides, 12 to 50 amino acids in length, are potent (at micromolar concentrations), broad-spectrum antibiotics, and function as an integral component of the innate immune system.[57] The mechanism of AMPs includes cell membrane damage, inhibition of cell wall synthesis formation of pores, disruption of the membrane bilayer, and inhibition of nucleic acid and protein synthesis.[58-61] Currently approved Antimicrobial peptides by the FDA include bacitracin, colistin, and polymyxin B.[62]

1.4.4. Combination therapy

In the face of rising concerns over the development of antibiotic resistance, sole drug clinical treatment approaches may not be suitable to combat the issues. Based on the scientific literature and clinically proven recommendations and treatments, combination approaches are more effective in combating multi-drug resistance.[63]

- Studies have shown that few cationic polypeptide compounds increase the effectivity of the existing antibiotics against antibiotic-resistant Gram-negative bacteria. These compounds, when given in combination with antibiotics, enhance the permeability of the antibiotic. *S. aureus* shows drug resistance because of its drug efflux activity.
- Dual-drug delivery approaches that combine antibiotics targeting different pathways are the most studied and successful approaches to combat antibiotic resistance. Antibiotic combinations such as a combination of roxithromycin/doxycycline have proven much more effective against MRSA strains when compared to two antibiotics separately.[64]
- Using a combination therapy capable of delivering a bactericidal antibiotic while concurrently inhibiting the mechanism of resistance is a very effective strategy to overcome certain resistance mechanisms. This approach is particularly useful in cases of potential enzymatic disruption of the antibiotic, such as in the case of augmentin, which pairs a β-lactam antibiotic (amoxicillin) with a β-lactamase inhibitor (e.g., clavulanic acid). Another very good example is celecoxib, a nonsteroidal anti-

inflammatory drug (NSAID) that inhibits the MDR1 efflux pump and enhances the sensitivity of *S. aureus* to a variety of antibiotics, including ampicillin, kanamycin, chloramphenicol, and ciprofloxacin.[63]

1.4.5. Local and stimuli-responsive antibiotic delivery

Systemic antibiotic administration has traditionally been the foundation of clinical therapies to address the ever-present infectious attack. In case of the patients going through a plethora of medical procedures systemic administration is often not effective, as it does not provide local tissue concentrations sufficient to kill bacteria prior to incurring serious side effects, such as renal and liver damage.[65] Local delivery of current antibiotics and other antimicrobial biologics (e.g., AMPs, anti-quorum sensors, bacteriophage, and others) may preserve and extend their efficacy in the evolutionary race between antimicrobial development and bacterial resistance. Vancomycin, tobramycin, amoxicillin, gentamicin, cefamandole, cephalothin, and carbenicillin have all been incorporated into commercially available local release systems. The duration and level of sustained release are dependent on the host tissue matrix, the type and mechanism of the antibiotic, and the clinically established critical postoperative period. Unfortunately, several local antibiotic drug delivery vehicles suffer from premature burst release with subsequent sub-therapeutic activity, inadvertently evoking bacterial antibiotic resistance. Nanoparticles and liposomes are currently used for controlled drug delivery systems and provide an advantage over traditional systemic delivery systems.[66] Many of these advantages are thought to stem from the membrane-like structure that allows them to fuse with the cellular membrane and deliver a drug payload directly to the cytoplasmic compartment[21]. There have been a few important studies on antimicrobial liposome vesicles, which can be used in chemotherapy as a dual approach to deliver the drug. Along with the drug carrying capability they can act as an antimicrobial agent to combat the hindrance in therapy caused by bacterial superbugs.[67, 68] There have been few efforts given in the field of stimuli-responsive antibiotic drug delivery such as magnate, ultrasound, pH, redox responsive, enzymatic, and others.

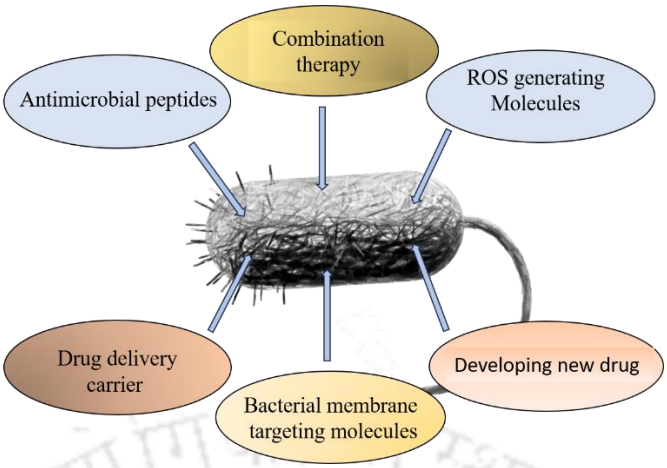

Figure 1.6 Diagram to show the strategy to combat drug resistance

1.4.6. Bacterial membrane targeting molecules

As mentioned in the section mentioned above, antibacterial drug molecules with membrane-oriented activity have an important role in antibacterial activity and comparatively better counteract the bacterial resistance system. Membrane active molecules can iron out the resistance caused by efflux transporters, enzyme inhibitors, and the low permeability of the drug into the cell. Membrane-disrupting molecules should have a cationic group that can convey membrane-oriented activity because the peptidoglycan present in Gram-negative and teichoic acid in GP bacterium is negatively charged. Cationic-charged molecules can selectively attach to the bacterial cell membrane over mammalian cells. The molecular basis of this difference is the asymmetric nature of the outer membrane leaflet in which neutral-charged lipid molecules consist of phosphatidylethanolamine, phosphatidylcholine, and sphingomyelin while the inner membrane surface contains negative phosphatidylserine. Contrary to this, the Bacterial cell membrane contains phosphatidylglycerol or cardiolipin and phosphatidylserine, making the surface more negative.[38] Hydrophobicity and negative charge in the bacterial cell wall and membrane offer the idea to hypothesize the plausible drug design to interact with the cell membrane. In this area, Zhiliang and co-workers studied the polymyxin synthesis and structural activity aspects with respect to its antibacterial efficacy. They discovered the structural importance of amphiphilic molecules as- polymyxin contains cyclic heptapeptide with a tripeptide side chain acylated by a fatty side chain on the amino group. But their use is limited because of the serious side effects of the neurotoxic nature of the parent compound.[69] To avoid toxicity now, various polymyxin derivatives have been

synthesized.[70] Electrostatic interaction stabilizes the molecule on the cell membrane, and an acylated long hydrophobic chain helps the drug enter the cell and disrupts the osmotic balance.[71, 72] Alteration of the membrane potential of bacterial membranes is responsible for increasing the collateral sensitivity of antibiotic-resistant microbes. Collateral sensitivity refers to mutations that cause multi-drug resistance in bacteria which can simultaneously enhance sensitivity to many other unrelated drugs.[73] Regarding aminoglycoside antibiotics, their cellular uptake demands an active proton motive force. [32, 74, 75]

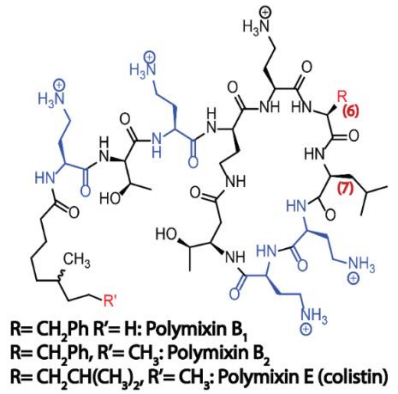

Figure 1.7 Chemical structures of lipopeptide polymyxin and its derivatives

1.4.6.1. Cationic amphiphilic molecule as suitable antimicrobial drugs

Cationic amphiphilic molecules are of great interest in targeting the bacterial cell membrane. Alisha and co-workers designed different cationic amphiphiles (CAM) classes to target and compromise the structural integrity of bacteria membranes, leading to cell rupture and death. The impact of cationic conformational flexibility, hydrophobic domain flexibility, and hydrophobic domain architecture were evaluated.

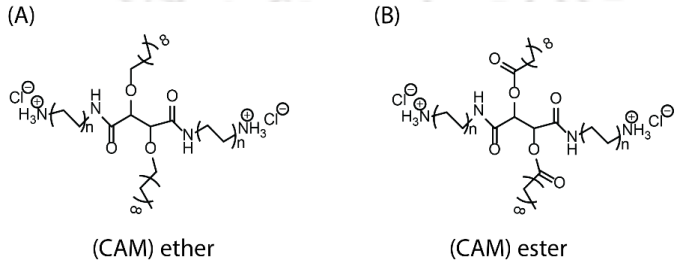

Figure 1.8 Cationic antimicrobial amphiphiles.

The membrane activity of the CAM was evaluated to assess the impact of selected chemical features, namely, flexibility and hydrophobic architecture, on antimicrobial

efficacy and selectivity. They observed that the branched hydrophobic architecture had the most detrimental effect on the Gram-negative bacteria. [76]

Aiyagari Ramesh and co-workers synthesized the amphiphile molecule with planar fluorogenic pyrin, a pyridine head group, and a long hydrocarbon chain. They also synthesized another variable of the same molecule with reduced hydrocarbon chain length to show the effect of a long hydrocarbon chain and hypothesized that a long hydrocarbon chain length is essential for an amphiphile to insert into the bacterial cell membrane. The positive charge of pyridinium helps in electrostatic interaction and planer pyrin molecule stacks in DNA nitrogenous bases.[77]

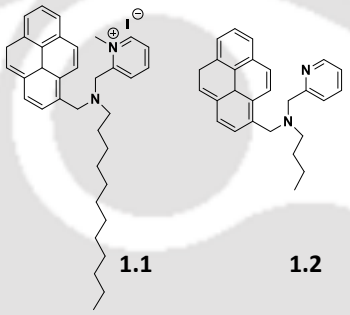

Figure 1.9 Synthesised amphiphile molecule with variable chain length.

1.4.6.2. Antimicrobial lipophilic molecules as a drug and carrier of drug

During and post-golden era of antibiotics, numerous hydrophobic and phenolic compounds were extracted and characterized by its property and applications. Many of these molecules were found to be studded with antimicrobial and antifungal properties. This led to a search for antimicrobial properties in other natural lipophilic molecules.[78] Few lipophilic molecules are already present in mammalian cell membranes fulfilling multiple roles as a signalling molecule, hormone, and as part of the immune system. Cholic acid bile salts, sphingosine, etc. are such natural antimicrobial lipophilic molecules, and their derivatives are profoundly used as antibiotics such as Squalamine and ceragenin (figure 1.10).[79-81]

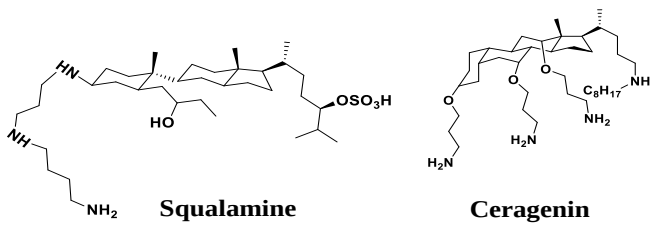

Figure 1.10 Lipophilic antibiotics.

Sphingosine's antimicrobial activity has been reported in skin and respiratory epithelial cells, and its deficiency causes serious infection in these cells. Grace E. M. and co-workers demonstrated the role of sphingosine as an antimicrobial agent.[82] Kauss, and co-workers synthesized some lipid oligonucleotides with variable nucleotide head groups and long hydrophobic chains in order to facilitate its entry into the cell.[83] This lipid oligo nucleotide had some inherent antimicrobial activity, and it was used to encapsulate the commercial antibiotic cephalosporin derivatives. Vesicles encapsulated with antibiotics have a plethora of paybacks, including (1) enhanced activity of the antibiotic in a synergistic manner, (2) leads to local delivery of drug to avoid the side effects and concentrate the drug at the infection site of tissue (3) can be used in nebulizer to treat chronic respiratory infection as in cystic fibrosis patients.[83] Use of inhaled liposomal antimicrobial treatment in lung Infections results in targeting of the antimicrobial agent at the site of infection to the infectious organism, increasing intracellular antibiotic concentrations, reducing drug toxicity, and improving tolerability.[84] In this series Angelique and co-workers synthesized antimicrobial lipophilic *N*-heterocyclic carbene silver complexes for aerosolization (figure 1.11). They tested their antibacterial activity against *P. aeruginosa* and *S. aureus,* which are frequent residents of respiratory in patients with lung disease and cystic fibrosis.[85]

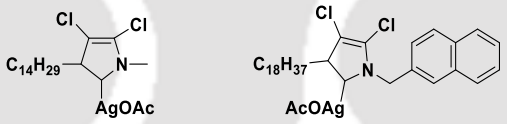

1.3 **1.4**

Figure 1.11 Structures of the antimicrobial *N*-heterocyclic carbenes with different chain length.

The most important liposomal antimicrobial drugs for inhalation include amikacin, tobramycin, ciprofloxacin, and amphotericin B.[86, 87] New avenues of research in the delivery of lung-targeted liposomal antimicrobials alone or in association with other treatment alternatives are being investigated. The antimicrobial aerosol particles must dissolve in the epithelial lining fluid and mucus. Secondly, the need for antibiotic diffusion toward the bacteria depends on the site since, in the case of cystic fibrosis with *Pseudomonas aeruginosa* chronic infections, the location is most likely intraluminal within the mucus. An important benefit of an inhaled liposome formulation is to cross the mucous barrier to reach the epithelial cell of the respiratory system and provides a slow release of

the antibiotic, which reduces the dosing frequency and continuously maintains high drug concentrations in the lung above the MIC. Lipophilic molecules with average hydrocarbon chain length have the tendency to form vesicles in aqueous environment. These vesicular structures have been used to encapsulate the drugs and transport them to the destined site. Active targeting could be accomplished by coupling targeted ligands to the surface of liposomes, such as proteins, peptides, carbohydrates, or monoclonal antibodies or their fragments. Liposomes intended to incorporate drug molecules or antigens can be designed with specific signal transduction-inducing molecules that can activate the adaptive immune response. Hence lipid oriented innate and adaptive immune response of the host gives a glimpse of therapeutic or prophylactic opportunities to design amphiphilic or lipophilic molecules to combat drug-resistant and chronic infections. For instance, liposomes are formulated during vaccine preparation by encapsulating with lipids, nucleic acid, peptides or proteins as an antigen to provide adjuvant properties. These can help to modulate the inflammation in the responsive microenvironment of T lymphocyte priming. Currently, few liposomes are under clinical trials, which can be used as an adjuvant in future medical practices to fight deadly infectious diseases like malaria, tuberculosis, and others. Antimicrobial lipophilic molecules have few benefits over antimicrobial peptides, and one of them is that they are resistant to bacterial proteases and also difficult to modify by bacterial enzymes. Additionally, they can easily cross hydrophobic cell membranes. In recent years few researchers have modified the existing antibiotics by conjugating the hydrophobic fatty acid side chains to add on antimicrobial activity against drug-resistant bacterial strains. In this series, Jayanta Haldar and co-workers modified the vancomycin with a long hydrocarbon chain containing a quaternary ammonium group.[88] These modified glycopeptides revealed a broad spectrum of activity against both Gram-negative and Gram-positive activity and had additional mechanisms of cell division inhibition earlier unidentified for antimicrobial glycopeptides. These findings suggest that cationic amphiphilic molecules have a bright future in the designing of suitable antimicrobial compounds to combat drug resistance and rejuvenate the activity of clinically approved antibiotics. Very few liposomes with inherent antimicrobial activity are known to date, but they are also the flag bearer components to synergistically fight the drug resistance, reducing the multiple drug dosing and to render the synergistic activity after the encapsulation of the antibiotics.

1.4.6.3 Sulfonium amphiphile as an antimicrobial agent

Among the compounds with membrane-directed activity, sulfonium-based compounds have gained special attention over other analogues. There is a plethora of research confirming the antibacterial activity of sulfonium compounds. Kanazawa and co-workers in 1993 prepared poly(p-vinylbenzyl tetramethylenesulfonium tetrafluoroborate)s with capricious molecular weights. The authors observed that polymeric sulfonium salts exhibited high antibacterial activity against Gram-positive bacteria. Activity against *S. aureus* was presented with MIC of 3.4 μM, and to kill the bacteria required 34 μM or more within the time duration of 30- or 60-min. Activity against Gram-negative bacteria was much smaller. A decent antibacterial effect was also presented for the sulfonium *N*-chloramines, which were chemically synthesized. The action of sulfonium *N*-chloramine in a concentration 20 μg/mL during 10 min showed 100% reduction of *S. aureus* and *E. coli.*[89] However, some sulfonium compound work in higher concentrations and examples are S-methylsulfonium and S-oxo-S-methylsulfonium salts. Their MICs are 25-100 μg/mL for *S. aureus* and *P. aeruginosa*, 50-100 μg/mL for *E. coli*, 100 μg/mL for *Proteus vulgaris* and 25-50 μg/mL for *Candida albicans*. Moreover, the authors presented moderate antiphage activity of these salts.[90] Hirayama and co-workers worked on a sulfonium compound and compared its antimicrobial activity with some ammonium compounds like benzalkonium chloride and found that the sulfonium compounds were less toxic to human cell lines and more effective on bacterial cells.[91] R. G Carden and co-workers studied the antimicrobial activity of tetrahydrthiophene-based amphiphiles and revealed that sulfonium amphiphiles had similar or higher antimicrobial activity than its quaternary ammonium analog against drug-sensitive and resistant bacterial strain.[92]

This could be due to the mammalian metabolic system being well adopted for sulfonium molecules (as it has S-adenosyl methionine) and least adopted with quaternary ammonium compounds; additionally, sulfonium compounds possess less cationic charge density compared to its ammonium analogue. In recent years sulfonium amphiphiles have been synthesized and explored for their antimicrobial activity. Moreover, sulfonium analogues have also been used to enhance the activity of existing antibiotics; for instance, conjugation of a small sulfonium molecule to the vancomycin rejuvenated its activity against drug-resistant bacterial strains under in-vitro and in-vivo conditions. Conjugation of small sulfonium molecule with vancomycin rendered its enhanced activity against some gram-negative bacterial strains, too, and it provided the cationic nature to the vancomycin causing

better interaction with the negatively charged cell surface and membrane disrupting bactericidal activity. Another research group conjugated similar sulfonium molecules to the norvancomycin, which is the methylated vancomycin. They observed an increment of 4-to-2048-fold antibacterial activity against drug-resistant bacterial strains. By conjugating various lipo-sulfonium moieties to the vancomycin antibiotic, they studied the structure-activity relationship.[93] Overall, these sulfonium-based modifications of glycopeptide antibiotics gave an idea to rejuvenate the antibiotic activity to combat the resistance by using the existing antibiotics. The amphiphilicity in sulfonium molecules needs to be optimized akin to other hydrophobic antimicrobial peptides for selective antimicrobial activity and compatibility towards host cell lines and blood cells. Sulfonium amphiphiles, being cationic in nature, renders membrane-oriented antimicrobial activity and hence can facilitate the entry of other antibiotics with their targets in the cytosolic region. Jing Sun and co-workers reported about the antimicrobial polymers containing sulfonium molecules, which were more stable and presented better processibility than the small molecules. They prepared chlorepoxypropane-modified polysulfonium with tuned amphiphilicity to render high selectivity against Gram-positive and Gram-negative bacterial strains than erythrocytes cells (figure 1.12). These polymers were efficient enough to eradicate the robust bacterial biofilm. Its bactericidal activity was impervious for up to 25 days, suggesting its ability to counteract the resistance mechanism of the bacterial cells. Polysulfonium compound also exhibited antimicrobial activity under in-vivo conditions on infected mouse skin.[94] Anzar Khan and co-workers investigated the antimicrobial activity analysis of poly(β-hydroxy sulfonium) compounds with long hydrocarbon chains and found that it had similar antimicrobial activity as vancomycin and kanamycin against *E. coli* and *S. aureus* selective compatibility against mammalian cell lines. This compound was also effective in terminating tuberculosis infection caused by mycobacterium. The mechanistic study revealed that the compound had obvious membrane-disrupting bactericidal activity.[95] Jingyi Rao and co-workers reported the sulfonium-containing homopolymers **PS$^+$** (figure 1.12) and sulfonium-containing gel with broad spectrum activity against drug-sensitive and drug-resistant bacterial strains. They developed a group of sulfonium-containing compounds with altered monomeric precursors in an effort to vary the hydrophobicity, which rendered the antimicrobial activity with MIC value ranging from 1.25 -10 µg/mL against clinical microbes. In a different study, they prepared sulfonium-based gel (**TEE-S$^+$** and **ETT-S$^+$**) with good antimicrobial activity, but its toxicity towards

mammalian cell lines limited its further study.[96] In a recent study, they developed similar sulfonium compounds by varying the hydrophobicity and charge densities by controlled methylation of the polythioether compound. At sub-inhibitory concentration, the sulfonium compound represented synergistic antibacterial and antibiofilm activity with rifampicin against Gram-negative bacterial strains under in-vitro conditions.[97] Laconically, the sulfonium molecules primmed with lipophilicity can be the rising tool to combat the antibacterial drug resistance by its membrane-oriented bactericidal activity and by tunning its charge density and hydrophilicity its specificity towards bacterial cells can be defined. Additionally, biocompatible biopolymers can also be used to stabilise the small sulfonium and other antibacterial compounds to fight the resistance and for better biocompatibility.

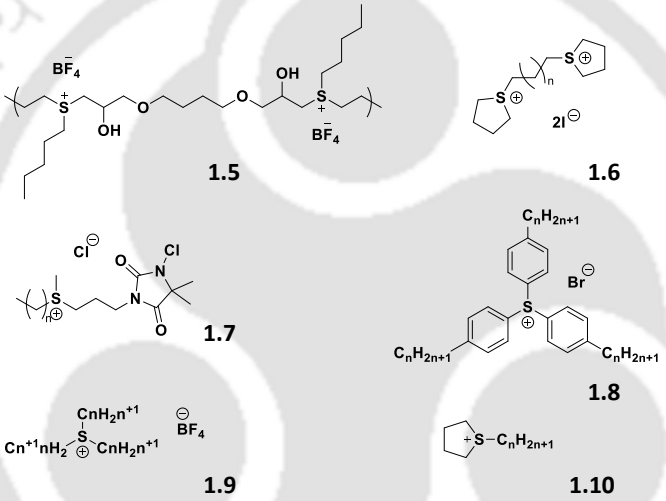

Figure 1.12 Few examples of sulfonium-based antimicrobial compound

1.4.6.4. Antimicrobial biopolymer

While the aforementioned section summarises the efficient antimicrobial activity of amphiphiles and sulfonium, it was observed that polymers play an important role in stabilizing these sulfonium molecules. Hence developing a polymer with sulfonium conjugate or stabilizing them onto biocompatible polymeric materials seems to be a good option to prepare highly selective antimicrobial material with better biocompatibility while harbouring the specific features of the biopolymers. These biologically active polymers fill a critical niche in the development of new biocompatible, active medical devices. Such antimicrobial devices may effectively ease the burden on systemic antibiotics, essentially promoting antibiotic stewardship, prolonging the life of conventional antibiotic therapies,

and curbing the evolution of antibiotic-resistant microbes. Integrating an antibiotic agent into a polymer matrix minimizes antibiotic toxicity, increases antibiotic stability, and improves antibiotic half-life and efficacy. Biopolymers such as albumin, hyaluronic acid (HA), chitosan, chitin, guar gum, and some essential oil extracted from medicinal plants have been a great source of antimicrobial agents and have been modified to have enhanced antimicrobial efficacy.[98, 99] The benefit of using these biopolymers is that they are rich in functional groups and hence can be modified for better tuning in their antimicrobial activity and host cell cytocompatibility. Modifying these polymers is cost-effective and eco-friendly, establishing a new archetype of ecological conservation. In this series, albumin biopolymer has been modified by a few research groups to render it bacterial membrane damaging effect, which leads to the bactericidal fate; for instance, Chia-Yu Tsai, and co-workers conjugated the albumin from different sources by its mannosylation and verified its antimicrobial activity against Gram-negative and Gram-positive bacterial strains.[100, 101] Albumin has been exploited to cross-link with Tetrakis (hydroxymethyl) phosphonium sulfate to get hydrogel with self-healing and antimicrobial properties.[102] Albumin has an inherent property to interact with small molecules and drugs, and this property can be harvested to make it a drug transporter as well as by its modification, antimicrobial activity can be immured in it. Another interesting biopolymer is HA which has been utilized in clinical settings and cosmetics for its wound healing and hygroscopic properties. HA is a ligand for CD44, which after the interaction, promotes the epithelial cell migration followed by an accelerated wound healing process. Hyaluronic acid has been chemically modified extensively by targeting its functional groups: carboxylic, glucuronic, *N*-acetyl, and hydroxyl groups. Out of this, carboxylic acid has been modified extensively by cross-linking with other small molecules by esterification, etherification, bis-epoxide cross-linking, and others. [103]

1.5 Summary

The information mentioned above summarises the development of antibiotic resistance in bacterial strains and discusses important strategies to combat this problem. It has been observed that a simple and smart bacterial genetic system has always been evolving, which is how it has acquired the resistance mechanism. Hence it can be predicted that current and future genera need to develop an advanced strategy to cope up the pathogenicity of these superbugs. Out of the various mechanism opted by antibacterial drugs, membrane-

disrupting activity makes it more efficient to fight the drug resistance mechanism of the pathogens. It has been well established that amphiphilicity and cationic charge density of the molecules have a prominent role in revealing membrane-directed antibacterial activity or adding these properties to the existing clinically proven antibiotics rejuvenating its activity. Different structural moieties have been utilized to synthesize bactericidal antimicrobial compounds, including benzalkonium, guanidinium, pyridinium, sulfonium, ammonium, and others. Hereby, we have discussed the importance of sulfonium molecules in antimicrobial activity and their role; in rejuvenating the activity of last-resort antibiotics such as vancomycin. Sulfonium molecules with membrane-directed activity can be the next-generation antibacterial agent to combat the drug-resistant bacterial superbug. Biocompatibility of these cationic molecules remains a challenge to design membrane-disrupting antibacterial agents and to address this problem, biopolymers played a ground-changing role. These biopolymers can be conjugated with cationic and amphiphilic molecules to assess the antimicrobial activity and harbour the specific features of these polymers.

As per our aforementioned literature study in the presented thesis we have designed the different group of sulfonium containing drug carriers with inherent antibacterial activity. We have developed series of sulfonium containing liposomes with variable head group and hydrocarbon chain length. It showed that the sulfonium containing liposome with pyridinium and head group was potent antibacterial activity and also a long hydrocarbon chain length of C_{12} was helpful to exhibit the better antibacterial activity. It was surprising to note that the potent liposome had antibiotic encapsulation efficiency which presented synergistic antibacterial activity against various bacterial strains including drug sensitive and resistant one. Thought the compound presented negligible toxicity against blood cells and mammalian cell lines at MIC value but at higher concentration it had some toxicity. Hence in next chapter we explored a way to design antibacterial sulfonium compound with better biocompatibility and efficient drug encapsulation property. Towards this approach we selected a biopolymer for better biocompatibility and inherent drug carrier for better drug encapsulation efficacy. These two parameters are fulfilled by the albumin and hence we modified bovine serum albumin protein with small sulfonium molecule to render antimicrobial activity and long hydrocarbon chain in an effort to make it nano aggregate for antibiotic encapsulation. Sulfonium and long hydrocarbon chain conjugated protein

aggregates presented moderate antibacterial activity and negligible toxicity against blood cell lines and mammalian cell lines. Protein based nanoaggregate presented higher drug encapsulation efficacy and it had synergistic activity. Furthermore, to ensure the safety and applicability, this nanoaggregate was tested under in-vivo condition in mice model. Furthermore, the installation of sulfonium molecule in other biopolymer was also performed for its versatile use to combat drug resistance for topical use. In this regard sulfonium cross linker molecule was introduced in HA which plays imperative role in wound healing process. Antibacterial activity of the gel helps to combat the infection and fastens the healing process. Sulfonium containing gel was tested against drug sensitive and drug resistant bacterial strains. Various class of antibiotics were incorporated in to the gel and its antimicrobial activity have been tested to check whether it exhibits the synergistic efficacy. In-vitro results of the hydrogel invoked us to explore the similar study under in-vivo condition to ensure its safety and efficiency in animal model. The importance of in-vivo study of any biopolymer destined to be used in biomedical is to ensure its safety and efficiency in animals. This practice also increases the reliability of the drug and material for further study. After a in-vivo results we investigated its use as a band-aid by coating it on to fabric and further testing its antimicrobial examination.

1.6 References

1. Mack, A.; Choffnes, E. R.; Hamburg, M. A.; Relman, D. A., Microbial evolution and co-adaptation: a tribute to the life and scientific legacies of Joshua Lederberg: workshop summary. National Academies Press: **2009**.
2. Chaguza, C., Bacterial survival: evolve and adapt or perish. *Nat. Rev. Microbiol.* **2020,** *18* (1), 5-5.
3. Aminov, R. A brief history of the antibiotic era: lessons learned and challenges for the future. *Front Microbiol* **2010,** *1*, 134.
4. Birnbaum, J.; Kahan, F. M.; Kropp, H.; Macdonald, J., Carbapenems, a new class of beta-lactam antibiotics: discovery and development of imipenem/cilastatin. *Am. J. Med.* **1985,** *78* (6), 3-21.
5. Hutchings, M. I.; Truman, A. W.; Wilkinson, B., Antibiotics: past, present and future. *Curr. Opin. Microbiol.* **2019,** *51*, 72-80.
6. Aminov, R., The role of antibiotics and antibiotic resistance in nature. *Environ. Microbiol.* **2009,** *11* (12), 2970-2988.
7. Andrews, T.; Thompson, M.; Buckley, D. I.; Heneghan, C.; Deyo, R.; Redmond, N.; Lucas, P. J.; Blair, P. S.; Hay, A., Interventions to influence consulting and antibiotic use for acute respiratory tract infections in children: a systematic review and meta-analysis. *PLoS One* **2012,** *7* (1), e30334.
8. Ağagündüz, D.; Cocozza, E.; Cemali, Ö.; Bayazıt, A. D.; Nanì, M. F.; Cerqua, I.; Morgillo, F.; Saygılı, S. K.; Berni Canani, R.; Amero, P., Understanding the role of the gut microbiome in gastrointestinal cancer: A review. *Front. Pharmacol.* **2023,** *14*, 1130562.

9. MacGregor, R. R.; Graziani, A., Oral administration of antibiotics: a rational alternative to the parenteral route. *Clin. Infect. Dis.* **1997,** *24* (3), 457-467.
10. Ocampo, P. S.; Lázár, V.; Papp, B.; Arnoldini, M.; Abel zur Wiesch, P.; Busa-Fekete, R.; Fekete, G.; Pál, C.; Ackermann, M.; Bonhoeffer, S.; chemotherapy, Antagonism between bacteriostatic and bactericidal antibiotics is prevalent. *Int. J. Antimicrob. Agents* **2014,** *58* (8), 4573-4582.
11. Nemeth, J.; Oesch, G.; Kuster, S., Bacteriostatic versus bactericidal antibiotics for patients with serious bacterial infections: systematic review and meta-analysis. *J. Antimicrob. Chemother.* **2015,** *70* (2), 382-395.
12. de Pedro, M. A.; Cava, F., Structural constraints and dynamics of bacterial cell wall architecture. *Front Microbiol.* **2015,** *6*, 449.

13. Pasquina-Lemonche, L.; Burns, J.; Turner, R.; Kumar, S.; Tank, R.; Mullin, N.; Wilson, J.; Chakrabarti, B.; Bullough, P.; Foster, S. , The architecture of the Gram-positive bacterial cell wall. *Nature* **2020,** *582* (7811), 294-297.
14. Schneider, T.; Sahl, H., An oldie but a goodie–cell wall biosynthesis as antibiotic target pathway. *Int. J. Med. Microbiol.* **2010,** *300* (2-3), 161-169.
15. Sarkar, P.; Yarlagadda, V.; Ghosh, C.; Haldar, J., A review on cell wall synthesis inhibitors with an emphasis on glycopeptide antibiotics. *MedChemComm* **2017,** *8* (3), 516-533.
16. Elsbroek, L.; Amiteye, D.; Schreiber, S.; Herrmann, F., Molecular Imaging of Isolated Escherichia coli DH5α Peptidoglycan Sacculi Identifies the Mechanism of Action of Cell Wall-Inhibiting Antibiotics. *ACS Chem. Biol.* **2023,** *18* (4), 848-860.
17. Silver, L., Novel inhibitors of bacterial cell wall synthesis. *Curr. Opin. Microbiol.* **2003,** *6* (5), 431-438.
18. Kavčič, B.; Tkačik, G.; Bollenbach, T., Mechanisms of drug interactions between translation-inhibiting antibiotics. *Nat. Commun.* **2020,** *11* (1), 4013.
19. Scaiola, A.; Leibundgut, M.; Boehringer, D.; Caspers, P.; Bur, D.; Locher, H. H.; Rueedi, G.; Ritz, D. J. S. r., Structural basis of translation inhibition by cadazolid, a novel quinoxolidinone antibiotic. *Sci. Rep.* **2019,** *9* (1), 5634.
20. Scaiola, A.; Leibundgut, M.; Boehringer, D.; Caspers, P.; Bur, D.; Locher, H. H.; Rueedi, G.; Ritz, D., Structural basis of translation inhibition by cadazolid, a novel quinoxolidinone antibiotic. *Sci. Rep.* **2019,** *9* (1), 5634.

21. Loree, J.; Lappin, S. L., Bacteriostatic antibiotics. **2019**.
22. Baquero, F.; Levin, B., Proximate and ultimate causes of the bactericidal action of antibiotics. *Nat. Rev. Microbiol.* **2021,** *19* (2), 123-132.
23. Hangas, A.; Aasumets, K.; Kekäläinen, N. J.; Paloheinä, M.; Pohjoismäki, J. L.; Gerhold, J. M.; Goffart, S., Ciprofloxacin impairs mitochondrial DNA replication initiation through inhibition of Topoisomerase 2. *Nucleic Acids Res.* **2018,** *46* (18), 9625-9636.
24. Pontes, M. H.; Groisman, E., A physiological basis for nonheritable antibiotic resistance. *Mbio* **2020,** *11* (3), e00817-20.
25. Villain-Guillot, P.; Bastide, L.; Gualtieri, M.; Leonetti, J., Progress in targeting bacterial transcription. *Drug Discov. Today* **2007,** *12* (5-6), 200-208.
26. Mingeot-Leclercq, M.-P.; Décout, J., Bacterial lipid membranes as promising targets to fight antimicrobial resistance, molecular foundations and illustration through the renewal of aminoglycoside antibiotics and emergence of amphiphilic aminoglycosides. *MedChemComm* **2016,** *7* (4), 586-611.

27. Teng, P.; Nimmagadda, A.; Su, M.; Hong, Y.; Shen, N.; Li, C.; Tsai, L.-Y.; Cao, J.; Li, Q.; Cai, J., Novel bis-cyclic guanidines as potent membrane-active antibacterial agents with therapeutic potential. *Chem. Commun.* **2017,** *53* (87), 11948-11951.
28. Toyofuku, M.; Schild, S.; Kaparakis-Liaskos, M.; Eberl, L., Composition and functions of bacterial membrane vesicles. *Nat. Rev. Microbiol.* **2023**, 1-16.

29. Vooturi, S.; Firestine, S., Synthetic membrane-targeted antibiotics. *Curr. Med. Chem.* **2010,** *17* (21), 2292-2300.
30. Lee, M.-T.; Hung, W.-C.; Hsieh, M.-H.; Chen, H.; Chang, Y.-Y.; Huang, H. W. J. B. J., Molecular state of the membrane-active antibiotic daptomycin. *Biophys. J.* **2017,** *113* (1), 82-90.
31. Walsh, C. , Molecular mechanisms that confer antibacterial drug resistance. *Nature* **2000,** *406* (6797), 775-781.
32. Christaki, E.; Marcou, M.; Tofarides, A., Antimicrobial resistance in bacteria: mechanisms, evolution, and persistence. *J. Mol. Evol.* **2020,** *88*, 26-40.
33. Alexander, J. A. N.; Worrall, L. J.; Hu, J.; Vuckovic, M.; Satishkumar, N.; Poon, R.; Sobhanifar, S.; Rosell, F. I.; Jenkins, J.; Chiang, D. J. N., Structural basis of broad-spectrum β-lactam resistance in Staphylococcus aureus. *Nature* **2023**, 1-8.

34. Wang, Y.-L.; Liu, S.; Yu, Z.-J.; Lei, Y.; Huang, M.-Y.; Yan, Y.-H.; Ma, Q.; Zheng, Y.; Deng, H.; Sun, Y., Structure-based development of (1-(3′-mercaptopropanamido) methyl) boronic acid derived broad-spectrum, dual-action inhibitors of metallo-and serine-β-lactamases. *J. Med. Chem.* **2019,** *62* (15), 7160-7184.
35. van Duin, D.; Kaye, K. S.; Neuner, E. A.; Bonomo, R.; disease, i., Carbapenem-resistant Enterobacteriaceae: a review of treatment and outcomes. *J. Mol. Evol.* **2013,** *75* (2), 115-120.
36. Schaenzer, A. J.; Wright, G., Antibiotic resistance by enzymatic modification of antibiotic targets. *Trends Mol. Med0* **2020,** *26* (8), 768-782.
37. Hotta, K.; Kondo, S., Kanamycin and its derivative, arbekacin: significance and impact. *J. Antibiot.* **2018,** *71* (4), 417-424.
38. Magnet, S.; Blanchard, J., Molecular insights into aminoglycoside action and resistance. *Chem. Rev.* **2005,** *105* (2), 477-498.
39. Wright, G., Molecular mechanisms of antibiotic resistance. *Chem. Commun.***2011,** *47* (14), 4055-4061.

40. Liu, Y.; Tong, Z.; Shi, J.; Li, R.; Upton, M.; Wang, Z. J. T., Drug repurposing for next-generation combination therapies against multidrug-resistant bacteria. *Theranostics* **2021,** *11* (10), 4910.
41. Fernández, L.; Hancock, R., Adaptive and mutational resistance: role of porins and efflux pumps in drug resistance. *Clin. Microbiol. Rev.* **2012,** *25* (4), 661-681.
42. Tessier, J.; Lecluse, M.; Gravel, J.; Schmitzer, A., Antimicrobial and antibiofilm activity of disubstituted bis-benzimidazolium salts. *ChemMedChem* **2018,** *13* (23), 2567-2572.
43. Flemming, H.-C.; van Hullebusch, E. D.; Neu, T. R.; Nielsen, P. H.; Seviour, T.; Stoodley, P.; Wingender, J.; Wuertz, S., The biofilm matrix: Multitasking in a shared space. *Nat. Rev. Microbiol.* **2023,** *21* (2), 70-86.
44. Singh, T.; Dar, S. A.; Das, S.; Haque, S., New strategies to combat drug resistance in bacteria. In *Drug Discovery Targeting Drug-Resistant Bacteria*, Elsevier: 2020; pp 377-398.

45. Si, Z.; Lim, H. W.; Tay, M. Y.; Du, Y.; Ruan, L.; Qiu, H.; Zamudio-Vazquez, R.; Reghu, S.; Chen, Y.; Tiong, W., A glycosylated cationic block poly (β-peptide) reverses intrinsic antibiotic resistance in all ESKAPE gram-negative bacteria. *Angew. Chem.* **2020,** *59* (17), 6819-6826.
46. NurhannaáRiduan, S., Antibiotic resistance mitigation: The development of alternative general strategies. *J. Mater. Chem. B* **2020,** *8* (30), 6317-6321.
47. Si, Z.; Zheng, W.; Prananty, D.; Li, J.; Koh, C. H.; Kang, E.-T.; Pethe, K.; Chan-Park, M. B. J. C. S., Polymers as advanced antibacterial and antibiofilm agents for direct and combination therapies. *Chem. Sci.* **2022,** *13* (2), 345-364.
48. Qiu, H.; Si, Z.; Luo, Y.; Feng, P.; Wu, X.; Hou, W.; Zhu, Y.; Chan-Park, M. B.; Xu, L.; Huang, D.; Biotechnology, The mechanisms and the applications of antibacterial polymers in surface modification on medical devices. *Front. Bioeng. Biotec* **2020,** *8*, 910.
49. Dantas, D.; Ribeiro, A. I.; Carvalho, F.; Gil-Martins, E.; Silva, R.; Remião, F.; Zille, A.; Cerqueira, F.; Pinto, E.; Dias, A., Red-shifted and pH-responsive imidazole-based azo dyes with potent antimicrobial activity. *Chem. Commun.* **2023,** *59* (19), 2791-2794.

50. Koschevic, M. T.; de Araújo, R. P.; dos Santos Garcia, V. A.; Fakhouri, F. M.; de Oliveira, K. M. P.; Arruda, E. J.; Dufresne, A.; Martelli, S., Antimicrobial activity of bleached cattail fibers (Typha domingensis) impregnated with silver nanoparticles and benzalkonium chloride. *J. Appl. Polym. Sci.* **2021,** *138* (35), 50885.
51. Kim, S.-H.; Semenya, D.; Castagnolo, D. , Antimicrobial drugs bearing guanidine moieties: A review. *Eur. J. Med. Chem.* **2021,** *216*, 113293.
52. Zhou, M.; Zheng, M.; Cai, J.; interfaces, Small molecules with membrane-active antibacterial activity. *ACS Appl. Mater. Interfaces* **2020,** *12* (19), 21292-21299.
53. Wang, H.; Li, F.; Yong, Y.; Lv, M.; Liu, C.; Xu, Q.; Du, G.; Xie, J.; You, Y.; Xiao, J., A novel full solar light spectrum responsive antimicrobial agent of WS 2 quantum dots for photocatalytic wound healing therapy. *J. Mater. Chem. B* **2023**.
54. Lakshmi, S.; Rubeena, A. S.; Subramaniyan, S. B.; Raman, T.; Vaseeharan, B.; Arockiaraj, J.; Karthikeyan, S.; Anbazhagan, V.; Preetham, E., Hybrid of Metapenaeus dobsoni lectin and platinum nanoparticles exert antimicrobial and immunostimulatory effects to reduce bacterial bioburden in infected Nile tilapia. *Sci. Rep.* **2023,** *13* (1), 525.

55. Wu, F.; Ma, J.; Wang, Y.; Xie, L.; Yan, X.; Shi, L.; Li, Y.; Liu, Y. J. A. n., Single copper atom photocatalyst powers an integrated catalytic cascade for drug-resistant bacteria elimination. *ACS Nano* **2023,** *17* (3), 2980-2991.
56. He, X.; Qian, Y.; Wu, C.; Feng, J.; Sun, X.; Zheng, Q.; Li, X.; Shen, J., Entropy-Mediated High-Entropy MXenes Nanotherapeutics: NIR-II-Enhanced Intrinsic Oxidase Mimic Activity to Combat Methicillin-Resistant Staphylococcus Aureus Infection. *Adv. Mater.* **2023**, 2211432.
57. Hancock, R. E.; Sahl, H.-G. J. N. b., Antimicrobial and host-defense peptides as new anti-infective therapeutic strategies. *Nat. Biotechnol.* **2006,** *24* (12), 1551-1557.
58. Fjell, C. D.; Hiss, J. A.; Hancock, R. E.; Schneider, G., Designing antimicrobial peptides: form follows function. *Nat. Rev. Drug Discov.* **2012,** *11* (1), 37-51.
59. Leontiadou, H.; Mark, A. E.; Marrink, S., Antimicrobial peptides in action. *J. Am. Chem. Soc.* **2006,** *128* (37), 12156-12161.
60. Lei, J.; Sun, L.; Huang, S.; Zhu, C.; Li, P.; He, J.; Mackey, V.; Coy, D., The antimicrobial peptides and their potential clinical applications. *Am. J. Transl. Res.* **2019,** *11* (7), 3919.

61. Magana, M.; Pushpanathan, M.; Santos, A. L.; Leanse, L.; Fernandez, M.; Ioannidis, A.; Giulianotti, M. A.; Apidianakis, Y.; Bradfute, S.; Ferguson, A., The value of antimicrobial peptides in the age of resistance. *Lancet Infect. Dis* **2020,** *20* (9), e216-e230.
62. Jorge, P.; Pérez-Pérez, M.; Rodríguez, G. P.; Pereira, M. O.; Lourenço, A., A network perspective on antimicrobial peptide combination therapies: the potential of colistin, polymyxin B and nisin. *Int. J. Antimicrob. Agents* **2017,** *49* (6), 668-676.
63. Si, Z.; Pethe, K.; Chan-Park, M., Chemical basis of combination therapy to combat antibiotic resistance. *J. Am. Chem. Soc. Au* **2023,** *3* (2), 276-292.
64. Kurt Yilmaz, N.; Schiffer, C. , Introduction: drug resistance. *Chem. Rev.* **2021,** *121* (6), 3235-3237.
65. Min, J. G.; Sanchez Rangel, U. J.; Franklin, A.; Oda, H.; Wang, Z.; Chang, J.; Fox, P.; Chemotherapy, Topical antibiotic elution in a collagen-rich hydrogel successfully inhibits bacterial growth and biofilm formation in vitro. *Int. J. Antimicrob. Agents* **2020,** *64* (10), e00136-20.
66. Gonzalez Gomez, A.; Hosseinidoust, Z., Liposomes for antibiotic encapsulation and delivery. *ACS Infect. Dis.* **2020,** *6* (5), 896-908.

67. Zhu, H.; Geng, Q.; Chen, W.; Zhu, Y.; Chen, J.; Du, J., Antibacterial high-genus polymer vesicle as an "armed" drug carrier. *J Mater Chem B* **2013,** *1* (40), 5496-5504.
68. Dey, S.; Patel, A.; Raina, K.; Pradhan, N.; Biswas, O.; Thummer, R. P.; Manna, D., A stimuli-responsive anticancer drug delivery system with inherent antibacterial activities. *Chem. Commun.* **2020,** *56* (11), 1661-1664.
69. Yu, Z.; Qin, W.; Lin, J.; Fang, S.; Qiu, J., Antibacterial mechanisms of polymyxin and bacterial resistance. *BioMed Res. Int.* **2015,** *2015* (679109).
70. Tang, C.; Song, Y.; Wang, Z.; Wang, D.; Yao, X.; Meng, Y.; Li, Y.; Yang, L. J. J. o. M. S., Hydrophobic modification Thr of polymyxin E: Effect on activity and toxicity. *J. Mol. Struct.* **2022,** *1265*, 133382.
71. Kaguchi, R.; Katsuyama, A.; Sato, T.; Takahashi, S.; Horiuchi, M.; Yokota, S.-i.; Ichikawa, S., Discovery of Biologically Optimized Polymyxin Derivatives Facilitated by Peptide Scanning and In Situ Screening Chemistry. *J. Am. Chem. Soc.* **2023,** *145* (6), 3665-3681.
72. Brown, P.; Dawson, M., Development of new polymyxin derivatives for multi-drug resistant Gram-negative infections. *J. Antibiot.* **2017,** *70* (4), 386-394.
73. Li, M.; Zhou, H.; Yang, C.; Wu, Y.; Zhou, X.; Liu, H.; Wang, Y., Bacterial outer membrane vesicles as a platform for biomedical applications: An update. *J. Control. Release* **2020,** *323*, 253-268.
74. Gul, R.; Rauf, M. K.; Badshah, A.; Azam, S. S.; Tahir, M. N.; Khan, A., Ferrocene-based guanidine derivatives: In vitro antimicrobial, DNA binding and docking supported urease inhibition studies. *Eur. J. Med. Chem.* **2014,** *85*, 438-449.
75. Garneau-Tsodikova, S.; Labby, K., Mechanisms of resistance to aminoglycoside antibiotics: overview and perspectives. *MedChemComm* **2016,** *7* (1), 11-27.
76. Algburi, A.; Zhang, Y.; Weeks, R.; Comito, N.; Zehm, S.; Pinto, J.; Uhrich, K. E.; Chikindas, M. L. J. A. a.; chemotherapy, Gemini cationic amphiphiles control biofilm formation by bacterial vaginosis pathogens. *Antimicrob. Agents Chemother.* **2017,** *61* (12), e00650-17.
77. Thiyagarajan, D.; Goswami, S.; Kar, C.; Das, G.; Ramesh, A., A prospective antibacterial for drug-resistant pathogens: a dual warhead amphiphile designed to track

interactions and kill pathogenic bacteria by membrane damage and cellular DNA cleavage. *ChemComm* **2014,** *50* (56), 7434-7436.
78. Nisini, R.; Poerio, N.; Mariotti, S.; De Santis, F.; Fraziano, M., The multirole of liposomes in therapy and prevention of infectious diseases. *Front. Immunol.* **2018,** *9*, 155.
79. Rahman, M. A.; Bam, M.; Luat, E.; Jui, M. S.; Ganewatta, M. S.; Shokfai, T.; Nagarkatti, M.; Decho, A. W.; Tang, C., Macromolecular-clustered facial amphiphilic antimicrobials. *Nat. Commun.* **2018,** *9* (1), 5231.
80. Sannasiddappa, T. H.; Lund, P. A.; Clarke, S., In vitro antibacterial activity of unconjugated and conjugated bile salts on Staphylococcus aureus. *Front Microbiol* **2017,** *8*, 1581.

81. Verhaegh, R.; Becker, K. A.; Edwards, M. J.; Gulbins, E., Sphingosine kills bacteria by binding to cardiolipin. *J. Biol. Chem.* **2020,** *295* (22), 7686-7696.

82. Martin, G. E.; Boudreau, R. M.; Couch, C.; Becker, K. A.; Edwards, M. J.; Caldwell, C. C.; Gulbins, E.; Seitz, A., Sphingosine's role in epithelial host defense: A natural antimicrobial and novel therapeutic. *Biochimie* **2017,** *141*, 91-96.
83. Kauss, T.; Arpin, C.; Bientz, L.; Vinh Nguyen, P.; Vialet, B.; Benizri, S.; Barthélémy, P., Lipid oligonucleotides as a new strategy for tackling the antibiotic resistance. *Sci. Rep.* **2020,** *10* (1), 1054.

84. Bassetti, M.; Vena, A.; Russo, A.; Peghin, M., Inhaled liposomal antimicrobial delivery in lung infections. *Drugs* **2020,** *80* (13), 1309-1318.

85. Mottais, A.; Berchel, M.; Le Gall, T.; Sibiril, Y.; d'Arbonneau, F.; Laurent, V.; Jaffrès, P.-A.; Montier, T., Antibacterial and transfection activities of nebulized formulations incorporating long n-alkyl chain silver N-heterocyclic carbene complexes. *Int. J. Pharm.* **2019,** *567*, 118500.
86. Vairo, C.; Vidal, M. V.; Hernandez, R. M.; Igartua, M.; Villullas, S., Colistin-and Amikacin-loaded lipid-based drug delivery systems for resistant gram-negative lung and wound bacterial infections. *Int. J. Pharm.* **2023**, 122739.
87. Rosita, N.; Miatmoko, A.; Cahyani, D. M.; Hariyadi, D. M., Lipid-Based Drug Delivery for Pneumonia Treatment. In *Infectious Diseases Drug Delivery Systems*, Springer: 2023; pp 307-329.
88. Sarkar, P.; De, K.; Modi, M.; Dhanda, G.; Priyadarshini, R.; Bandow, J. E.; Haldar, J., Next-generation membrane-active glycopeptide antibiotics that also inhibit bacterial cell division. *Chem. Sci.* **2023,** *14* (9), 2386-2398.
89. Kanazawa, A.; Ikeda, T.; Endo, T., Antibacterial activity of polymeric sulfonium salts. *J. Polym. Sci.* **1993,** *31* (11), 2873-2876.
90. Klimenko, S.; Stolbova, T.; Kulikova, L., Synthesis and the antimicrobial and antiphage activity of sulfonium and oxosulfonium salts of condensed thianes and thiacyclohexene. *Pharm. Chem. J.* **2001,** *35* (1), 22-25.
91. Hirayama, M., The antimicrobial activity, hydrophobicity and toxicity of sulfonium compounds, and their relationship. *Biocontrol Sci.* **2011,** *16* (1), 23-31.
92. Feliciano, J. A.; Leitgeb, A. J.; Schrank, C. L.; Allen, R. A.; Minbiole, K. P.; Wuest, W. M.; Carden, R.; letters, m. c., Trivalent sulfonium compounds (TSCs): Tetrahydrothiophene-based amphiphiles exhibit similar antimicrobial activity to analogous ammonium-based amphiphiles. *Bioorg. Med. Chem. Lett.* **2021,** *37*, 127809.

93. Guan, D.; Chen, F.; Shi, W.; Lan, L.; Huang, W. J. C., Single Modification at the N-Terminus of Norvancomycin to Combat Drug-Resistant Gram-Positive Bacteria. *ChemMedChem* **2023,** *18* (9), e202200708.
94. Sun, J.; Li, M.; Lin, M.; Zhang, B.; Chen, X., High antibacterial activity and selectivity of the versatile polysulfoniums that combat drug resistance. *Adv. Mater.* **2021,** *33* (41), 2104402.
95. Oh, J.; Khan, A. J. B., Main-chain polysulfonium salts: development of non-ammonium antibacterial polymers similar in their activity to antibiotic drugs vancomycin and kanamycin. *Biomacromolecules* **2021,** *22* (8), 3534-3542.
96. Zhao, J.; Zhu, Z.; Rao, J., Development of cationic sulfonium-based gels with inherent antibacterial, excellent antibiofilm, and tunable swelling properties. *Eur. Polym. J.* **2022,** *179*, 111551.
97. Zhao, Y.; Wang, X.; Hu, Y.; Zhao, J.; Sun, M.; Yang, M.; Xuan, H.; Wang, X.; Zhang, J.; Zhu, Z., Enhanced Synergistic Antibacterial and Antibiofilm Efficacy of Main-Chain Polysulfoniums with Antibiotics by Balancing Charge Density and Amphiphilicity. *ACS Appl. Polym. Mater.* **2023**.
98. Nosrati, H.; Heydari, M.; Tootiaei, Z.; Ganjbar, S.; Khodaei, M.; Technology, Delivery of antibacterial agents for wound healing applications using polysaccharide-based scaffolds. *J Drug Deliv Sci Technol* **2023**, 104516.
99. Feketshane, Z.; Adeyemi, S.; Ubanako, P.; Ndinteh, D.; Ray, S.; Choonara, Y.; Aderibigbe, B., Dissolvable sodium alginate-based antibacterial wound dressing patches: Design, characterization, and in vitro biological studies. *Int. J. Biol. Macromol.* **2023,** *232*, 123460.
100. Tsai, C.-Y.; Chen, Y.-J.; Fu, Y.-S.; Chang, L.; biophysics, Antibacterial and membrane-damaging activities of mannosylated bovine serum albumin. *Arch. Biochem. Biophys.* **2015,** *573*, 14-22.
101. Shi, Y.-J.; Wang, R.-T.; Chu, Y.-H.; Chen, Y.-J.; Tang, C.-C.; Fu, Y.-S.; Lee, Y.-C.; Wang, L.-J.; Huang, C.-H.; Chang, L.; biophysics, Membrane-damaging activities of mannosylated ovalbumin are involved in its antibacterial action. *Arch. Biochem. Biophys.* **2018,** *639*, 1-8.
102. Xia, T.; Jiang, X.; Deng, L.; Yang, M.; Chen, X. J. C.; Biointerfaces, S. B., Albumin-based dynamic double cross-linked hydrogel with self-healing property for antimicrobial application. *Colloids Surf. B . B .* **2021,** *208*, 112042.
103. Burdick, J. A.; Prestwich, G., Hyaluronic acid hydrogels for biomedical applications. *Adv mater* **2011,** *23* (12), H41-H56.

CHAPTER 2

SULFONIUM-BASED LIPOSOME-ENCAPSULATED ANTIBIOTICS DELIVER A SYNERGISTIC ANTIBACTERIAL ACTIVITY

2.1 Background and objective of the present work

A brief introduction about the importance of cationic sulfonium molecules with amphiphilicity gave us the idea to analyze the antibacterial activity of sulfonium compounds. It has been observed that amphiphilic molecules with long hydrocarbon chain helps the compound to interact and traverse the hydrophobic bacterial cell membrane. Long fatty acid chain conjugated with polar head group can assemble to form liposome also which can be utilized to encapsulate the drug and its delivery reducing the multiple dosing of the drug and enhancing the efficacy. An antibiotic drug carrier with inherent bactericidal activity can provide the synergistic activity. As per the report the conjugation of sulfonium molecule to the antibiotics rejuvenated the activity of antibiotic vancomycin and norvancomycin against vancomycin resistant bacterial strains hence we can hypothesize that encapsulation of antibiotics in sulfonium containing liposomes can help it restore its activity against drug resistant bacterial strains such as MRSA and *P. aeruginosa*. This strategy seems more cost effective as design and synthesis of even single sulfonium containing antimicrobial nano carrier can be used to encapsulate and rejuvenate the activity of multiple antibiotics as per the requirements.

In our previous study, we demonstrated that the sulfonium lipids encapsulate and deliver the anticancer drug, doxorubicin, to a mammalian cell.[1] The self-assembly properties of those sulfonium lipids could be utilized to deliver both aqueous soluble and insoluble antibiotics at the target site. The amphiphilicity and the presence of cationic sulfonium moieties would also allow the sulfonium-based lipids to fuse with the outer membrane of the bacteria cells and release the encapsulated antibiotics.[2] Recently, polymeric amphiphilic systems with inherent antibacterial activity were reported.[3] However, a small molecule-based biocompatible amphiphilic system could augment the therapeutic benefits.

Herein, we report the synthesis and mechanism of the antibacterial activity of sulfonium-based amphiphilic compounds. The role of cationic charge and hydrocarbon chain length in antimicrobial activity was investigated by their structural modification against both gram-positive and gram-negative strains of bacteria. The amphiphilic molecule with the pyridinium head group showed the most potent antibacterial activity among the tested compounds against gram-negative, gram-positive, and even drug-resistant bacteria. The less-toxic sulfonium compound was also found to be effective to prevent the formation of biofilm and to eradicate the mature robust biofilm. In addition, commercial antibiotics

amoxicillin and tetracycline were encapsulated in pyridinium containing potent compound followed by its encapsulation and release profile study. Antibacterial efficacies of the composite were also investigated against drug sensitive and drug resistant bacterial strains to calculate the synergistic activity. The composite showed moderate loading of water-soluble antibiotics and sustained release profile. Overall, our studies propose that electrostatic interaction of cationic liposomes with the bacterial membrane allows its disassembly and insertion of the amphiphilic compound to the bacterial membrane, resulting in the concomitant release of antibiotics at the target site to achieve synergistic antibacterial activities.

2.2 Results and discussion

2.2.1 Design and synthesis of compounds

The anticancer drug delivery and moderate antimicrobial activities of the sulfonium lipids motivated us to synthesize a new series of sulfonium-based compounds.[4] The key features in designing the compounds were the installation of cationic (pyridinium) or anionic (sulfonic acid) headgroup and variation of alkyl chain length in addition to the sulfonium moieties (Scheme 2.1). The variation in alkyl chain length would allow us to investigate the role of hydrophobicity and antimicrobial activity. We envisage that the hydrophobicity of dialkyl chain lengths could allow the compounds to self-aggregate in an aqueous medium, which could be useful in encapsulating the commercial antibiotics. The presence of both sulfonium moieties and antibiotic encapsulation ability would generate a composite antibacterial agent, which can increase the bactericidal effect, reduce the antibiotic-related toxicity, and enhance the efficacy of the antibiotics at lower doses (Figure 2.1A). Most of the conventional liposomes, micelles, or nanoparticle-based delivery systems lack such a dual mode of action, suggesting that the combined antibacterial activity of these sulfonium-based compounds can improve the killings of drug-resistant pathogenic bacteria.

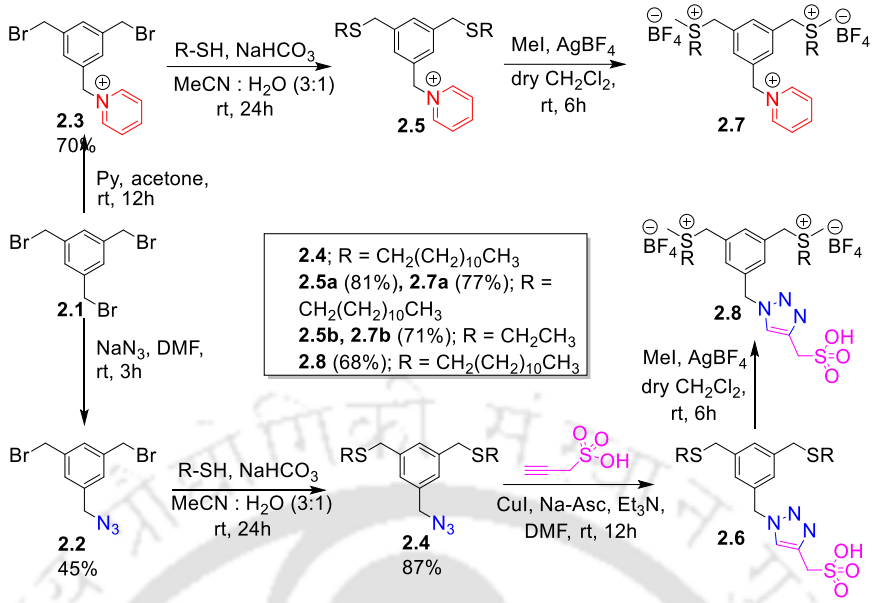

Scheme 2.1. Synthetic routes to the sulfonium-based compounds.

The compounds were synthesized according to our reported methods with minor modifications (Scheme 2.1).[4] The compounds for the current study were synthesized using 1,3,5-tris(bromomethyl)benzene. The mono-modification of 1,3,5-tris(bromomethyl)benzene with azide and pyridine resulted in compounds **2.2** and **2.3**, which were further modified with aliphatic thiols to provide compounds **2.4** and **2.5**, respectively. The azide-alkyne click reaction of compound **2.4** with prop-2-yne-1-sulfonic acid produced compound **2.6**. Finally, the treatment of compounds **2.5** and **2.6** with methyl iodide in the presence of $AgBF_4$ provided the desired product **2.7** and **2.8** with satisfactory yield. These compounds were characterized by nuclear magnetic resonance (NMR), high-resolution mass spectrometry (HRMS).

2.2.2 Aggregation behavior in aqueous solution

To investigate the behavior of these amphiphilic compounds under an aqueous environment, the compounds were dissolved in phosphate-buffered saline (PBS).[4] The compounds **2.7b** was completely soluble, but compound **2.7a** and **2.8** formed a suspended aqueous solution. The presence of short alkyl chain length and sulfonic acid could be reasons for their aqueous solubility. The field-emission transmission electron microscope (FE-TEM) analysis showed that compound **2.7a** form spherical aggregates in an aqueous medium (Figure 1B). The dynamic light scattering (DLS) study showed that the size of the spherical aggregates varies between 270-340 nm at different pH of the respective buffers at 25 ˚C (Figure 2.1C, 2.1D). The zeta-potential measurements showed that the overall

surface charge of the spherical aggregates was positive, and the positive charge increases with the decrease in pH of the buffer, which could be due to a decrease in solvation number in acidic medium. Hence, TEM, DLS, and zeta-potential measurements revealed that compound **2.7a** form stable spherical aggregates with positive surface potential.

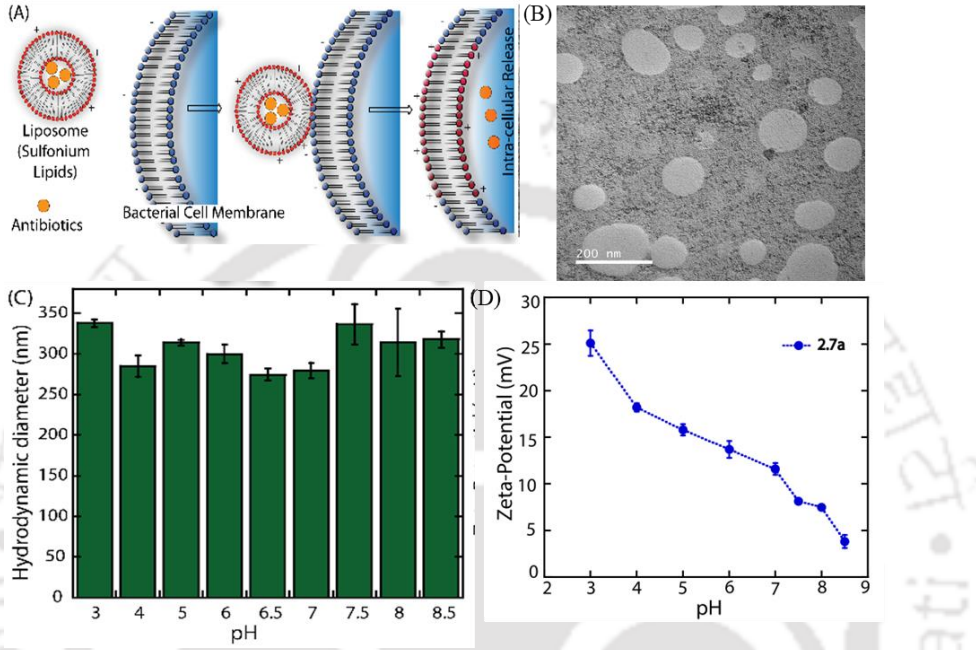

Figure 2.1. Cartoon diagram demonstrating the probable pathway for the bactericidal effect of antibiotics encapsulated liposomes of compound **2.7a** (A). Representative TEM image of the soluble aggregates generated from the 100% **compound 2.7a** (B). The scale bar for the TEM image is 200 nm. Variation of the hydrodynamic diameter of the soluble aggregates generated from the 100% compound **2.7a** at different pH was measured by DLS analysis **(C)**. The surface potential of the soluble aggregates generated from the 100% **compound 2.7a** at different pH (D)

2.2.3 Antibacterial activities of the compounds

The sulfonium-based compounds showed antibacterial activity against both gram-positive and gram-negative bacteria.[4, 5] The minimum inhibitory concentrations (MIC) of the compounds were calculated against gram-negative bacteria such as *Escherichia coli* MTCC 1687 (*E. coli*) and *Pseudomonas aeruginosa* MTCC 2488 and gram-positive bacteria such as *Staphylococcus aureus* MTCC 96 and methicillin-resistant *Staphylococcus aureus* (MRSA) by micro broth dilution method.[6] Highly infectious E. coli strain resides in the

intestine and causes various diseases, including pneumonia, diarrhea, and urinary tract infection (UTI). The bacterial strains of *S. aureus* and *P. aeruginosa* are the frequent residents of bronchioles and alveoli of cystic fibrosis patients. The MIC values were reckoned as the minimum concentration of the compounds, which caused no visible growth, or the optical density (OD) of the compound treated bacterial culture was close to that of control (without any bacteria). The compounds **2.7a** and **2.8** showed very good antibacterial activity against all the four tested bacterial strains (Table 2.1). The MIC values of the pyridinium containing compound **2.7a** were within 6.3-12 μM. Whereas the sulfonic acid-containing compound **2.8** had little higher MIC values of 12-24 μM. It was emboldening to observe that the drug-resistant strain of *S. aureus* (MRSA) showed a similar MIC value to that of its drug-sensitive strain. Further antibacterial studies of compounds **2.7a** and **2.8** were performed to investigate the impetus of different structural moieties in the compound, which provide the observed antimicrobial property. However, compound **2.4** with azide but no sulfonium moieties showed no antibacterial activity even at 100 μM.[4] Compound **2.5a,** with only pyridinium but no sulfonium moieties, showed no antibacterial activity even at 100 μM, suggesting the role of sulfonium moieties in the antibacterial activities of compound **2.7a**. Compound **2.7b,** with the same head group, but with short alkyl chain (ethyl group) length to that of compound **2.7a**, showed no antibacterial activity even at 100 μM, suggesting that the long hydrocarbon chain is as important as other moieties in the compound. Compound **2.5b** with short alkyl chain length also showed no antibacterial activity. Probably, the sulfonium and pyridinium or sulfonic acid moieties could be involved in electrostatic or hydrogen bond interactions with the phosphoryl and carboxyl groups of the bacterial membrane lipids and elicit the insertion of the long hydrocarbon chain lengths of compounds **2.7a** and **2.8** to the bacterial membrane.[5] The higher antibacterial activity of compound **2.7a** over **2.8** could be due to much stronger electrostatic interaction of pyridinium moiety with anionic lipids of the bacterial membrane than that with the sulfonic acid moiety. The cationic moieties showed better antibacterial activity over neutral or anionic moieties.[7-9] Similar antibacterial activities were reported when sulfonium moiety was appended to vancomycin.[5] The sulfonium containing vancomycin analog showed improved antibacterial activity against vancomycin-resistant bacteria, suggesting the potential of sulfonium moiety in antibacterial activities. The attachment of sulfonium moiety also alters the innate feature of vancomycin, leading to its activity against gram-negative bacteria.[5] Interestingly, the antibacterial activity of these

sulfonium lipids **2.7a** and **2.8** are similar to other substances, especially to some widely used antiseptics. The MIC values of those antiseptics against *P. aeruginosa* are the following: for octenidine dihydrochloride 3.9-31.25 μg/mL (6.25-50.1 μM) for chlorhexidine digluconate 15.63-64 μg/mL (30.9-126.6 μM), and for polyhexamethylene biguanide 2-31.25 μg/mL.[10, 11] Simultaneously, the activity of sulfonium compounds **2.7a** and **2.8** against *P. aeruginosa* is significantly higher than other very important antiseptics like benzalkonium chloride (MICs 32-512 μg/ml), povidone-iodine (MICs 62.5-1024 μg/ml) and triclosan (MICs >512 μg/ml).[10, 11] several sulfonium-based compounds showed better antimicrobial activities than some common cationic antimicrobials including cetylpyridinium chloride and benzalkonium chloride.[12] Recently, developed sulfonium *N*-chloramines showed higher antibacterial activities than the formerly reported quaternary ammonium counterpart.[13] The polymeric salts of *p*-vinylbenzyl tetramethylenesulfonium tetrafluoroborate exhibited high antibacterial activity against Gram-positive bacteria.[14]

Table 2.1. Antibacterial activities of the synthesized compounds.

Compound			MIC (μM)/ MBC (μM)				HC_{50} (μM)
	n	R	*E. coli*	*P. aeruginosa*	*S. aureus*	*S. aureus* (MRSA)	
2.4	11	$-N_3$	>100	>100	>100	>100	-
2.5a	11	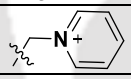	>100	>100	>100	>100	-
2.5b	2	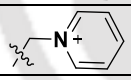	>100	>100	>100	>100	-
2.7a	11	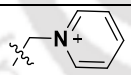	7.5 ± 1 / 10 ± 1	12 ± 0.5 / 24 ± 1	6.3 ± 1 / 12.5 ± 1	6.3 ± 1 / 12.5 ± 1.5	29
2.7b	2	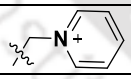	>100	>100	>100	>100	-
2.8	11	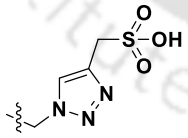	12 ± 1 / 20 ± 1	25 ± 1 / 50 ± 1	10 ± 0.5 / 12.5 ± 1	25 ± 1 / >100	35
Octenidine dihydrochloride				6.25-50.1			
Chlorhexidine digluconate				30.9-126.6			
Triclosan				>1,766			

The bactericidal activity of the compounds was tested against the same bacterial strains.[15] The minimum bactericidal concentration (MBC) of the compound was greater than the minimum bacteriostatic concentration, suggesting that a greater concentration of the compound is required to demolish the bacterial membrane or metabolic activity at a rate

with which they might not be able to repair it and die off (Table 2.1). Thus, these amphiphiles proficient in the bacterial cell at a low concentration, which makes them good antimicrobial agents for immunocompromised patients also. The bactericidal activity of the compounds was further confirmed by FESEM analysis.[4] A significant difference in morphology of the bacterial cells was observed between the control and compound treated samples. The cocci shape of the *S. aureus* and the rod shape of *E. coli* were disfigured or fragmented in the drug-treated bacterial sample, which could be due to the relentless disruption of the bacterial membrane. These morphological changes of bacterial cells suggest that compound **2.7a** may induce bacterial programmed cell death.[16]

Additionally, the antibiofilm activity of the compound was tested because a plethora of bacterial strain constructs a sturdy biofilm to protect their colony from drugs and other unpropitious conditions. Extra polymeric substance or biofilm is essentially composed of extracellular DNA (eDNA), peptide or protein, and intercellular polysaccharide with different ratios and architecture depending upon the bacterial strain. Biofilm has been implicated in many infectious diseases, including chronic sinusitis, atherosclerosis, chronic wounds, endocarditis, and many more.[17] The antibiofilm assay by the crystal violet staining method showed that compound **2.7a** inhibits the formation of biofilm by *S. aureus* strain in a dose-dependent manner.[18] However, the concentration of compound **2.7a** required in inhibiting 90% biofilm (12 μM) or complete abolishment of mature biofilm (24 μM) was 2-4 fold higher than its MIC values against *S. aureus* cells (Figure 2.2B and 2.2C). Thus, amphiphile has the capability to degrade the mature biofilm and efficiently can inhibit its reformation. The presence of both pyridinium and sulfonium moieties (cationic) of compound **2.7a** could be the driving for its electrostatic interactions with the TA and LPS of the gram-positive and gram-negative bacterial cells which led to the membrane-mediated antibacterial activities (Figure 2.2D).

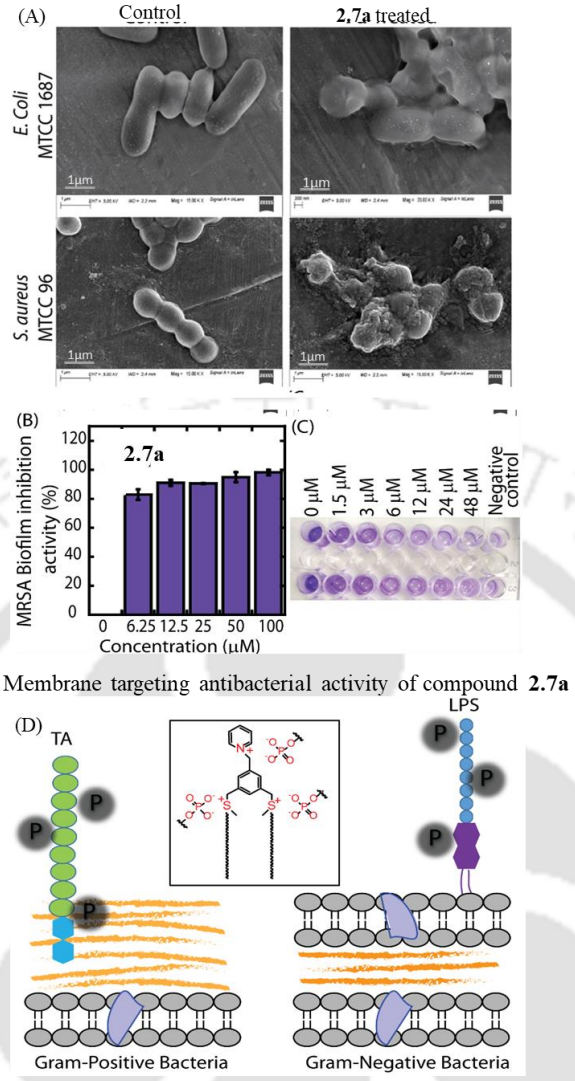

Membrane targeting antibacterial activity of compound **2.7a**

Figure 2.2. Representative FESEM images of untreated and compound **2.7a**-treated bacterial cells (A). The scale bar for the images is 1.0 µm. Compound **2.7a** mediated eradication of *S. aureus* (MRSA) biofilm was investigated by crystal violet staining assay The experiment was performed in triplicates (B and C). Cartoon diagram demonstrating the probable interaction of the compound **2.7a** with the negatively charged TA and LPS in the gram-positive and gram-negative bacteria, respectively (D).

The mechanism of bactericidal activity was studied by propidium iodide (PI) uptake assay.[19, 20] The fluorescent DNA intercalating agent, PI can cross the damaged cell membrane but impermeable to the intact and live cell. The PI uptake assay was performed at different concentrations and time intervals using *S. aureus* cells. The increase in fluorescence intensity of PI revealed that the antibacterial activity of compound **2.7a** is

membrane directed and time-dependent, suggesting that the number of dead cells increases with time (Figure 2.3A). Further mechanistic studies were performed by membrane depolarization assay using $DiSC_3(5)$ dye.[20] The fluorescence intensity of this dye gets quenched on the negatively charged bacterial membrane. However, it showed higher fluorescence intensity on the disrupted membrane. The $DiSC_3(5)$ assay was tested on S. *aureus* at various concentrations of compound **2.7a** along with positive control (valinomycin), and a significant disparity was observed in fluorescence intensity even at a very low concentration range, which increased with the increase in concentration. The increase in fluorescence intensity of $DiSC_3(5)$ dye of the compound **2.7a** treated cells suggests the disruption in membrane integrity of *S. aureus* cells (Figure 2.3B). Fluorescence-based live and dead cell imaging study by staining the drug-treated cells with PI and 5(6)-carboxyfluorescein diacetate *N*-succinimidyl ester (cFDA-SE) was also done to investigate the bactericidal activity of the compound (Figure 2.3C). The membrane-permeable nonfluorescent cFDA-SE dye only shows fluorescence due to the formation of carboxyfluorescein succinimidyl ester (CFSE) in the presence of esterase enzyme, which is an indicator of bacterial cell viability. During the measurements, the *S. aureus* cells were stained with the cFDA-SE dye, and microscopic fluorescence images were recorded. The analysis revealed that the compound **2.7a**-treated *S. aureus* cells lacked CFSE fluorescence, which exclaimed the inactivity of bacterial metabolism due to superior membrane damage, which results in cell death.

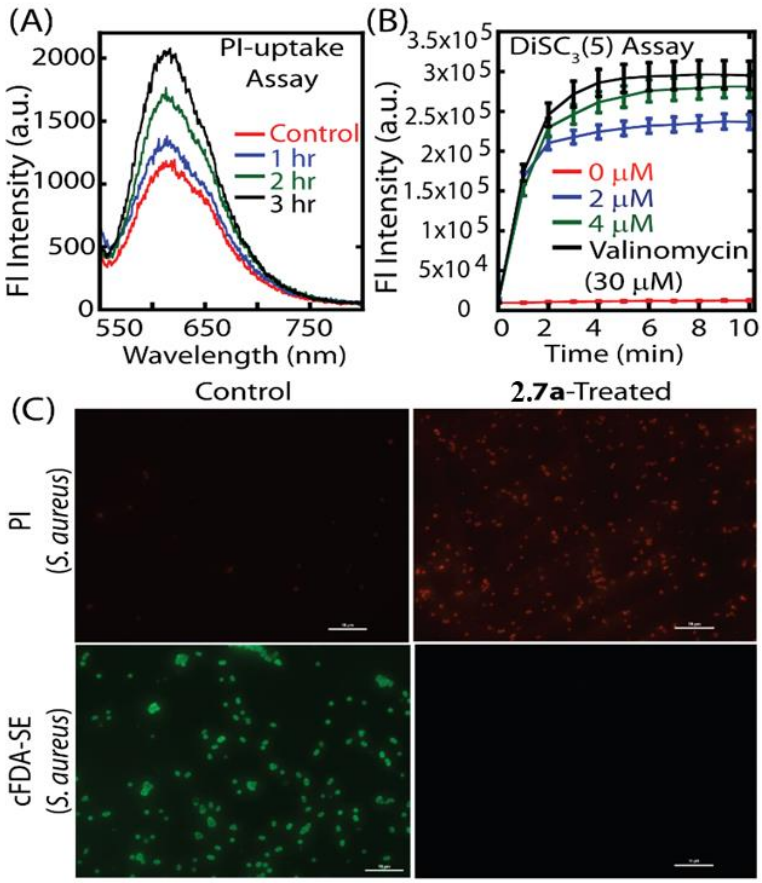

Figure 2.3. Fluorescence-based PI-uptake assay of compound **2.7a** using *S. aureus* (MRSA) cells (A). Compound **2.7a**-treated membrane depolarization assay using $DiSC_3(5)$ dye on *S. aureus* (MRSA) cells (B). Representative fluorescence microscopic images of untreated and compound **2.7a**-treated bacterial cells (C). The scale bar for the images is 10 μm.

2.2.4 Antibiotics encapsulation and antibacterial efficacy

The self-assemble property of compound **2.7a** inspired us to encapsulate antibiotics and generate an antibacterial composite, where both antibiotic and sulfonium-based compound would show a potential synergistic effect. Antibiotics and other drugs, when encapsulated in liposomes, are more effective and protected from the adverse environment of the cell. To explore the antibiotic encapsulation, both bacteriostatic and bactericidal antibiotics tetracycline and amoxicillin, respectively, were selected. Encapsulation and release profiles of antibiotics in compound **2.7a** were investigated by the fluorometric method (Figure 2.5 and 2.6B). Compound **2.7a** showed satisfactory loading ability for tetracycline (18%) and amoxicillin (28%) at pH 7.4, suggesting that these water-soluble antibiotics could be

entrapped within the hydrophilic core of the self-assembled structure (Figure 2.6A). Fluorescence measurements of these antibiotics showed sustained release profiles with 40% and 60% of tetracycline and amoxicillin, respectively, which were released after 60 hours of incubation at 37 °C (Figure 2.6B). These sustained antibiotics release profiles of compound **2.7a** are advantageous for their biological applications, including a reduction in antibiotic-associated toxicity, augmentation of the activity of the antibiotics at lower doses, and others.

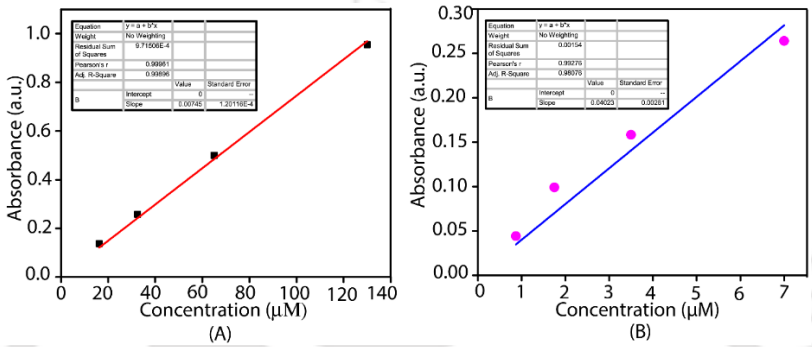

Fig.2.4. Standard plot for the calculation of extinction coefficient (ε) for Tetracycline (A) and Amoxicillin (B).

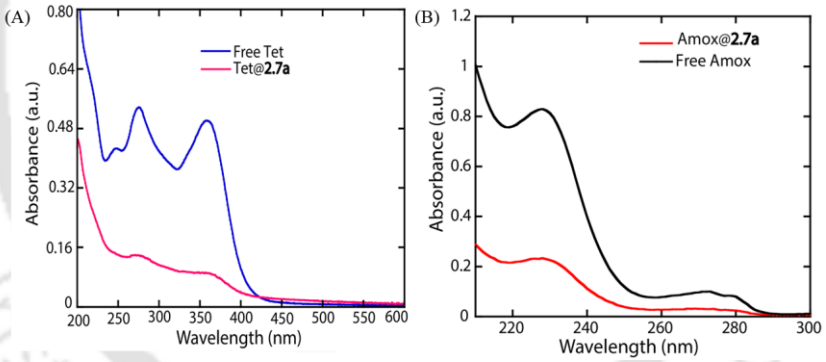

Fig. 2.5. UV-Vis spectra of free antibiotics, antibiotic encapsulated vesicles of **2.7a** at pH 7.4 tetracycline (A) amoxicillin (B)

The antibacterial activity of tetracycline and amoxicillin encapsulated liposomes of **2.7a** (**2.7a**@tetracycline and **2.7a**@amoxicillin) showed synergistic effects, and the antibacterial activities were 4 to 6.5-folds higher (lower MIC) than free tetracycline and amoxicillin, suggesting the accomplishment of dual activity of compound **2.7a** and antibiotics encapsulated within the liposome (Table 2.2). Therefore, the encapsulation of these antibiotics increases the drug efficacy, and the controlled release of drugs could provide the long-term effect and minimize the necessity of multiple dosing. However, it is important to mention that tetracycline and amoxicillin loading efficiencies of compound **2.7a** were 18%

and 28%, respectively; hence much lower concentrations of the encapsulated antibiotics were required to have a similar antibacterial activity than the free antibiotics.

Table 2.2. Antibacterial activities of the commercial antibiotics and antibiotic encapsulated sulfonium based amphiphilic compound.

Antibiotic	Bacterial train	MIC (μg/mL)	MIC (**2.7a**@antibiotic (μg/mL)
Tetracycline	S. *aureus*	1.87	0.31
	E. *coli*	3.75	0.87
Amoxicillin	S. *aureus*	2.50	0.44
	E. *coli*	4.0	0.62

2.2.5 Synergy calculation

Synergy measurement of the antibiotic encapsulated **2.7a** lipid was calculated by checkerboard analysis. To quantify the synergistic effect of antibiotic encapsulated **2.7a** following equation was used-

$$\frac{MIC\ of\ \mathbf{2.7a}\ loaded\ with\ antibiotic\ (\frac{\mu g}{mL})}{MIC\ of\ \mathbf{2.7a}(\frac{\mu g}{mL})} + \frac{MIC\ of\ antibiotic\ loaded\ in\ \mathbf{2.7a}(\frac{\mu g}{mL})}{MIC\ of\ antibiotic(\frac{\mu g}{mL})} = FIC\ Index$$

A fractional inhibitory concentration (FIC) value less than 0.5 indicates the synergy.

Table 2.3: fractional inhibitory concentration (FIC) value of antibiotic encapsulated in **2.7a** vesicles

Compound name	Bacterial strain	FIC value
Tet@2.7a	S. *aureus*	0.31
	E. *coli*	0.41
Amox@2.7a	S. *aureus*	0.30
	E. *coli*	0.24

An antimicrobial agent can be used for further bio-application only when it is biocompatible and non-toxic to human cells. As our drug targets the bacterial membrane, it should be specific to that only. Though bacterial membrane differs from the mammalian cell membrane and red blood cell membrane architecture but because of few similarities in membrane nature, the drug should be tested against mammalian cells. In this regard, the

cytocompatibility of synthesized potent amphiphiles and antibiotic-loaded amphiphiles were verified against HeLa (human cervical cancer) and HaCaT (human keratinocyte) cells by assessing the NADH dependent cellular oxidoreductase enzyme activity was evaluated with the MTT dye (3-(4,5-dimethylthiazol-2-yl)-2,5-diphenyltetrazolium bromide) (Figure 2.6C). The HaCaT cell line showed no toxicity up to 100 µM against compound **2.8**. The calculated IC_{50} value of compound **2.7a** was 27 µM. Meanwhile, the IC_{50} values of 7a@tetracycline and 7a@amoxicillin were 8 and 29.41 µM, respectively (Figure 2.6D). Furthermore, the toxicity of the synthesized amphiphiles was tested against the membrane of red cells, which is very much elastic, and the only structural component it has is the plasma membrane that provides the mechanical support to the cell. To ensure the compatibility of the sulfonium-based amphiphiles against red blood cells, hemolytic activity was performed. Disruption of the membrane of the red blood cells causes heme leakage from the cell that can be measured by the spectrophotometric method (Figure 2.6E). Amphiphiles at various concentration ranges were incubated with 5% hematocrit at room temperature. The extent of heme release was measured by UV-Vis spectroscopy at 410 nm after the centrifugation. The result was compared with negative (no compound) and positive controls (0.1% Triton X-100) and was found that at MIC and MBC value compound has very less or no hemolytic activity (Table 1).

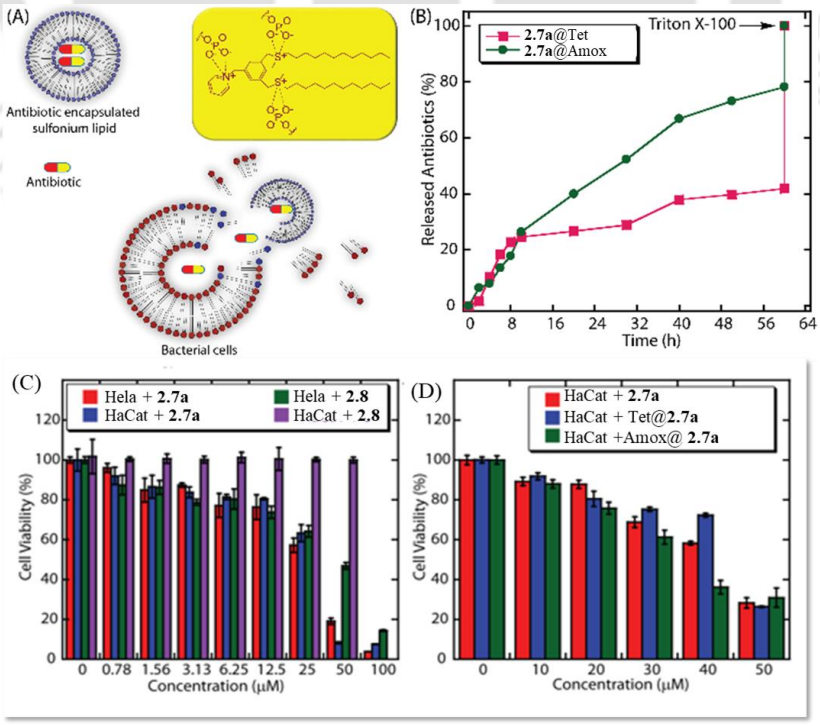

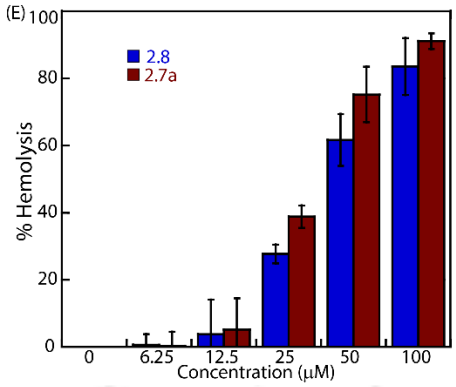

Figure 2.6. Cartoon diagram demonstrating the antibiotic release pathways from the liposomes of compound **2.7a** (A). The antibiotics (tetracycline and amoxicillin) release profile of compound **2.7a** at pH 7.4 (B). Concentration-dependent viabilities of the HeLa and HaCaT cells in the presence of compounds **2.**7a and **2.**8 (C). Concentration-dependent viabilities of the HaCaT cells in the presence of compounds **2.7a** and antibiotics encapsulated compound **2.7a** (D). Hemolytic activity of **2.7a** and **2.8** in the human red blood cell (E).

2.3 Conclusion

Bacterial infections and antibiotic resistance is rapidly becoming one of the most daunting healthcare burden of our day which immediately need effective therapeutic strategies. The current study demonstrates that the modular synthesis of membrane active sulfonium-based lipids can effectively form liposome and encapsulate the commercially available antibiotics to have synergistic effect against bacterial strains responsible for respiratory infection like cystic fibrosis. Liposomal aggregates are the rising armor to strive against such respiratory syndromes. The fascinating properties of the antibiotic-encapsulated liposomes were the prudent assimilation of two weapons, which permitted harnessing their concomitant activity. Membrane directed activity of the lipids make them less prone to drug resistance, and the most potent lipid also augment the activity of commercial antibiotics. We envisage that this inherent antimicrobial drug carrier can be proven as the panacea, towards the path of antibiotic stewardship.

2.4 Experimental section

2.4.1. General information —All the required reagents were purchased from Sigma-Aldrich, Merck, and other commercial sources and bacterial media from Himedia, which

were used directly without further purification. The bacterial culture was acquired from the Microbial Type Culture Collection (MTCC). The synthesized compound was purified by column chromatography using 60–120 mesh silica gels. Reactions were monitored by thin-layer chromatography (TLC) on silica gel 60 F254 (0.25 mm). The 1H NMR and 13C NMR were recorded at 400 or 600 and 100 or 151 MHz with Varian AS400 spectrometer and Brucker spectrometer, respectively. The chemical shifts were reported in parts per million (δ) using DMSO-d6, CDCl3 as the internal solvent. The coupling constants (J values) and chemical shifts (δppm) were reported in Hertz (Hz) and parts per million (ppm), respectively, downfield from tetramethylsilane using residual chloroform (d = 7.28 for 1H NMR, d = 77.23 for 13C NMR) as an internal standard. Multiplicities are reported as follows: s (singlet), d (doublet), t (triplet), m (multiplet), and br (broadened). High-resolution mass spectra were recorded at Agilent Q-TOF mass spectrometer with Z-spray source using built-in software for analysis of the recorded data. Ultrapure water (Milli-Q system, Millipore, Billerica, MA) was used for the preparation of buffers.

2.4.2. Synthesis and characterization of the compounds

Synthesis of 1-(azidomethyl)-3,5-bis(bromomethyl)benzene (2.2) — To stirring solution of 1,3,5-tris(bromomethyl)benzene (**1**) (1.40 mmol) in dry DMF solvent, sodium azide (1.2 mmol) was added portion-wise, and the resulting mixture was stirred for 3 hours at room temperature. The progress of the reaction was monitored by thin-layer chromatography (TLC). After maximum consumption of compound **2.1**, the solvent was removed under reduced pressure, and CH_2Cl_2 (25 mL) was added. The salt was filtered off, and the filtrate was concentrated under reduced pressure. The crude product was purified through silica gel column chromatography with a solvent gradient system using ethyl acetate and hexane (0-1.5% EtOAc in hexanes) to obtain the pure product **2.2** as a clear yellow oil (200 mg; 45% yield). The compound was characterized by ^{1}H and ^{13}C NMR, which is in accordance with the literature report.[21]

Synthesis of 1-(3,5-bis(bromomethyl)benzyl)pyridin-1-ium (2.3) — To stirring solution of 1,3,5-tris(bromomethyl)benzene (**1**, 1.40 mmol) in acetone solvent pyridine (1.3 mmol) was added, and the resulting mixture was stirred for 12 hours at room temperature. A white precipitate was observed, which was filtered, and washed with acetone to afford the desired product **2.3** as a white solid (350 mg, 70%). The compound was characterized by ^{1}H and ^{13}C NMR, which is in accordance with the literature report.[22]

Synthesis of ((5-(azidomethyl)-1,3-phenylene)bis(methylene))bis(dodecylsulfane) (2.4) — To a stirring solution of 1-(azidomethyl)-3,5-bis(bromomethyl)benzene (**2.2**, 0.31 mmol) in CH_3CN/H_2O (3:1 in volume) was slowly added (dropwise) a previously stirring solution of dodecanthiol and sodium bicarbonate in CH_3CN/H_2O (3:1 in volume) at room temperature. The resulting reaction mixture was stirred for 36 hours. After that, the solvent was removed under reduced pressure. Then the reaction mixture was diluted with cold water and ethyl acetate. The organic layer was extracted with EtOAc (3 × 50 mL) and washed with brine, and dried over anhydrous Na_2SO_4. The organic solvent was removed under reduced pressure. The crude reaction mixture was purified through silica gel column chromatography with a solvent gradient system using ethyl acetate and hexane (0-10% EtOAc in hexane) to afford compound **2.4** as a colorless gummy solid. Characterization of the compound : Colourless gummy liquid (yield – 87%) ^{1}H NMR (600 MHz, $CDCl_3$) δ_{ppm} 7.23 – 7.22 (s, 1H), 7.14 (s, 2H),, 4.31 (s, 2H), 3.69 – 3.66 (m, 4H), 2.42 – 2.37 (m, 4H), 1.57 – 1.50 (m, 4H), 1.35 – 1.24 (m, 36H), 0.88 (t, 3H); ^{13}C NMR (151 MHz, $CDCl_3$) δ_{ppm} 139.7, 135.8, 129.3, 127.2, 54.5, 36.0, 31.9, 31.4, 29.7, 29.6, 29.6, 29.5, 29.4, 29.3, 29.2, 28.9, 22.7, 14.1; HRMS (ESI) calcd. for $C_{33}H_{63}N_4S_2$ $[M+NH_4]^+$: 579.4494, found: 579.4463.

Synthesis of 1-(3,5-bis((dodecylthio)methyl)benzyl)pyridin-1-ium (2.5a) — To a stirring solution of 1-(3,5-bis(bromomethyl)benzyl)pyridin-1-ium (**3**, 0.14 mmol) in CH_3CN/H_2O (3:1 in volume) was slowly added (dropwise) a previously stirring solution of dodecanthiol (0.30 mmol) and sodium bicarbonate (0.30 mmol) in CH_3CN/H_2O (3:1 in volume) at room temperature. The resulting reaction mixture was stirred for 36 hours, after that the solvent was removed under reduced pressure. Then the reaction mixture was diluted with cold water and ethyl acetate. The aqueous layer was extracted with EtOAc (3 × 50 mL) and washed with brine, and dried over anhydrous Na_2SO_4. The organic solvent was removed under reduced pressure. The crude reaction mixture was purified through silica gel column chromatography with a solvent gradient system using ethyl acetate and hexane (0.1-10% EtOAc in hexanes) to afford compound **2.5a** as a colorless gummy liquid. Characterization of compound: colorless gummy liquid (yield – 81%) ^{1}H NMR (600 MHz, $CDCl_3$ + DMSO-d_6) 9.38 – 9.37 (m, 2H), 8.38 – 8.34 (m, H), 7.99 – 7.95 (m, 1H), 7.33 (s, 1H), 7.27 (s, 1H), 7.20 (s, 1H), 6.17 (s, 2H), 2.68 (s, 1H), 2.37 – 2.30 (m, 4H), 1.51 – 1.43 (m, 4H), 1.25 – 1.18 (m, 38H), 0.81 (t, 3H); ^{13}C NMR (151 MHz, $CDCl_3$) δ_{ppm} 145.2, 145.0, 140.9, 132.9,

130.9, 128.3, 128.2, 64.3, 41.0, 36.0, 32.1, 31.9, 29.6, 29.5, 29.3, 29.2, 28.9, 22.6, 14.0; HRMS (ESI) calcd. for $C_{38}H_{64}NS_2$ $[M]^+$: 598.4480, found: 598.4487

***Synthesis of ((5-(pyridin-1-ium-1-ylmethyl)-1,3-phenylene)bis(methylene))bis(dodecyl(methyl)sulfonium)* (2.7*a*)** — To stirring solution of 1-(3,5-bis((dodecylthio)methyl)benzyl)pyridin-1-ium (**2.5a**, 0.08 mmol) in dry DCM solvent was added $AgBF_4$ (0.08 mmol) and methyl iodide (0.2 mmol) and the resulting mixture was stirred for 5 hours at room temperature. The progress of the reaction was monitored by TLC. After consumption of compound **2.5a**, the solvent was removed under reduced pressure and the resulting mixture was filtered off using a pad of celite to remove silver salt. Then the crude mixture was washed with ether and CH_3CN to afford compound **2.7a** as a brown gummy liquid. Characterization of compound: Brown gummy liquid (yield – 77%); ^{1}H NMR (600 MHz, DMSO-*d*$_6$) δ_{ppm} 9.14 – 9.13 (m, 2H), 8.70 – 8.67 (m, 1H), 8.24 – 8.21 (m, 2H), 7.63 (s, 2H), 7.57 (s, 1H), 5.93 (s, 1H), 4.80 – 4.63 (m, 4H), 2.79 (s, 6H), 1.76 – 1.63 (m, 4H), 1.34 – 1.18 (m, 39H), 0.86 (t, 6H); ^{13}C NMR (151 MHz, DMSO-*d*$_6$) δ_{ppm} 146.8, 145.5, 136.6, 132.4, 130.9, 128.9, 62.9, 46.1, 44.1, 40.91, 31.7, 29.5, 29.4, 29.2, 29.1, 28.8, 28.2, 23.7, 22.5, 21.9, 14.4; ES-MS (ESI+) m/z: $[(M + 3BF_4^-]$ 609.4756.

***Synthesis of ((5-(pyridin-1-ium-1-ylmethyl)-1,3-phenylene)bis(methylene))bis(ethyl(methyl)sulfonium)* (2.7*b*)** — To a stirring solution of 1-(3,5-bis(bromomethyl)benzyl)pyridin-1-ium (**2.3**, 0.28 mmol) in in CH_3CN/H_2O (3:1 in volume) was slowly added (dropwise) a previously stirring solution of ethanethiol (0.60 mmol) and sodium bicarbonate (0.60 mmol) in CH_3CN/H_2O (3:1 in volume) at room temperature. The resulting reaction mixture was stirred for 36 hours. After that, the solvent was removed under reduced pressure. Then the reaction mixture was diluted with cold water and ethyl acetate. The organic layer was extracted with EtOAc (3 × 50 mL) and washed with brine, and dried over anhydrous Na_2SO_4. After that, the solvent was removed under reduced pressure to afford a white solid which was used for the next reaction without further purification. Then to the stirring solution of above white solid 1-(3,5-bis((ethylthio)methyl)benzyl)pyridin-1-ium (0.06 mmol) (**2.5b**) in dry DCM was added $AgBF_4$ (0.06 mmol), and methyl iodide (0.16 mmol), and the resulting mixture was stirred for 5 hours at room temperature. The progress of the reaction was monitored by TLC. After total consumption of the starting compound, the solvent was removed under reduced

pressure, and the resulting mixture was filtered off using a pad of celite to remove silver salt. Then the crude mixture was washed with ether and CH_3CN to afford compound **2.7b** as a brown gummy liquid. Characterization of compound: Dark Brown gummy liquid (yield – 71%) ^1H NMR (600 MHz, DMSO-d_6) δ_{ppm} 9.15 – 9.08 (m, 2H), 8.69 – 8.61 (m, 1H), 8.23 – 8.21 (m, 2H), 7.95 (s, 1H), 7.58 (s, 2H), 5.93 (s, 2H), 4.71 – 4.62 (m, 4H), 2.89 (m, 2H), 2.77 (s, 6H), 2.73 (s, 2H), 1.33 (t, 3H); ^{13}C NMR (151 MHz, DMSO-d_6) δ_{ppm} 162.8, 146.8, 145.5, 136.6, 133.8, 132.2, 130.9, 128.9, 66.1, 62.9, 59.3, 43.4, 35.5, 31.2, 21.2, 11.25, 8.84; ES-MS (ESI^+) m/z: [$(M + 3BF_4^-$] 889.525.

Synthesis of ((5-((4-(sulfomethyl)-1H-1,2,3-triazol-1-yl)methyl)-1,3-phenylene)bis(methylene))bis(dodecyl(methyl)sulfonium) (2.8) — To a stirring solution of ((5-(azidomethyl)-1,3-phenylene)bis(methylene))bis(dodecylsulfane) (**2.4**, 0.09 mmol) in DMF (3 mL) was added prop-2-yne-1-sulfonic acid (0.09 mmol) and the mixture was stirred for 10 minutes. After that, sodium ascorbate (0.003 mmol) and CuI (0.002 mmol) were added to the reaction mixture and the solution was allowed to stir for 24 hours at room temperature, and the reaction was monitored by TLC. After that, the unused solvent was removed under reduced pressure and diluted with ethyl acetate. The organic layer was separated, washed with brine, and dried over anhydrous Na_2SO_4. The solid crude product was washed with distilled hexane, the desired product **2.6** was almost pure, and the reaction mixture was used for the next reaction without further purification. To a stirring solution of compound **2.6** (0.58 mmol) in dry DCM $AgBF_4$ (0.058 mmol) was added, then methyl iodide (0.15 mmol), and the resulting mixture was stirred for 5 hours at room temperature. The progress of the reaction was monitored by TLC. After maximum consumption of compound **2.6**, the solvent was removed under reduced pressure, and the resulting mixture was filtered off using a pad of celite to remove silver salt. Then the crude mixture was washed with ether and CH_3CN to afford compound **2.8** as a brown gummy solid. Characterization of compound: Dark Brown gummy solid (yield – 68%) - ^1H NMR (600 MHz, $CDCl_3$) δ_{ppm} 9.82 (s, 1H), 8.02 (s, 2H), 7.95 (s, 1H), 4.71 – 4.62 (m, 2H), 3.78 – 3.76 (m, 2H), 3.34 – 3.17 (m, 4H), 2.81 (s, 6H), 2.35 – 2.28 (m, 1H), 1.87 – 1.78 (m, 4H), 1.44 – 1.40 (m, 4H), 1.29 – 1.23 (m, 41H), 0.86 (t, 6H); ^{13}C NMR (151 MHz, $CDCl_3$) δ_{ppm} 138.3, 133.0, 130.1, 129.0, 128.0, 125.3, 68.1, 47.2, 44.6, 41.4, 31.9, 29.7, 29.7, 29.6, 29.4, 29.0, 28.4, 25.6, 24.1, 22.7, 21.3, 14.1; ES-MS (ESI+) m/z: [$(M/2 + 2BF4^- + Na^+$] 552.0522.

2.4.3. Stock and working compound preparation —The stock solutions of the compounds were prepared in chloroform and stored at -20˚C. For working standard, the compounds were taken in a separate vial, and chloroform was removed under reduced pressure. The required concentration of the compound was prepared by adding a buffer to the dried compound and kept for 12 hours for hydration, and vortexed with intermittent sonication to form liposomes.

2.4.4. Zeta-potential and DLS measurement — Surface potential and hydrodynamic diameter of the compounds in the aqueous environment was measured by zeta potential and dynamic light scattering (DLS) using Zeta sizer ZS90 (Malvern, Westborough, MA) instrument at 25 °C. The stock solution of the compound was prepared in chloroform, and multi-layered vesicles were prepared by rotary evaporation method with the help of a vacuum pump. To this dried compound, phosphate-buffered saline (PBS; 137 mM NaCl, 2.7 mM KCl, 8 mM Na_2HPO_4, and 2 mM KH_2PO_4 at pH 7.4) buffer was added and kept for hydration overnight at 50˚C. To obtain the unilamellar vesicles sample vial was underwent vertexing and intermittent sonication. Disposable zeta cells (DTS1061) and 3 mL fluorescence cuvette were used for surface potential and DLS measurement.

2.4.5. Transmission electron microscopic measurements — The transmission electron microscope (TEM) was used to investigate the morphology of the aqueous soluble aggregates of the lipids. The lipid solution was prepared by the method mentioned above in PBS, pH 7.4. The freshly prepared lipid solution (without extrusion) was diluted to half of its original concentration using 1 mL PBS, pH 7.4. Then 10 µL of lipid solution was taken and placed onto a carbon-coated copper grid and allowed to absorb for 1 minute. The grid was then carefully blotted with filter paper, and only a trace amount of the solution in the middle of the grid was kept. After that, the grid was allowed to dry for 10 minutes at 30 °C. Finally, 5-10 µL of 2% uranyl acetate solution (in water) was added to the grid and allowed to dry for another 1 min. The excess uranyl acetate solution was wicked off, and the grid was dried overnight at 30 °C. The images were collected using a JEOL JEM 2100 transmission electron microscope (operated at a maximum accelerating voltage of 200 kV).

2.4.6. Antimicrobial activity and bactericidal activity — The antimicrobial activities of the compounds were tested by using broth dilution assay in 96 well plate. *Escherichia coli* MTCC 1687, *Pseudomonas aeruginosa* MTCC 2488 were cultured in Luria Bertani (LB),

and *S. aureus* MTCC 96, MRSA cells were cultured in Brain Heart Infusion (BHI) broth media till the mid logarithmic phase at 37˚C in a shaker incubator and harvested by centrifugation. Then cells were washed with PBS buffer and resuspended in the same buffer. In the presence of varying concentrations of the compounds, bacterial cells were incubated at 10^6 CFU/mL at 37˚C. After 14-16 hours of incubation, the optical density (OD) was measured at 600 nm by using a Tecan infinite M200 Plate reader. For the bactericidal activity test, the solution with no visible growth was transferred into a fresh well containing only media. The plate was incubated for 24 hours at 37˚C, and then the OD was measured. To get the closest minimum inhibitory concentration (MIC) value, this antimicrobial experiment was repeated at the variable concentration range, and at the reported MIC value procedure was repeated thrice.

2.4.7. Antibiotic loading and release profile study — The stock solutions of tetracycline amoxicillin antibiotics were prepared in PBS. The
compound was dissolved in chloroform and dried by rotary evaporation method to form a multilayer film. To this dried vial containing a dried layer of the compound, the aqueous solution of antibiotic was added and incubated at 37°C in a water bath for hydration. For good encapsulation of the antibiotic, the liposomes were freeze and thaw for 7 to 8 times, followed by a vigorous vortex. The unloaded antibiotic was removed by centrifugation. The antibiotic loading efficacy was measured by UV-Visible spectrophotometer. Encapsulated liposome was treated with 5 % Triton X-100 to break the liposome, and released antibiotic was monitored by its absorbance, and only antibiotic absorption was also recorded. The concentration of loaded antibiotic was calculated by Lambert-Beer's law, $A = \varepsilon.C_{ab}.l$, where C_{ab} is the released antibiotic concentration from the liposome, and for this calculation, the calibration curve was obtained to calculate extinction coefficient (ε) by the absorption of antibiotics at different concentration. The drug release profile was observed at different time intervals up to 60 hours by fluorescence spectrofluorometer, and for 100 % release of antibiotic, liposome suspension was treated with Triton X-100 followed by sonication and fluorescence measurement. The antimicrobial activity of the antibiotic encapsulated liposome was measured by the same experimental protocol.

2.4.8. Antibiofilm activity study — The antibiofilm activity study was performed by the crystal violet staining method. The *S. aureus* MTCC 96 is a well-known non-motile, sessile

strain and forms a biofilm on the bottom of the wells. The bacterial cells were grown and treated with compounds, as mentioned earlier section. After the overnight incubation, the planktonic cells were pipetted out, and wells were rinsed with PBS. The wells were air-dried under laminar airflow. Then, the crystal violet solution (1%, v/v) was added to each well, and the plate was incubated for 20 minutes. After incubation, the crystal violet solution was taken out, and the wells were dried. Then ethanol (95%) was added to each well, and absorbance was taken at 590 nm by using a 96 micro-titre plate reader (Infinite M200, TECAN, Switzerland).

2.4.9. Propidium iodide uptake assay — The stock solution (1.5 mM) of propidium iodide (PI) was prepared in sterile MilliQ water and stored at 4˚C. The *S. aureus* MTCC 96 cells were cultured overnight and collected by centrifugation, and resuspended in the same media. Cells were again diluted in media at 10^6 CFU/mL, and after the addition of the compound, the cells were incubated at 37˚C at 180 rpm. The sample (1 mL) was collected at the 1st, 2nd, 3rd hour. The culture was centrifuged and washed with PBS, and the cells were incubated with PI at 30 µM concentration for half an hour. Cells were again centrifuged and washed with and resuspended in the PBS, and the fluorescence measurement was recorded at an excitation wavelength of 535 and emission wavelength of 617 in the spectrofluorometer (HORIBA, flioroMax-4).

2.4.10. Fluorescence imaging assay — The PI and cFDA-SE dyes were used to stain dying and viable bacterial cells. The *S. aureus* cells were cultured and harvested, as mentioned in the earlier section. Cells were treated with the compound, and as a control, the only buffer was added to the cell culture. After 5 hrs of incubation, the cells were collected by centrifugation and washed with buffer, and diluted up to 10^6 CFU/mL. The cells were separately stained with PI at a concentration of 30 µM and cFDA-SE at a concentration of 10 µM. After 30 min of incubation, 10 µL of the stained sample was taken on a thin glass slide and observed under the fluorescence microscope.

2.4.11. Morphological Study — Morphological assessment was done by field emission scanning electron microscope (FESEM). The S. *aureus* MTCC 96 and *E. coli* MTCC 1687 cells were cultured and harvested by centrifugation at 5000 rpm for 5 minutes. Cells were washed and treated with the compound, and control was taken as the bacterial culture

without compound treatment. After 5 hours of incubation, cells were collected by centrifugation, washed with Mili-Q water, and drop-casted on aluminium foil studded glass grid, and air-dried under laminar airflow. The drop-casted sample was again mounted on FESEM metal grid sandwiched by carbon tape before the FESEM analysis sample was double-coated by gold.

2.4.12. Membrane Depolarization Study — For this study S. aureus, MTCC 96 cells were grown as mentioned in the above section till mid-log phase and harvested, followed by resuspension in HEPES buffer (10 mM HEPES and 50 mM glucose). To this, $DiSC_35$ was added at a final concentration of 0.4 µM, and cells were incubated for 1 h, and after this, KCl was added to cells suspension at a concentration of 100 mM. After 10 min incubation, variable concentrations (0, 2, and 4 µM) of the compound and 30 µM valinomycin as a positive control were added to the cell suspension, and fluorescence spectra were recorded at excitation and emission wavelength of 620 nm and 650 nm.

2.4.13. Cytocompatibility Test — To test the viability of human cells in presence of antimicrobial drugs, HeLa cells ($1x10^4$ cells/well) were seeded into 96 well plates in 100 µL of DMEM per well and left overnight for attachment. The cells were then treated with variable concentrations of compound and only buffer as control. After incubation for 24h, 10 µL MTT reagent (5 mg/mL) was added to each well (containing cells in DMEM media with compounds) and then incubated for another 3h at 37 °C in a CO_2 incubator. Later, the MTT reagent was removed from the wells, and formazan crystals were dissolved by adding 100 µL of dimethyl sulfoxide (DMSO) in each well. Absorbance was recorded at 570 nm to measure the cell viability by using a plate reader.

2.4.14. Haemolytic Assay — To test the toxicity of the compound against the blood cells, hemolysis screening was performed according to the reported protocol. The hemolytic assay was performed with erythrocytes extracted from fresh human blood as per the guidelines given by Institutional Animal Ethical Committee (IAEC). Blood was centrifuged at 1500 rpm for 10 minutes, the supernatant was discarded, and cells were washed with PBS, and 5% hematocrit was prepared in the same media. Serially diluted sulfonium compounds were added in a vial up to 240 µL, including a negative control with only buffer and positive control with 0.5% Triton X-100 and 60 µL of the 5% hematocrit was added to each vial and incubated for 1 hour at 37˚C. After incubation, vials were centrifuged at 1500

rpm for 10 minutes, and 50 µL of the supernatant was added to fresh 96 well plates. The absorbance was recorded at 410 nm % hemolysis was calculated by comparing the absorbance of the sample with positive control and of the negative control.

2.4.15. ^{1}H NMR and ^{13}C NMR spectra of synthesized compounds:

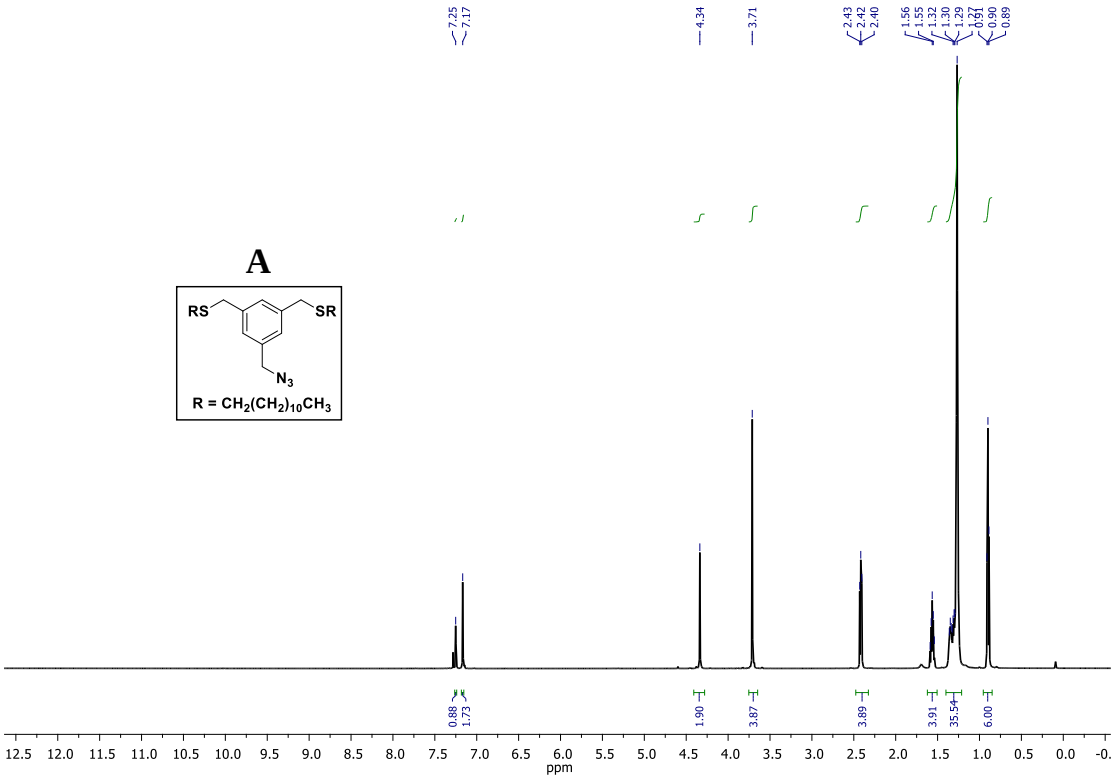

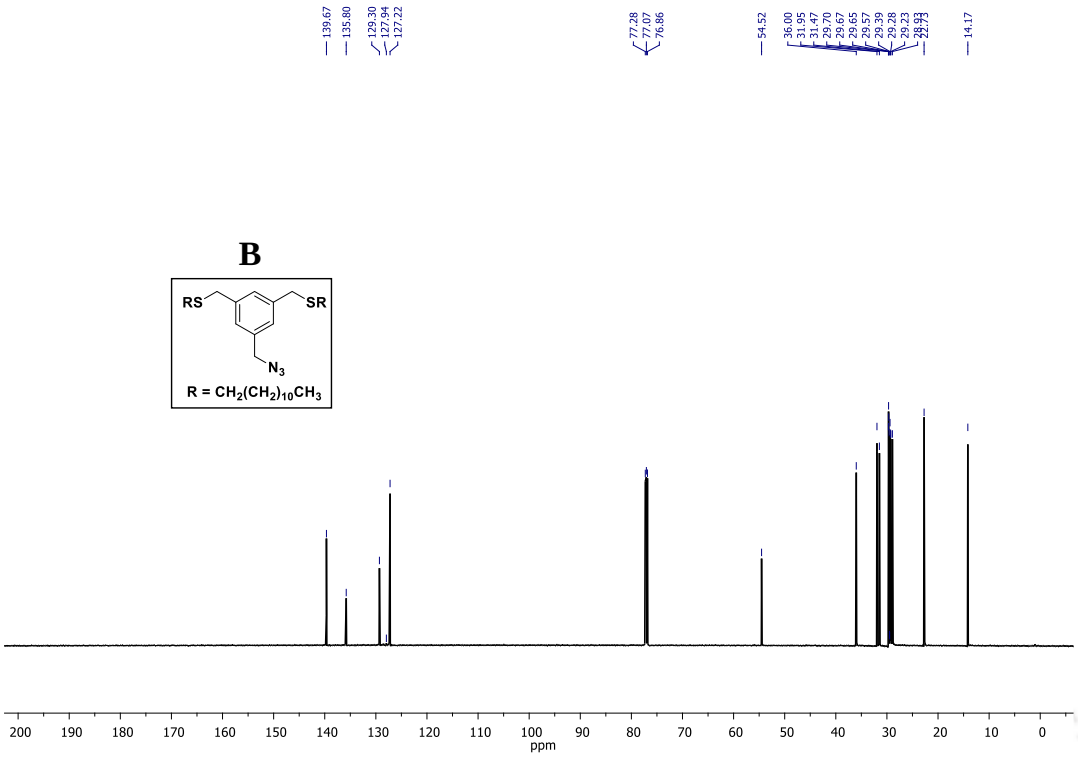

Fig. 2.7. ^{1}H NMR (A) and ^{13}C NMR (B) spectra of lipid **2.4.**

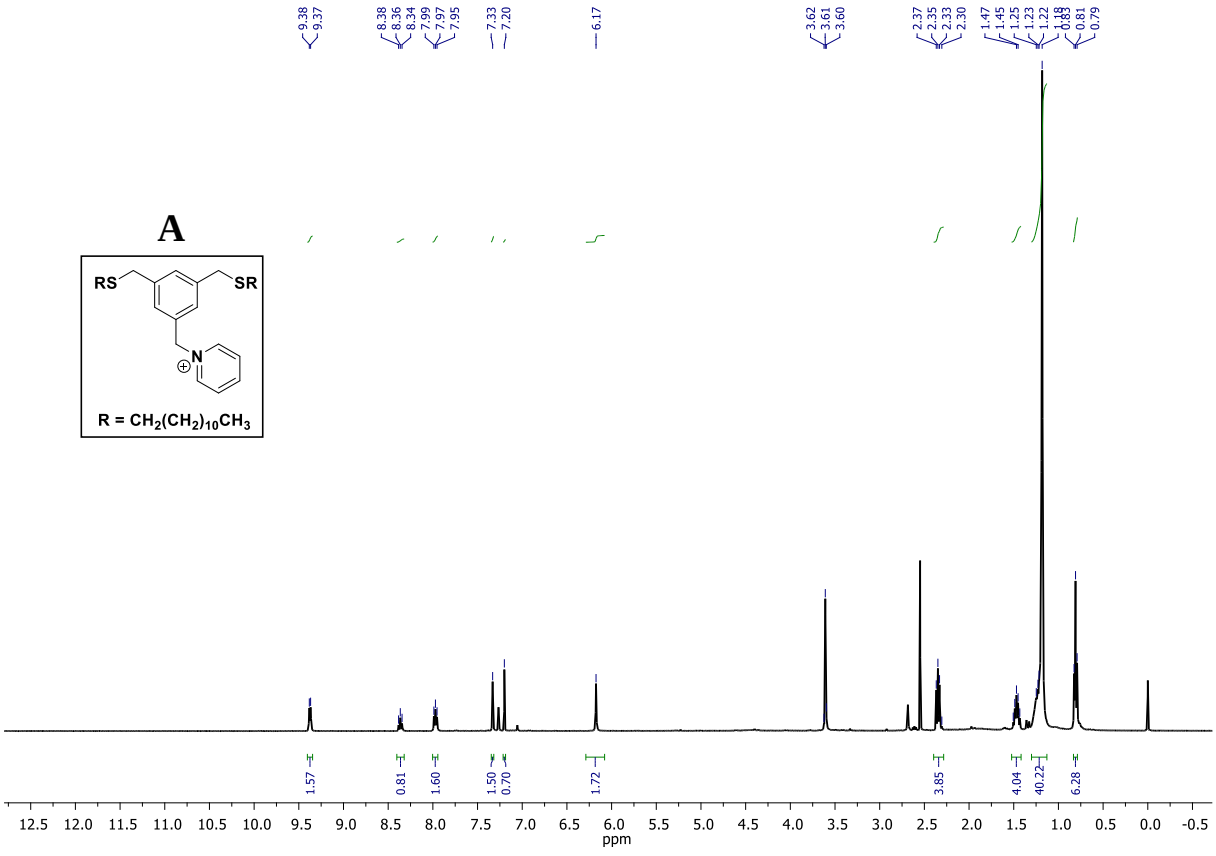

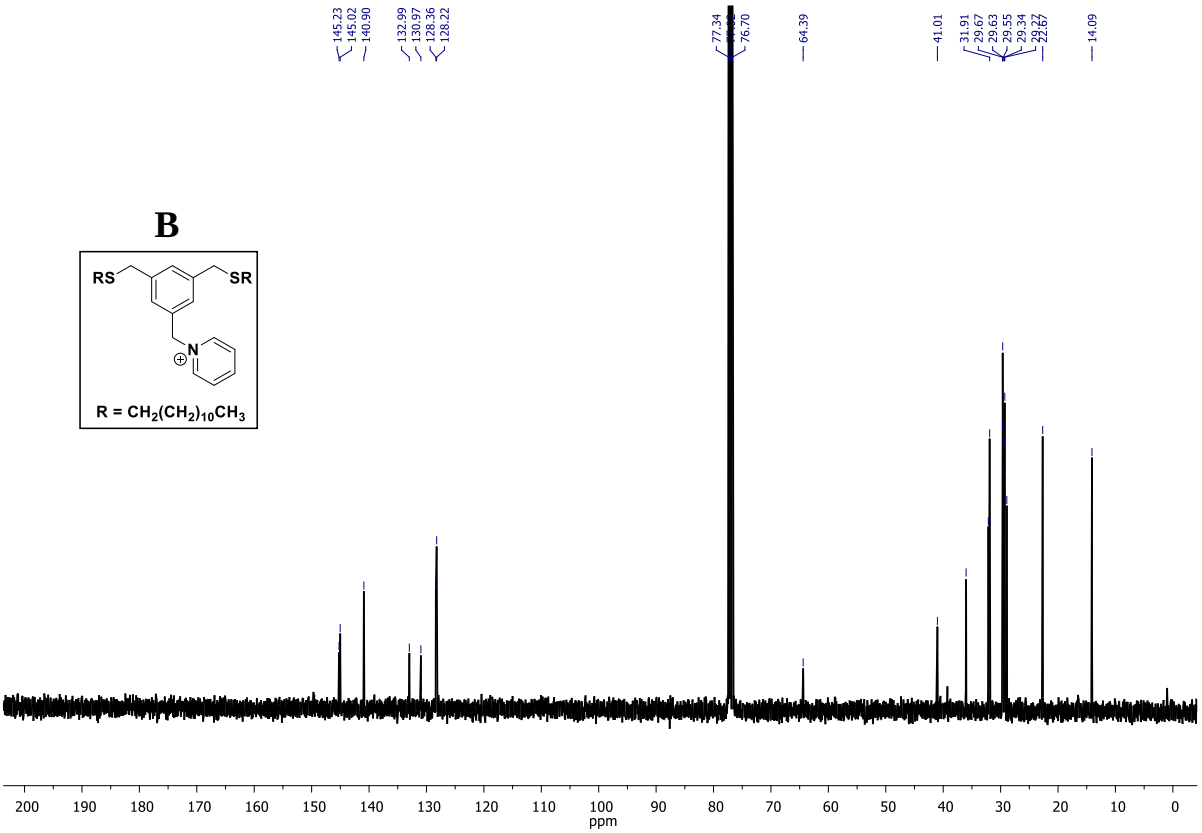

Fig. 2.8. ^{1}H NMR (A) and ^{13}C NMR (B) spectra of lipid **2.7a.**

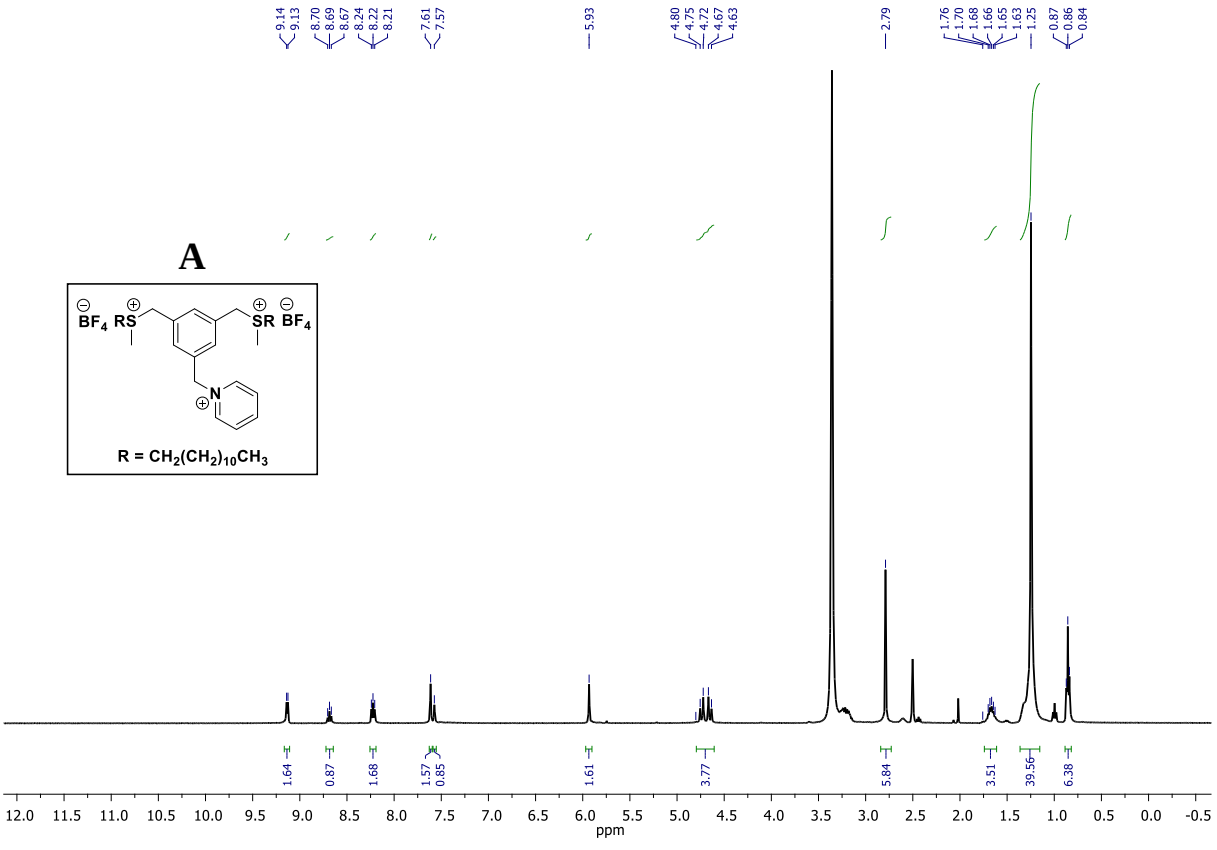

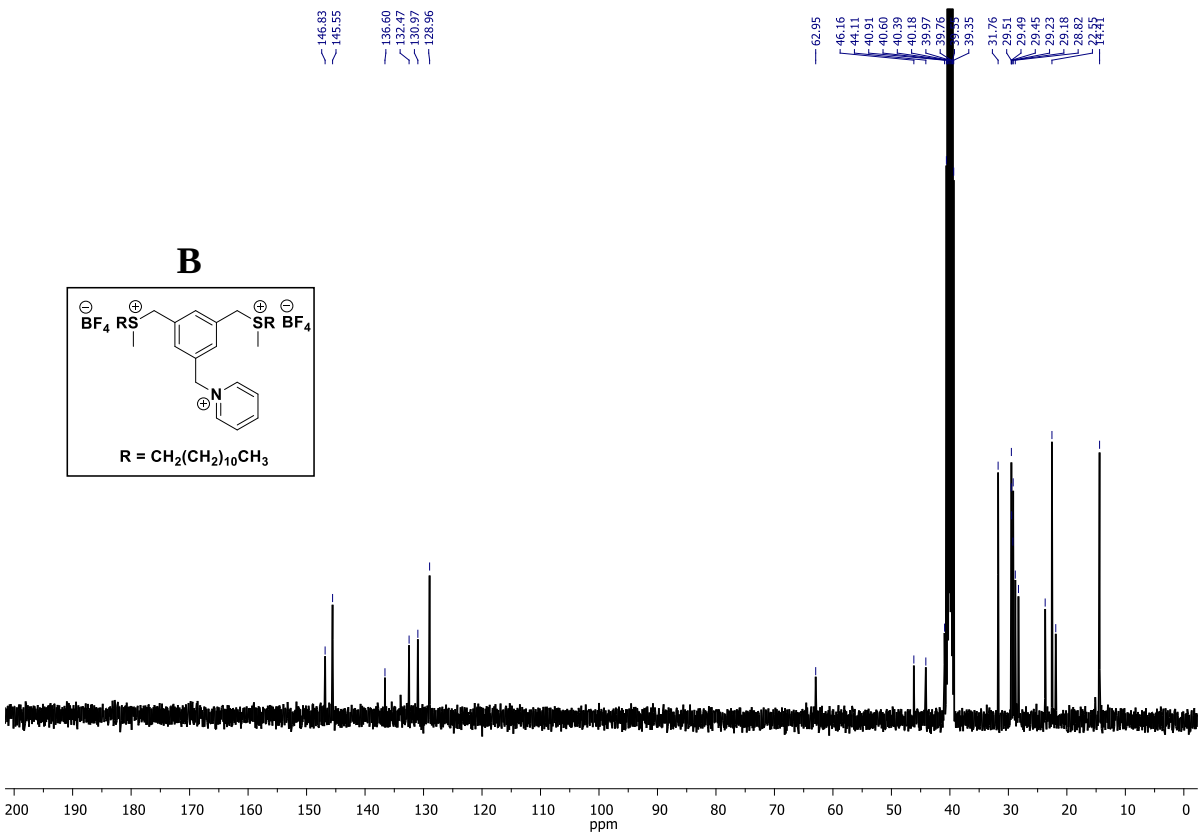

Fig. 2.9. ^{1}H NMR (A) and ^{13}C NMR (B) spectra of lipid **2.7b.**

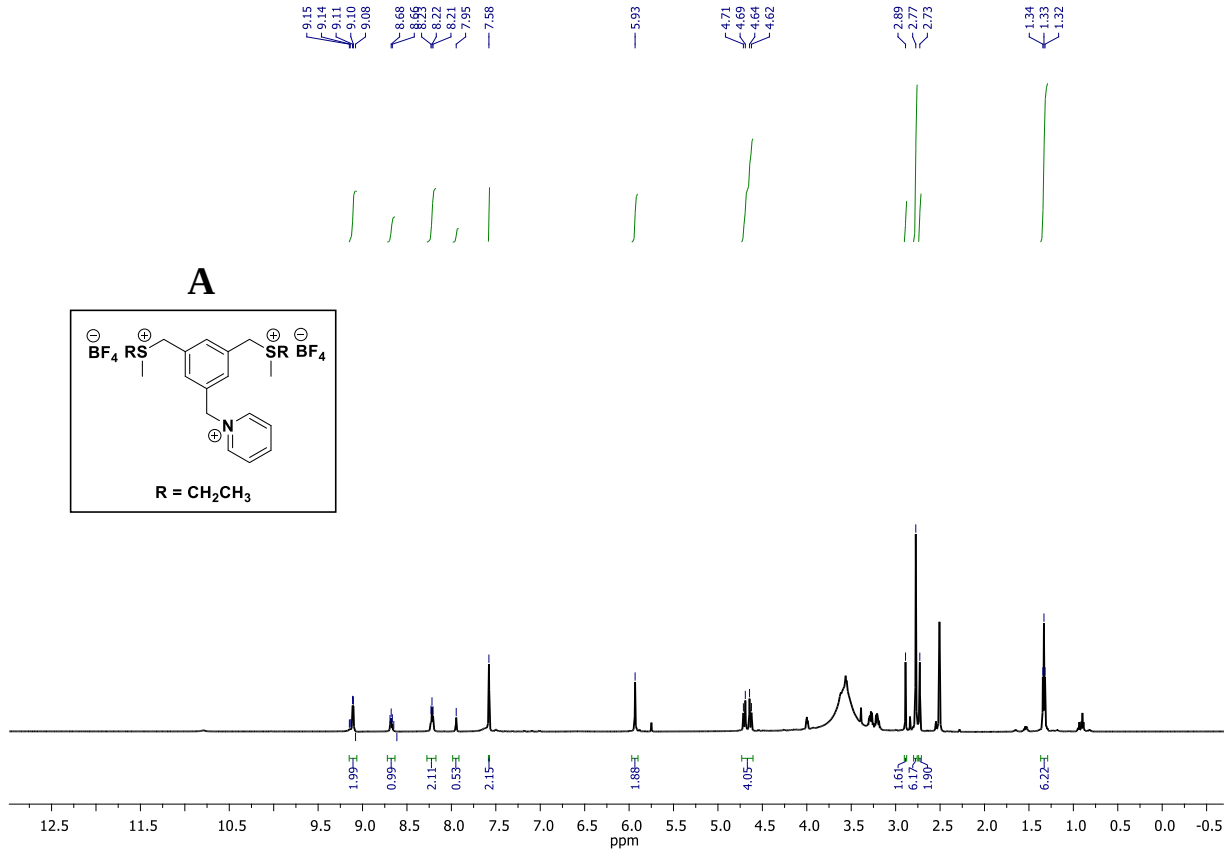

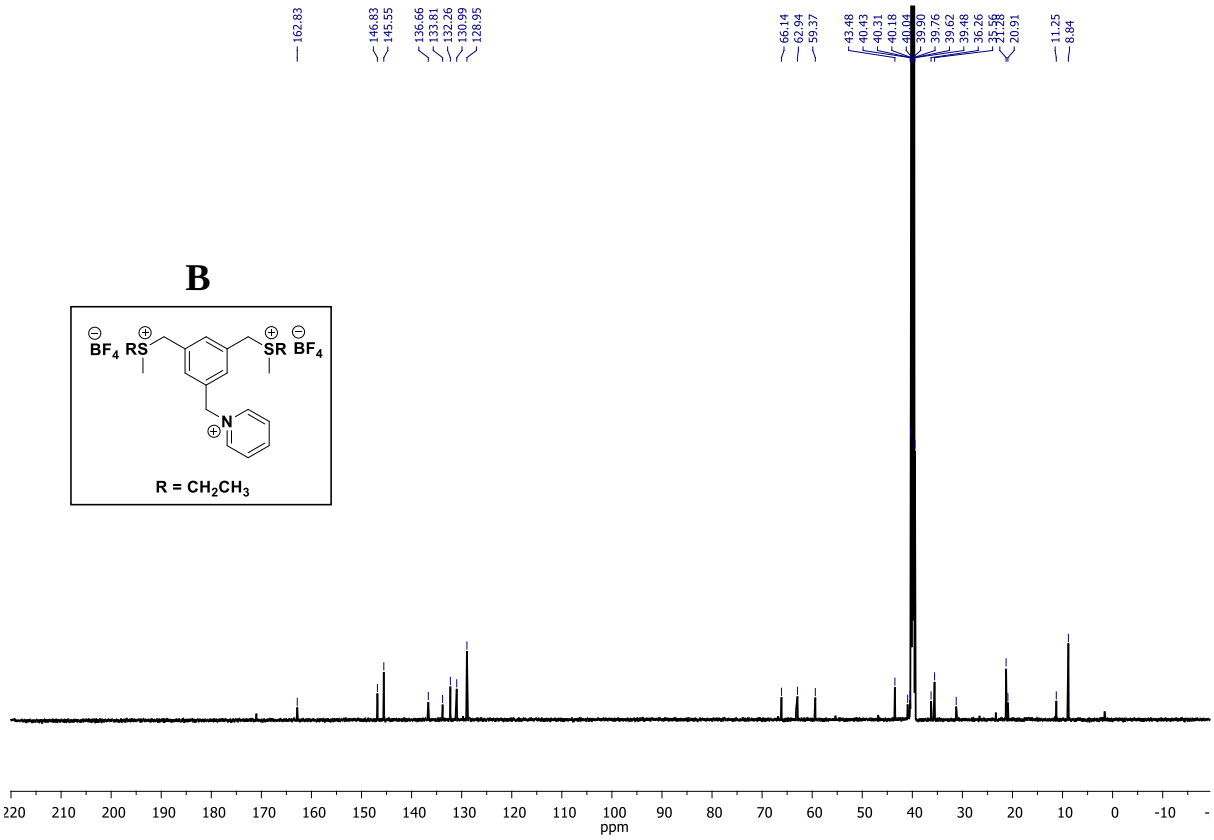

Fig. 2.10. ^{1}H NMR (A) and ^{13}C NMR (B) spectra of lipid **2.8.**

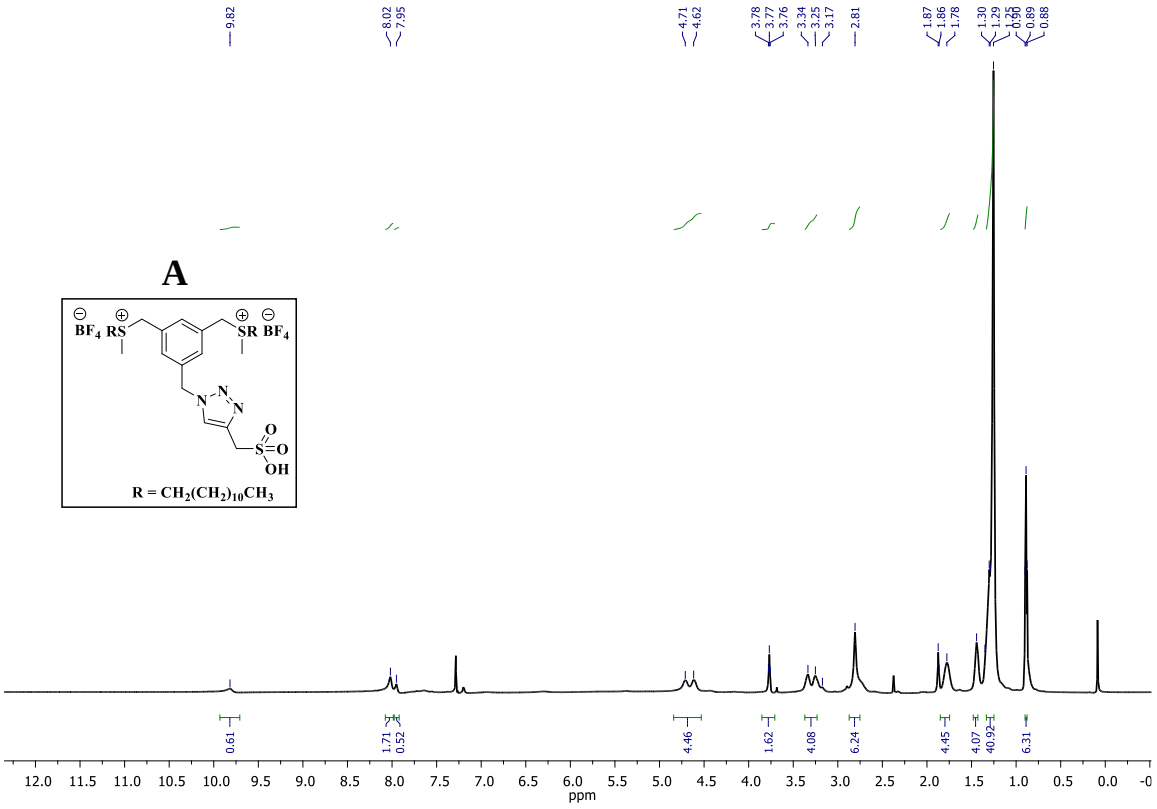

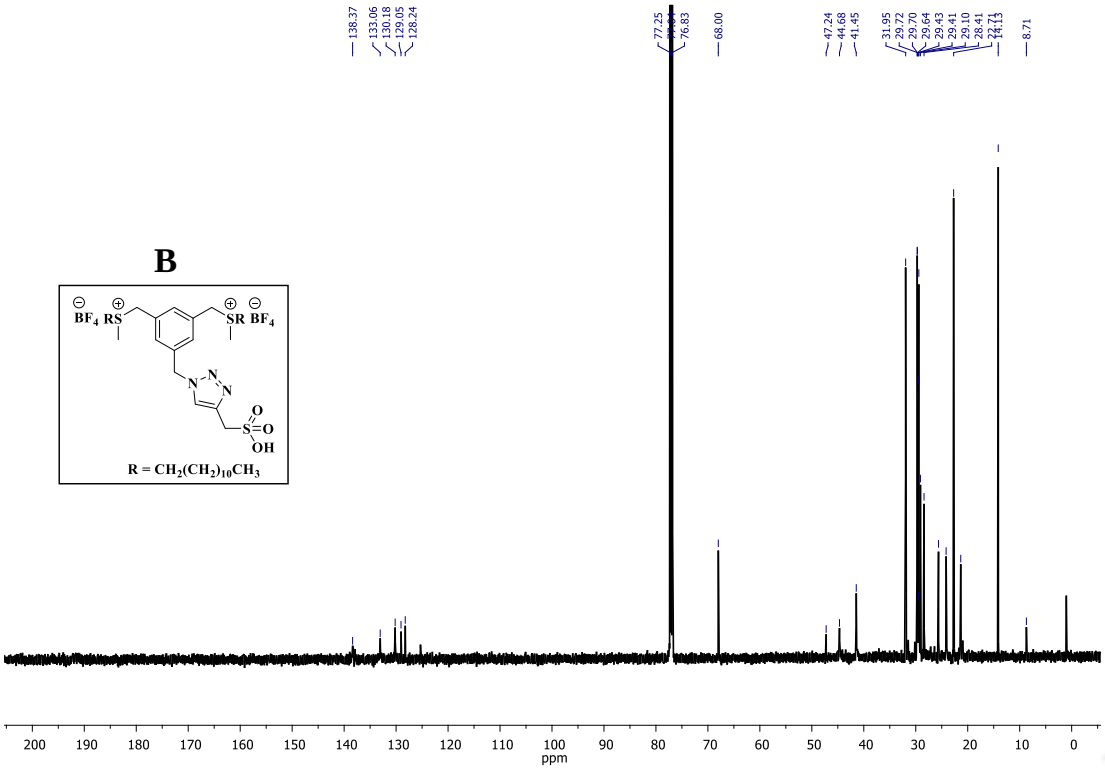

Fig. 2.11. ^{1}H NMR (A) and ^{13}C NMR (B) spectra of lipid **SL5.**

2.5 References:

1. Dey, S.; Patel, A.; Raina, K.; Pradhan, N.; Biswas, O.; Thummer, R. P.; Manna, D. J. C. C., A stimuli-responsive anticancer drug delivery system with inherent antibacterial activities. *Chem. Commun.* **2020,** *56* (11), 1661-1664.

2. Wang, D. Y.; van der Mei, H. C.; Ren, Y. J.; Busscher, H. J.; Shi, L. Q., Lipid-Based Antimicrobial Delivery-Systems for the Treatment of Bacterial Infections. *Front Chem* **2020,** *7*.

3. Kumar, A.; Boyer, C.; Nebhani, L.; Wong, E. H. H., Highly Bactericidal Macroporous Antimicrobial Polymeric Gel for Point-of-Use Water Disinfection. *Sci Rep* **2018,** *8* (1), 7965.

4. Dey, S.; Patel, A.; Raina, K.; Pradhan, N.; Biswas, O.; Thummer, R. P.; Manna, D., A stimuli-responsive anticancer drug delivery system with inherent antibacterial activities. *Chem Commun (Camb)* **2020,** *56* (11), 1661-1664.

5. Guan, D.; Chen, F.; Qiu, Y.; Jiang, B.; Gong, L.; Lan, L.; Huang, W., Sulfonium, an Underestimated Moiety for Structural Modification, Alters the Antibacterial Profile of Vancomycin Against Multidrug-Resistant Bacteria. *Angew Chem Int Ed Engl* **2019,** *58* (20), 6678-6682.

6. Balouiri, M.; Sadiki, M.; Ibnsouda, S. K., Methods for in vitro evaluating antimicrobial activity: A review. *J Pharm Anal* **2016,** *6* (2), 71-79.

7. Gilbert, P.; Moore, L. E., Cationic antiseptics: diversity of action under a common epithet. *J Appl Microbiol* **2005,** *99* (4), 703-15.

8. Moore, L. E.; Ledder, R. G.; Gilbert, P.; McBain, A. J., In vitro study of the effect of cationic biocides on bacterial population dynamics and susceptibility. *Appl Environ Microbiol* **2008,** *74* (15), 4825-34.
9. Papanicolas, L. E.; Gordon, D. L.; Wesselingh, S. L.; Rogers, G. B., Not Just Antibiotics: Is Cancer Chemotherapy Driving Antimicrobial Resistance? *Trends Microbiol* **2018,** *26* (5), 393-400.
10. Koburger, T.; Hübner, N.-O.; Braun, M.; Siebert, J.; Kramer, A., Standardized comparison of antiseptic efficacy of triclosan, PVP-iodine, octenidine dihydrochloride, polyhexanide and chlorhexidine digluconate. *J Antimicrob Chemother* **2010,** *65* (8), 1712-1719.
11. Karpiński, T. M., Efficacy of octenidine against Pseudomonas aeruginosa strains. *European Journal of Biological Research* **2019,** *3*, 135-140.
12. Hirayama, M., The antimicrobial activity, hydrophobicity and toxicity of sulfonium compounds, and their relationship *Biocontrol Sci* **2011,** *16* (1), 23-31.
13. Li, L.; Jia, D.; Wang, H.; Chang, C.; Yana, J.; Zhao, Z. K., Synthesis of sulfonium N-chloramines for antibacterial applications. *New J. Chem.* **2020,** *44*, 303-307.
14. Kanazawa, A.; Ikeda, T.; Endo, T., Antibacterial activity of polymeric sulfonium salts. *Polymer Chem.* **1993,** *31* (11), 2873-2876.
15. Uppu, D. S.; Akkapeddi, P.; Manjunath, G. B.; Yarlagadda, V.; Hoque, J.; Haldar, J., Polymers with tunable side-chain amphiphilicity as non-hemolytic antibacterial agents. *Chem Commun (Camb)* **2013,** *49* (82), 9389-91.
16. Bayles, K. W., Bacterial programmed cell death: making sense of a paradox. *Nat Rev Microbiol* **2014,** *12* (1), 63-9.
17. Zhao, G.; Usui, M. L.; Lippman, S. I.; James, G. A.; Stewart, P. S.; Fleckman, P.; Olerud, J. E., Biofilms and Inflammation in Chronic Wounds. *Adv Wound Care (New Rochelle)* **2013,** *2* (7), 389-399.
18. Funari, R.; Bhalla, N.; Chu, K. Y.; Soderstrom, B.; Shen, A. Q., Nanoplasmonics for Real-Time and Label-Free Monitoring of Microbial Biofilm Formation. *ACS Sens* **2018,** *3* (8), 1499-1509.
19. Yasir, M.; Dutta, D.; Willcox, M. D. P., Comparative mode of action of the antimicrobial peptide melimine and its derivative Mel4 against Pseudomonas aeruginosa. *Sci Rep* **2019,** *9* (1), 7063.
20. Kannan, R.; Prabakaran, P.; Basu, R.; Pindi, C.; Senapati, S.; Muthuvijayan, V.; Prasad, E., Mechanistic Study on the Antibacterial Activity of Self-Assembled Poly(aryl ether)-Based Amphiphilic Dendrimers *ACS Appl. Bio Mater.* **2019,** *8* (8), 3212–3224.
21. Werkhoven, P. R.; Elwakiel, M.; Meuleman, T. J.; van Ufford, H. C. Q.; Kruijtzer, J. A. W.; Liskamp, R. M. J., Molecular construction of HIV-gp120 discontinuous epitope mimics by assembly of cyclic peptides on an orthogonal alkyne functionalized TAC-scaffold. *Org Biomol Chem* **2016,** *14* (2), 701-710.
22. Marafino, J. N.; Gallagher, T. M.; Barragan, J.; Volkers, B. L.; LaDow, J. E.; Bonifer, K.; Fitzgerald, G.; Floyd, J. L.; McKenna, K.; Minahan, N. T.; Walsh, B.; Seifert, K.; Caran, K. L., Colloidal and antibacterial properties of novel triple-headed, double-tailed amphiphiles: exploring structure-activity relationships and synergistic mixtures. *Bioorg Med Chem* **2015,** *23* (13), 3566-73.

CHAPTER 3

ONIUM- AND ALKYL AMINE-DECORATED PROTEIN NANOPARTICLES AS ANTIMICROBIAL AGENTS AND CARRIERS OF ANTIBIOTICS TO PROMOTE SYNERGISTIC ANTIBACTERIAL AND ANTIBIOFILM ACTIVITIES

3.1. Background and objective of present work

Antibiotics-delivery systems (ADSs) are an attractive tool to fight against bacterial infections. The unique features of ADSs, such as improved solubility of hydrophobic antibiotics, prolonged antibiotic half-life, systematic circulation time, and sustained release profile, could reduce antibiotic resistance and systematic side effects. Various ADSs, including liposomes, dendrimers, nanoparticles, microspheres, and others, have been developed in this regard.[1, 2] The development of ADSs with inherent antimicrobial properties is considered a superior approach to tackling antibacterial resistance and a cost-effective strategy. Various biopolymers are currently being modified to develop antimicrobial agents or ADSs due to their superior biocompatibility and lower toxicity. In particular, the development of protein-based nanoparticles to deliver antibiotics is considered a potential strategy because of their efficient administration, protection, and transport of antibiotics.[3]

Membrane destabilizing agents can also aid the cytosol-targeted antibiotic's activity by facilitating its entry into the cell.[4, 5] However, the membrane-targeting antimicrobial drugs may also demonstrate toxicity to the host cell membrane. That is why these drugs should be prudently designed to accomplish superior biocompatibility. In this direction, the onium (quaternary ammonium, sulfonium, and phosphonium)-based molecules have been developed as membrane-disrupting antimicrobial agents.[6] Among these, sulfonium-based molecules have been found to be more biocompatible and more potent.[7]

Alkyl amine and onium-based small molecules were conjugated with albumin protein because of its few salient features over the other materials. Albumin is the most abundant and affordable transport protein with a long half-life period. It can be easily metabolized to amino acids and provide nutrients to the peripheral tissues. It contains multiple binding pockets to carry hydrophobic and hydrophilic drugs in the blood circulation system, maintains the osmotic pressure, and transports nutrients, proteins, and others. The polar surface allows it to be highly soluble in water. It can target the inflammation site with minimal toxicity. The albumin protein can be easily modified with simple biochemical reactions and does not require a lengthy process of purification. Various reports have revealed its importance to carry drugs to avoid resistance and multiple dosing in the case of anticancer and antibiotic drugs.[8-11] The proposed BSA modifications not only act as a carrier but also have inherent antimicrobial activity. BSA-based drug carrier (Nab-Paclitaxel) has been in use since 2005, and many more are ready for commercialization.[8,

[14] The mannosylated BSA has been reported to act against Gram-negative bacteria and Gram-positive bacterial strains.[12] Inspired by these observations, herein we report the development of BSA-based ADSs with inherent antimicrobial properties.

Our earlier study demonstrated the role of sulfonium-containing lipids with inherent antimicrobial activity and antibiotic delivery efficacy.[7] Its efficient bactericidal activity motivated us to explore the activity of sulfonium-modified BSA-based antibiotic carriers. We developed onium (sulfonium/ammonium) and lauryl amine tethered BSA-based nanoparticles and investigated their inherent antibacterial properties and antibiotic delivery aptitude (Figure 3.1). The sulfonium and lauryl amine conjugated BSA protein nanoparticles (PNPs) showed a synergistic effect when clinically proven antibiotics were encapsulated, fulfilling one goal of antibiotic stewardship: to reduce the effective dose of antibiotics and their exposure to other bacterial species. Initial antimicrobial studies showed that sulfonium-modified BSA (R-BSA-S) was more potent than ammonium derivative (R-BSA-N). Hence, R-BSA-S was further characterized for its nanoparticles forming aptitude in the aqueous environment and was used to encapsulate ciprofloxacin (CiproF) and ceftazidime (Cefta) antibiotics. The R-BSA-S showed membrane-disrupting activity and biofilm eradication activities to fight against the resistance mechanism of bacterial cells. It also showed negligible or no hemolytic activity and compatibility

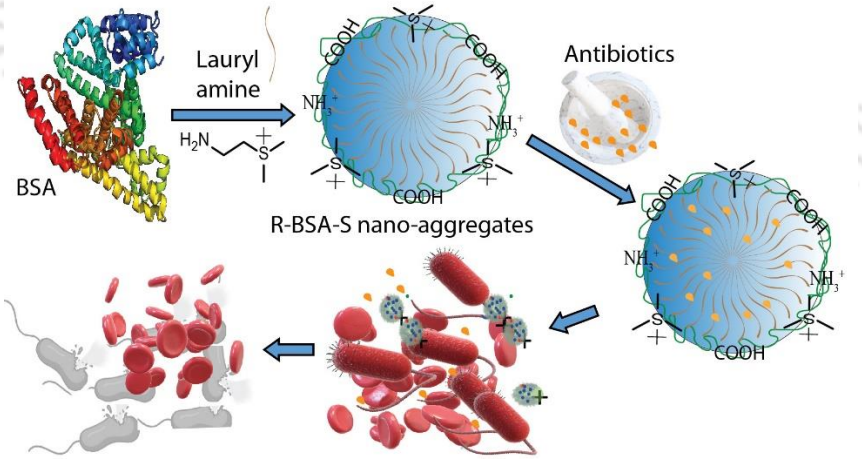

Figure 3.1. Schematic representation of the formation of modified BSA-based PNPs and their antibacterial activities.

with blood cells. Antibiofilm efficacy of the R-BSA-S and drug-encapsulated R-BSA-S was also investigated under in-vivo conditions, where compound treatment reduced the biofilm on the implanted catheter in mice. Overall, sulfonium-tethered BSA nanostructures

interact with the bacterial membranes and deliver their cargo antibiotics to achieve synergistic antibacterial and antibiofilm activities.

3.2 Result and discussion

3.2.1 Preparation and characterization of modified BSA

The BSA protein was modified with onium (sulfonium/ammonium)-based small molecules and lauryl amine and investigated their antimicrobial activity followed by antibiotic delivery efficiencies. The onium-based small molecules (2-aminoethyl)dimethylsulfonium and 2-amino-*N*,*N*,*N*-trimethylethan-1-aminium were synthesized from 2-aminoethane-1-thiol and ethylenediamine, respectively. The onium-based small molecules and lauryl amines were conjugated to the carboxyl group of acidic amino acids (aspartic and glutamic acid) of BSA by the amide-coupling method, as mentioned in our earlier reported method.[13] In our previous study, we observed that around 50 % of the acidic side chains of the BSA were modified by lauryl amine (BSA/ lauryl amine = 1:10). Hence, onium-based small molecules/lauryl amines were used in the ratio of 1:5 to modify BSA. Conjugation of onium-based small molecules and lauryl amine to the BSA were scrutinized using Fourier transform infrared (FTIR) and matrix-assisted laser desorption/ionization time-of-flight mass spectrometry (MALDI-TOF MS) techniques. The FTIR spectra of R-BSA-S revealed that the intensity of C-O-H in-plane bending (1390 cm^{-1}) was reduced, and the intensity of C-N stretching (1115 cm^{-1}) increased, suggesting the formation of amide bonds between the amine group of the onium-based molecule and carboxylic acid group of BSA protein (Figure 3.2A). The analysis of MALDI-TOF MS peaks shows an increase in the average molecular weight from 66258 Da (BSA) to 68505 Da (for sulfonium-modified BSA or BSA-S) and 69563 Da (for lauryl amine conjugated BSA-S or R-BSA-S) (Figure 3.2B). Similar changes in average molecular weight were observed for BSA-N (67746 Da; for ammonium-modified BSA) and R-BSN-N (69954 Da) (Figure 3.3B). The change in mass spectra showed that around 24 molecules of onium moiety and 6-8 molecules of lauryl amines were conjugated to the BSA protein. The Circular dichroism (CD) analysis revealed a complete loss of β-sheet and α-helix motifs, which suggests the unfolding of native BSA due to its conjugations with onium-based small molecules and lauryl amines (Figure 3.3C).[12-14]

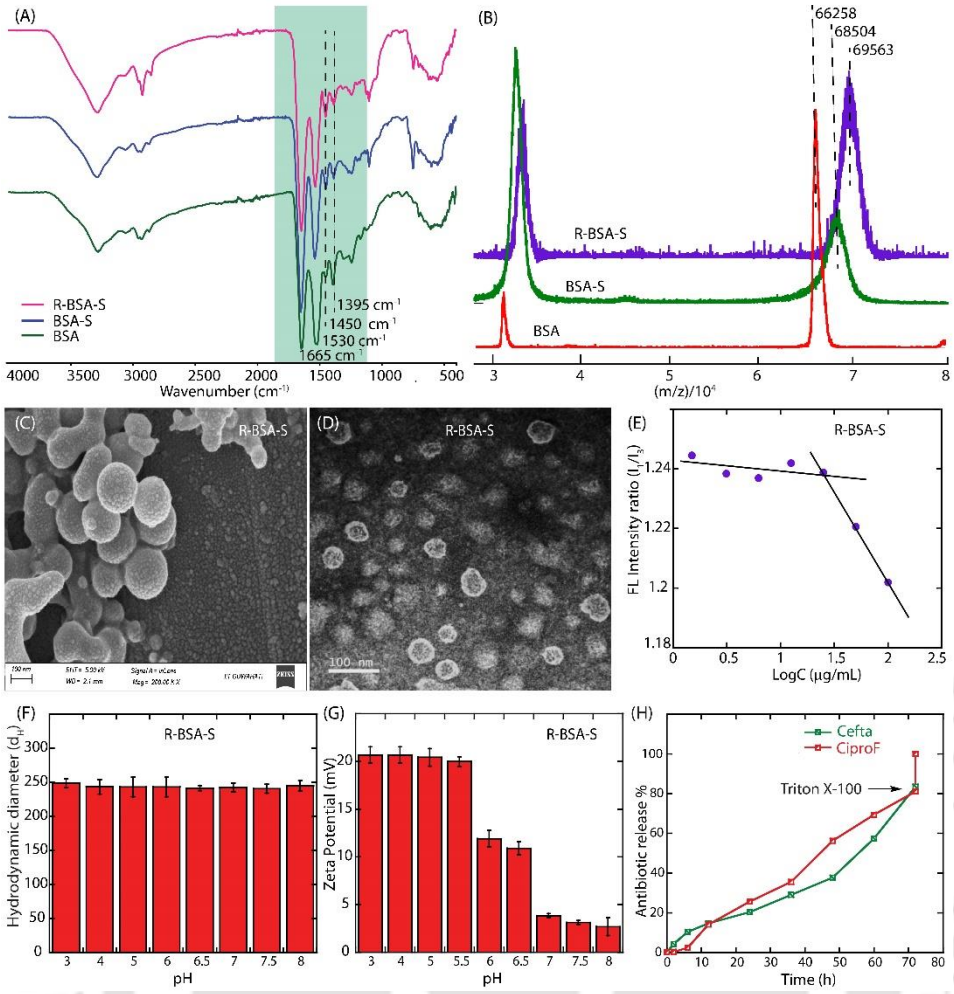

Figure 3.2. Characterization of BSA-based PNPs. Representative FTIR (A) and MALDI-TOF (B) spectra of BSA, BSA-S, and R-BSA-S. Representative FESEM (C) and FETEM (D) images of R-BSA-S. CAC measurements of R-BSA-S (E). DLS (F) and surface potential (G) of R-BSA-S across different pH. The antibiotics release profile of R-BSA-S (H).

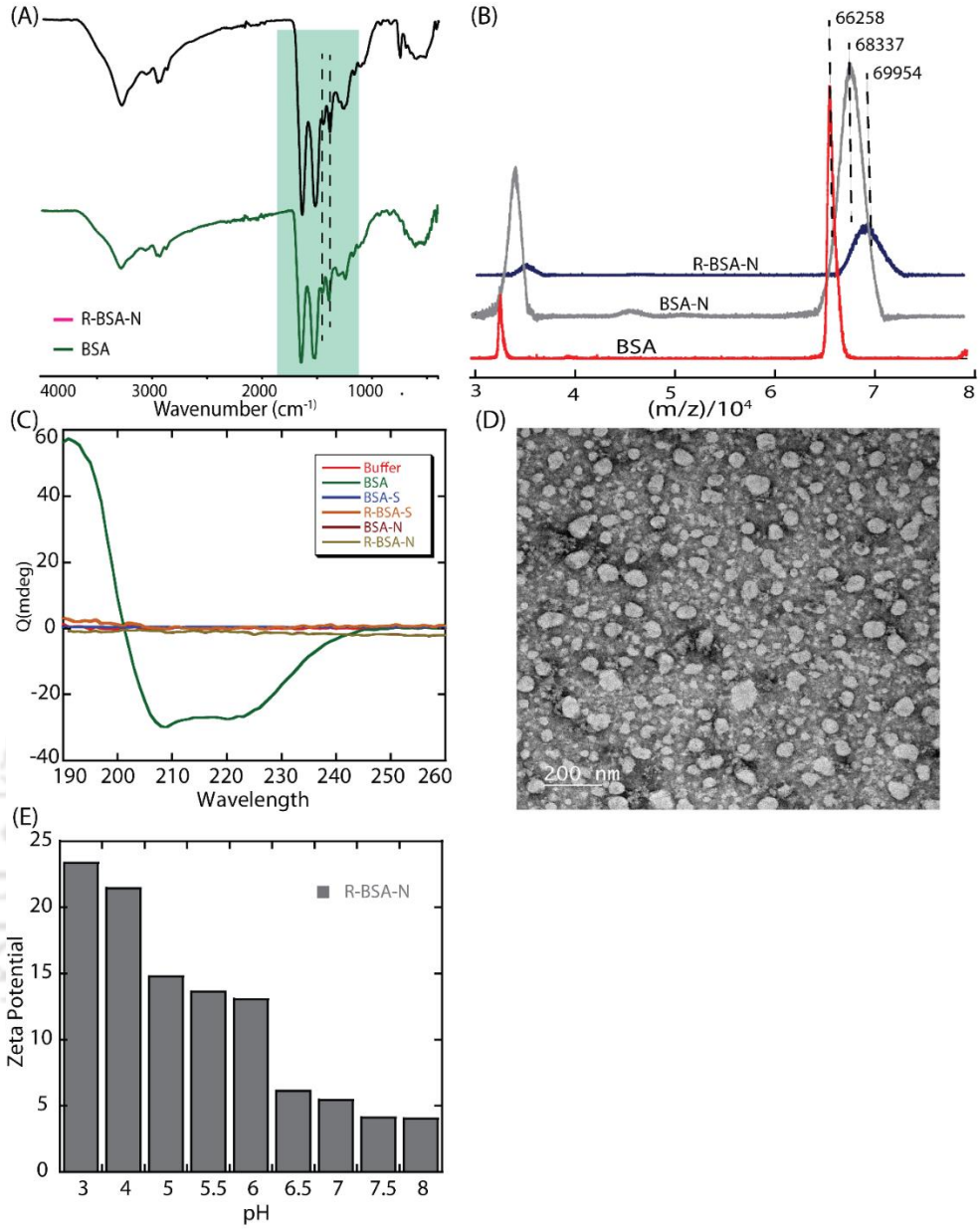

Figure 3.3. Representative FTIR (A) and MALDI-TOF (B) spectra of BSA and R-BSA-N. Representative CD spectra of BSA, BSA-N, and R-BSA-N in 10 mM PBS at pH 7.2 (C). Representative TEM images of R-BSA-N (D). The surface potential of R-BSA-N across different pH (E).

Modification of BSA with both onium-based small molecules and lauryl amines is supposed to increase the amphiphilicity, allowing it to form PNPs in an aqueous environment. Hence, FESEM and FETEM analyses were performed to investigate the morphology of the modified BSA (Figures 3.2C and 3.2D). The electron microscopic images showed the formation of spherical PNPs with a diameter of 70-90 nm. The

concentration at which R-BSA-S can form the PNPs was determined for its applicability to antibiotics loading. The critical aggregation concentration (CAC) of R-BSA-S was determined by using fluorescent probe-pyrene (Figure 3.2E). Pyrene fluorescence intensity was observed to show an enhancement on increasing the concentration of R-BSA-S to 12.5 µg/mL and was decreased (quenched) due to aggregation. The aggregation-induced quenching of the pyrene fluorescence indicated a CAC value of 12.5 µg/mL. A lower CAC value indicates its nanoaggregate forming capability, which could be useful to encapsulate the antibiotics. The hydrodynamic diameter and surface potential of the modified BSA were analyzed by dynamic light scattering (DLS) and Zetasizer within a pH range of 3 to 8. The average hydrodynamic size was found to be within 220-260 nm (Figure 3.2F), while the surface charge varies with the pH of the solution. The surface potential was positive at lower pH and decreased with the increase in pH of the solutions. At physiological pH, the surface potential was positive, which could help the molecule to interact with the negatively charged bacterial membrane (Figure 3.2G). Therefore, the morphological analyses suggested that the core of the PNPs contains the long alkyl chain, and the surface is decorated with onium-modified amino acids and other polar amino acids, which could be useful to carry both hydrophobic and hydrophilic antibiotics/drug molecules. The nano-sized cationic PNPs could show greater antibacterial activity due to passive targeting.

The antibiotics loading efficacy of R-BSA-S was investigated using commercial antibiotics, CiproF, and Cefta. The drug-loading studies were performed at a ratio of 1/5 of antibiotic to R-BSA-S using a Uv-Vis spectrophotometer (Figure 3.4 A and 3.4B). The antibiotics release profile was investigated by the high-pressure liquid chromatographic (HPLC) technique. The HPLC analysis showed that CiproF and Cefta loading efficiency of R-BSA-S were 53% and 60%, respectively. The drug-release kinetics showed a steady increase in the release rate, and 80-83% of drugs were released within 72 h (Figure 3.2H and 3.4C).

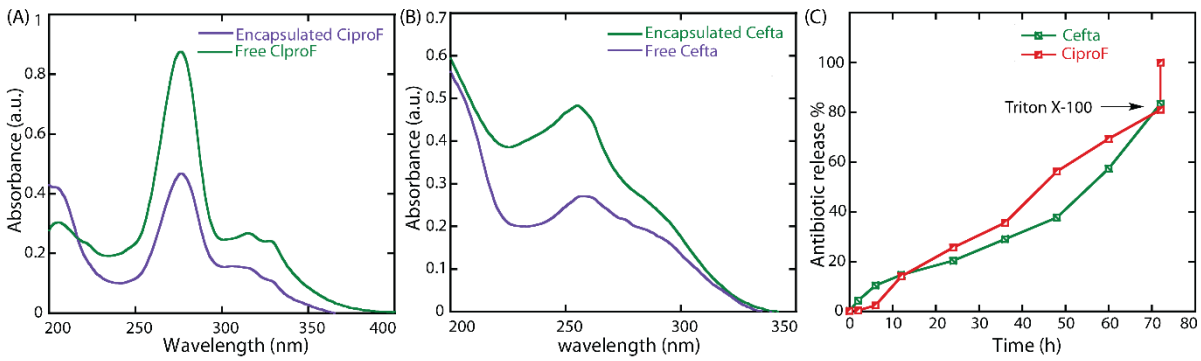

Figure 3.4. Antibiotics loading (A and B) and release profile (C) of R-BSA-S.

3.2.2 Biocidal activities of modified BSA

The biocidal activity of the modified BSA was investigated by comparing its antimicrobial and antibiofilm efficacy against Gram-negative and Gram-positive bacterial strains. Evaluation of these activities could assist in analyzing the importance of the modified BSA in fighting against drug-resistant bacterial strains. Herein, we investigated the biocidal activities of the modified BSA against both Gram-negative (*E. coli* and *P. aeruginosa*) and Gram-positive (*S. aureus* and gentamicin and methicillin-resistant *S. aureus* (GR-MRSA; ATCC 33592) bacterial stains using the micro broth dilution method (Table 1). The initial screening revealed that BSA, (2-aminoethyl)dimethylsulfonium, 2-amino-*N*,*N*,*N*-trimethylethan-1-aminium, lauryl amine, and R-BSA themselves showed no or negligible antibacterial activities. However, R-BSA-N, R-BSA-S, CiproF encapsulated R-BSA-S (CiproF@R-BSA-S), and Cefta encapsulated R-BSA-S (Cefta@R-BSA-S) express stronger potency against both Gram-positive and Gram-negative bacterial strains. The minimum inhibitory concentrations (MICs) of R-BSA-S were 15 and 20 µg/mL for *S. aureus* and GR-MRSA strains. In comparison, the MICs of R-BSA-S were 24 and 30 µg/mL for *E. coli* and *P. aeruginosa* strains. The higher MIC values of R-BSA-S for the Gram-negative strains could be due to the differences in membrane architecture. In addition, *P. aeruginosa* is known to form a sturdy biofilm matrix that protects it from harsh environments as well as from drugs. The modified BSA-based PNPs was found to be of greater or similar to the reported antimicrobial activity of the mannosylated albumin, where the MIC values were 0.85 and 0.61 µM against *E. coli* and *S. aureus* cells respectively.[12, 14] In addition, the concentration at which no visible growth was observed, was further cultured on agar plates to test the bactericidal activity. The outcome of the agar-plate assay showed no growth of bacterial cell colonies. This shows that the cationic R-BSA-S had the bactericidal activity.[15]

The antimicrobial activity of R-BSA-S was also examined after the treatment with blood serum to ensure that the interaction of blood components does not hamper the potency of the modified albumin protein. In this case, the R-BSA-S treated with blood serum for 1 h showed a similar MIC value as without treatment. Surprisingly, the ammonium counterpart, R-BSA-N, had higher MIC values than R-BSA-S against these tested bacterial strains. Various reports have shown that ammonium is more toxic than sulfonium moiety; hence,

R-BSA-S becomes more valuable for antibacterial treatments.[7, 16] Our findings revealed that the conjugation of sulfonium moiety and lauryl amine provided the BSA with potent antimicrobial properties.

3.2.3 Antibiofilm activity of R-BSA-S on MRSA

Further biocidal studies of R-BSA-S were performed against the GR-MRSA biofilm. Biofilm makes bacterial cells resistant to the defense system of the body and the drugs used to act against them. Hence, breaching the biofilm matrix is an imperative property of antimicrobial agents to counteract the resistance mechanism of bacterial cells.[4, 17] The GR-MRSA biofilm was cultured and treated with the R-BSA-S in 96-well plates at various concentrations and incubated for 14-16 h, then removed the planktonic cells. Biofilm attached to the surface of the wells was stained with crystal violet, and extra dyes were taken out and washed away with phosphate buffer saline (PBS) buffer. Biofilm-bound dye was dissolved in ethanol, and absorbance was measured at 550 nm. Biofilm formation was compared with the control (without R-BSA-S), and it was observed that more than 90 % biofilm was inhibited at 20 µg/mL concentration, and even at a lower concentration, it showed inhibition to some extent (Figure 3.5A), hence the 20 µg/mL was the minimum biofilm inhibitory concentration against MRSA. Triphenyl tetrazolium chloride (TTC) dye was used to investigate the viability of R-BSA-S treated biofilm. The TTC dye is an indicator of redox reaction occurring in viable cells or, here, in this case, biofilm, which after reduction, shows red color. The viability of the biofilm was observed below 20 µg/mL of CiproF@R-BSA-S, and the viability was less than 40 % at 10 µg/mL. The viability of the biofilm was observed to be below 5% at 20 µg/mL of R-BSA-S, and the viability was less than 40 % at 10 µg/mL (Figure 3.5B).

Table 3.1. Antibacterial activities of the modified BSA.

Bacterial strains MIC (µg/mL)				
Antimicrobial agents	***S. aureus***	**GR-MRSA**	***E. coli***	***P. aeruginosa***
BSA	>100	>100	>100	>100
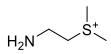	>100	>100	>100	>100

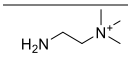	>100	>100	>100	>100
Lauryl amine	>100	>100	>100	>100
R-BSA	>100	>100	>100	>100
R-BSA-S	15 ± 2	20 ± 3	24 ± 1	30 ± 4
R-BSA-N	37.5 ± 2.5	40 ± 4	42 ± 3	>45
CiproF	0.019 ± 0.001	0.15 ± 0.02	0.058 ± 0.002	0.156 ± 0.071
Cefta	1.25 ± 0.31	125	1 ± 0.12	2.5 ± 0.31
CiproF@R-BSA-S[a]	0.004 ± 0.001	0.12 ± 0.04	0.007 ± 0.002	0.018 ± 0.007
Cefta@R-BSA-S[a]	0.156 ± 0.01	15 ± 2	0.125 ± 0.07	0.625 ± 0.11

[a]MIC values were calculated based on the concentration of the encapsulated antibiotic (Cipro and Cefta).

The antibiofilm activity was also investigated by staining the R-BSA-S treated bacterial cells with acridine orange and analyzed by its fluorescence microscopic images. The R-BSA-S and CiproF@R-BSA-S treated biofilm displayed reduced fluorescence in comparison to the one without treatment (Figure 3.5C). It was observed that R-BSA-S at a dose of 10 µg/mL potentiates the antibiofilm efficacy of CiproF. The morphology of the R-BSA-S and CiproF@R-BSA-S treated GR-MRSA biofilm was analyzed by FESEM images which showed the eradication of the biofilm (Figure 3.5D). Extracellular polymeric substances (EPS) are natural polymers of high molecular weight (polysaccharides, proteins, nucleic acids, and lipids) secreted by bacteria into their environment and the fundamental constituents of biofilms. The presence of total protein and polysaccharides in EPS regulates the survivability of the biofilm-forming bacterial strains.[18] Hence, the effect of R-BSA-S on the protein and polysaccharide contents in the EPS was assessed by Bradford and phenol sulphuric acid-based assays, which displayed around a two-fold decrease in protein and carbohydrate content of the EPS after treatment with CiproF@R-BSA-S (Figure 3.5E).

Our morphological analysis revealed that R-BSA-S forms spherical PNPs in the aqueous environment (Figures 3.2C and3.2D). We hypothesize that the potent compound R-BSA-S can escort the activity of other antibiotics and can sensitize the bacterial cells at a lower concentration. Hence, it was used to encapsulate the clinically proven antibiotics CiproF and Cefta. The CiproF is a broad spectrum of antibiotics and is used to treat various

diseases, including respiratory infection, bone infection, pneumonia, diarrhea, and skin infection. The Cefta is the third generation of cephalosporin and is used to cure meningitis, septicemia, intra-abdominal infection, and other such diseases. The MIC values of antibiotic-encapsulated R-BSA-S were found to display a synergistic effect (Table 3.2). We hypothesize that the antimicrobial and anti-biofilm activity of the R-BSA-S supported the activities of these commercially available antibiotics.

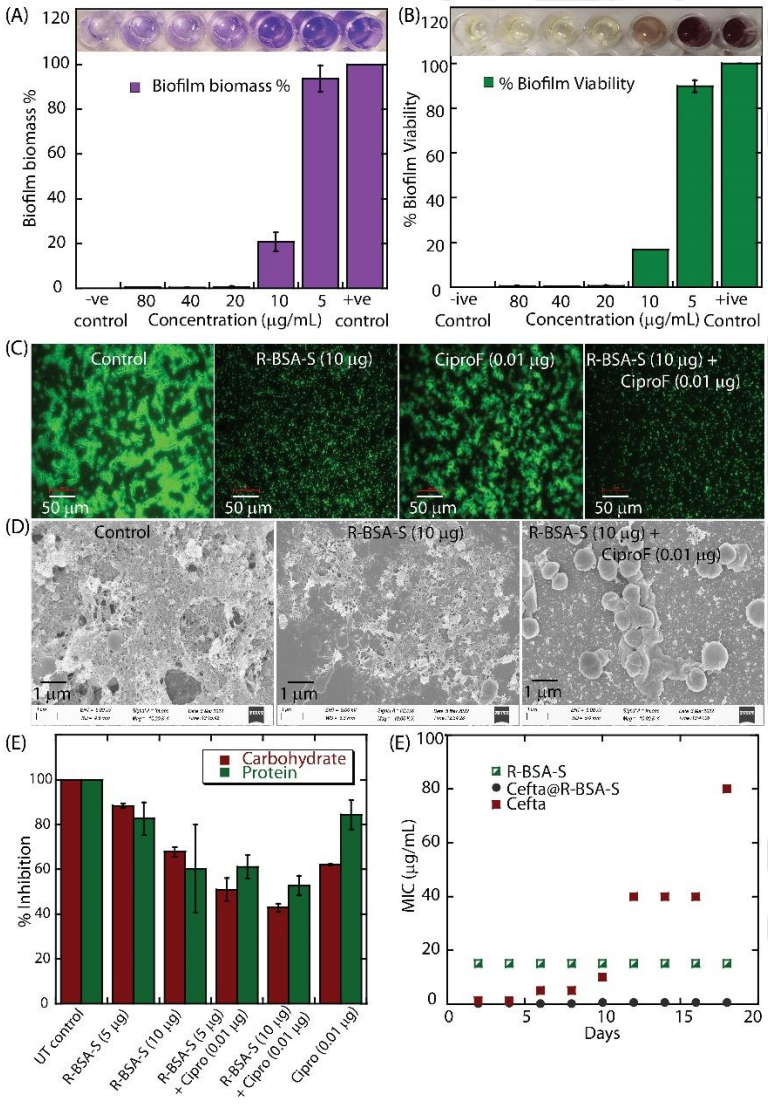

Figure 3.5. Antibiofilm activity of R-BSA-S alone and in combination with CiproF. Biomass (A) and viability (B) of GR-MRSA biofilm in the presence of different concentrations of R-BSA-S using crystal violet and TTC dye, respectively. Effect of R-BSA-S (10 µg/mL) alone and in combination with CiproF (0.01 µg/mL) on the MRSA biofilm formation. Acridine orange is used as a dye, and the attachments of MRSA biofilm

live cells on the glass surface are visualized under a fluorescence microscope (C). FESEM images of MRSA biofilm treated with R-BSA-S (10 µg/mL) and in combination with CiproF (0.01 µg/mL) (D). Estimation of polysaccharide (EPS) and total protein from MRSA biofilm. The samples were treated with R-BSA-S (5 µg/mL and 10 µg/mL) alone and in combination with CiproF (0.01 µg/mL) (E). Resistance studies against *S. aureus* cells (F).

The synergistic effect was calculated by fractional inhibitory concentration (FIC) index, where an FIC value less than 0.5 predicts the synergistic effect. The calculated MIC values of CiproF@R-BSA-S and Cefta@R-BSA-S against *S. aureus* revealed more than 4- and 8-fold decrease in MIC values compared to the only antibiotic. At the same time, GR-MRSA had a 1.25-fold reduction for CiproF@R-BSA-S, and on the other hand, it was found to be resistant to Cefta (MIC 125 µg/mL) and had a MIC value of 15 µg/mL for Cefta@R-BSA-S after encapsulation. The CiproF@R-BSA-S also showed a synergistic effect against both *E. coli* and *P. aeruginosa* bacterial strains with more than an 8-fold reduction in MIC values. The Cefta@R-BSA-S compared to only Cefta showed 8- and a 4-fold decrease in MIC values against *E. coli* and *P. aeruginosa*, respectively. The antibacterial efficacy of R-BSA-S against GR-MRSA and *P. aeruginosa* can be a prospective antibiotics delivery system. GR-MRSA and *P. aeruginosa*, are known to be resistant to numerous clinically proven antibiotics. It is also important to mention that there is no direct correlation between the CAC and MIC or MBEC values of R-BSA-S. However, the commercial antibiotics encapsulation efficacy is directly associated with the CAC value of R-BSA-S.

Table 3.2: Fractional Inhibitory concentration (FIC) index

Formulation	Bacterial Strain	MIC (µg/mL)	FIC Index
CiproF@R-BSA-S	*S. aureus*	0.004 ± 0.001	0.21
	GR-MRSA	0.12 ± 0.04	0.3
	E. coli	0.007 ± 0.002	0.12
	P. aeruginosa	0.018 ± 0.007	0.12
Cefta@R-BSA-S	*S. aureus*	0.156 ± 0.01	0.2
	GR-MRSA	15 ± 2	ND
	E. coli	0.125 ± 0.07	0.16

P.aeruginosa	0.625 ± 0.11	0.41

ND- Not determined.

3.2.4 Resistance test

We also investigated the capability of these PNPs in counteracting the drug-resistance ability of *S. aureus* (MTCC- 96). The multi-passage resistance studies were performed with only cefta, R-BSA-S, and cefta@R-BSA-S against the *S. aureus* bacterial cells. The outcome of this drug resistance study revealed that R-BSA-S developed the least resistance or no significant change in MIC value even after 18 days, while only cefta treatment showed a significant increase in MIC value within the same period of time. The cefta@R-BSA-S showed low or no significant resistance, suggesting that encapsulation of antibiotics could significantly reduce the drug-resistance ability of the bacterial cells (Figure 3.5F). Various reports demonstrated that membrane-subverting compounds develop the least resistance because cells are ruptured and inactivated before the drug counters the metabolic system of the bacterial cells.[19, 20] Hence drug encapsulated R-BSA-S composition, along with synergistic activity, could reduce the resistance mechanism of the bacterial cells.

3.2.5 Mechanistic studies

The antimicrobial activity of membrane-directed cationic amphiphilic compounds have been reported due to their electrostatic interaction with the negatively charged surface studded with lipopolysaccharide (Gram-negative bacteria) and teichoic acid (Gram-positive bacteria).[4-7] Hence, membrane disruption and depolarization properties of R-BSA-S were analyzed by propidium iodide (PI) uptake and 3,3′-dipropylthiadicarbocyanine iodide *(*$DiSC_35$)-assisted membrane depolarization analysis. The PI can enter only through the damaged membrane or dying cells and shows higher fluorescence intensity after binding with nucleic acid bases. The *S. aureus* cells were treated with different concentrations of R-BSA-S and at different time intervals samples were collected, and the change in fluorescence intensity was monitored (Figures 3.6A and 3.6B). It was observed that at various concentrations, fluorescence intensity was progressively increased, and the same observation was noted at different times, which denotes bactericidal activity of R-BSA-S has both time-dependent as well as dose-dependent activities. The CiproF@R-BSA-S and Cefta@R-BSA-S were also examined for their PI fluorescence at their MIC values, and the outcome of the study showed a moderate change in fluorescence intensity.

The fluorescence-based live and dead cell imaging assay using PI and 5(6)-carboxyfluorescein diacetate *N*-succinimidyl ester (cFDA-SE) revealed that the R-BSA-S-treated *S. aureus* cells lacked carboxyfluorescein succinimidyl ester (CFSE) fluorescence, which suggested the inactivity of bacterial metabolism due to superior membrane damage, which resulted in cell death (Figure 3.6C). The esterase-mediated conversion of cFDA-SE to CFSE only shows a fluorescence signal, which is an indicator of bacterial cell viability.[7]

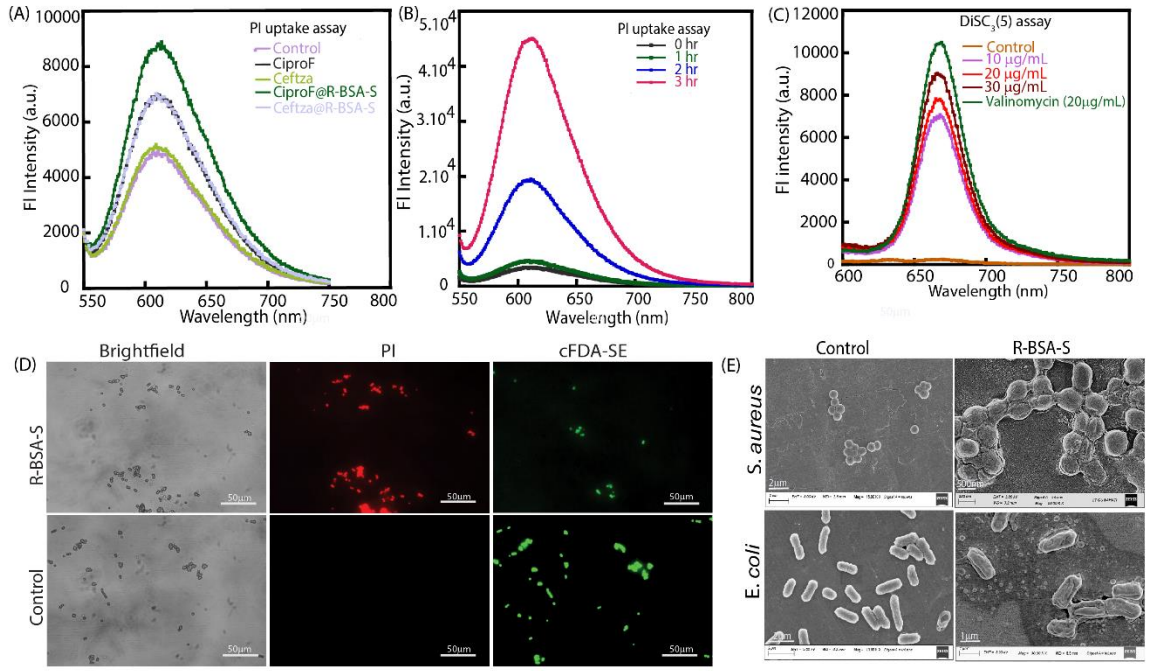

Figure 3.6. PI-uptake assay after treatment of *S. aureus* with CiproF, Ceftza, CiproF@R-BSA-S, and Ceftza@R-BSA-S (A). PI-uptake assay after treatment of *S. aureus* with CiproF@R-BSA-S at different time intervals (B). Representative fluorescence microscopic images of R-BSA-S and untreated *S. aureus* (C). The scale bar for the images is 50 µm. $DiSC_3(5)$–based membrane depolarization assay using *S. aureus* (D). Representative FESEM images of untreated and R-BSA-S treated bacterial cells (E)

The activities of both antibiotics CiproF and Cefta are not membrane oriented but by the inhibition of topoisomerase and cell wall synthesis inhibition, respectively.[21, 22] This predicts that even a slight change in membrane integrity was enough to support the action of the antibiotic. A loss of membrane integrity could lead to a change in osmotic pressure, followed by membrane depolarization. Hence, $DisC_3(5)$ dye was used to detect the depolarized state of the cell membrane (Figure 3.6D). Membrane depolarization of the bacterial cells due to the exposure to various concentrations of R-BSA-S was compared

with that of valinomycin, and it was found that even the subinhibitory concentration of the R-BSA-S caused membrane depolarization.

Viable bacterial cells have a characteristic shape that is defined and maintained by their membrane architecture and osmotic balance. In contrast, dying cells or membrane integrity-compromised cells are deprived of this specific feature.[4, 5] By observing the morphology of the bacterial cells, the viability state and mechanism of microbicidal activity can be confirmed. The morphology of R-BSA-S treated *S. aureus* and *E. coli* cells were examined by FESEM (Figure 3.6E), which revealed the visible change in the coccus and rod-shaped morphology of the *S. aureus* and *E. coli* cells, suggesting its membrane disruptive bactericidal activities.

3.2.6 Cell viability assay

The viability of R-BSA-S against mammalian peripheral blood mononuclear cells (PBMC) was investigated by the MTT assay. It has been observed that R-BSA-S alone at different doses (5, 10, 20, 40, 80, and 160 µg/mL) and in combinations with CiproF (0.01 µg/mL) did not significantly affect PBMC viability in comparison to untreated control (Figure 3.7).

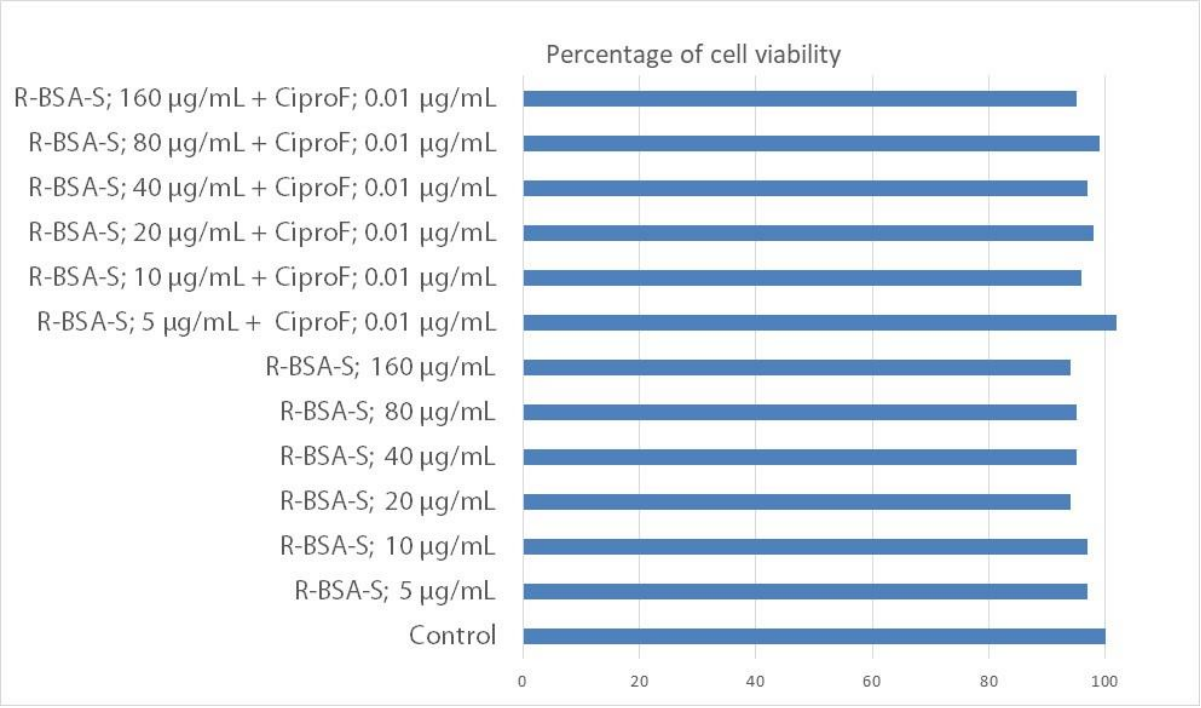

Figure 3.7. Viability of peripheral blood mononuclear cells (PBMC) after 24 h of treatments with R-BSA-S without or with CiproF.

3.2.7 Hemolytic assessment

Red blood corpuscles (RBC) cytocompatibility was performed by the hemolytic assay, corresponding to the measurement of heme release from compound-treated blood cells or the erythrocytes. The membrane architecture of erythrocytes is different from other mammalian cells, which are more fragile and control the endosomatic balance.[23] The presence or the interaction of the antibacterial agents should not hinder the membrane integrity of the erythrocyte. The outcome of the hemolytic assay revealed that the sulfonium-modified R-BSA-S, which was more toxic to bacterial cells, was more compatible with RBC than ammonium-modified R-BSA-N (Figure 3.8A). The hemolytic activity for R-BSA-S was less than 10 % up to 200 µg/mL. These results show that the antimicrobial activity of R-BSA-S is only specific to bacterial cell membranes. The outcome of this study revealed that the R-BSA-S did not show any toxicity against blood cells, and blood serum components also did not hinder its antimicrobial activity.

3.2.8 The effectiveness of R-BSA-S on a biofilm model implanted in a mouse with a catheter

To investigate the antibiofilm activity and potential side effects of the R-BSA-S-based nanoparticles, *in vivo* studies were performed. The *in vivo* antibiofilm activities of R-BSA-S alone or in combination with ciproF were assessed using a mouse model of catheter-associated infection. The *S. aureus* (MTCC 96) was grown *in vitro* on implantable catheters before being implanted in BALB/c mice. Histology and CFU count were used to examine the effect of R-BSA-S alone or in combination with ciproF at various doses on mouse liver and spleen. The CFU count was also used to assess the dispersion of catheter-associated biofilm. Figure 3.8B demonstrates the effects of R-BSA-S alone and in combination with ciproF on catheter-associated *in vivo* biofilm. The R-BSA-S-treated mouse had 326 CFU/liver compared to 588 CFU/liver in the untreated control. The combination of R-BSA-S and ciproF results in the highest inhibition in CFU count 176 CFU/liver,

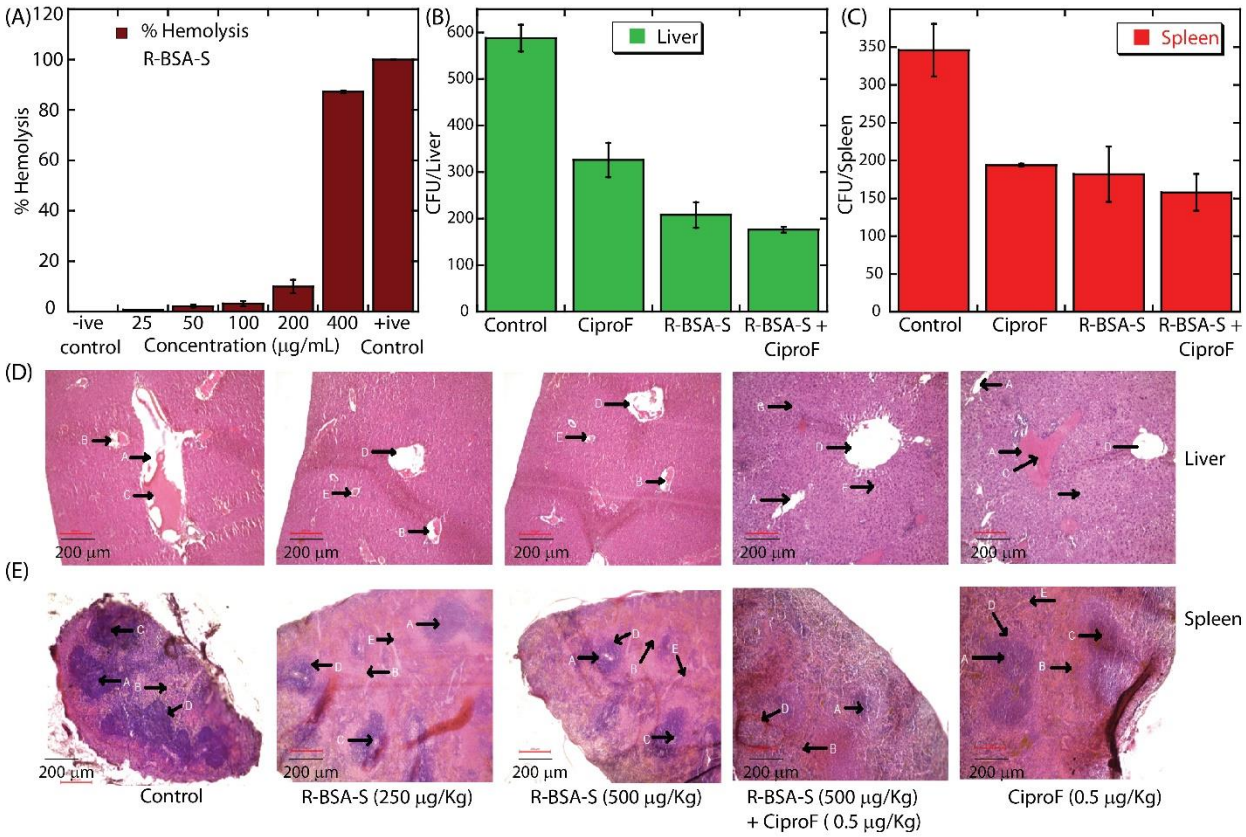

Figure 3.8. The extent of hemolysis in the presence of different concentrations of R-BSA-S and R-BSA-N (A). Effect of R-BSA-S alone or in combination with ciproF on a mouse model of catheter-associated infection. Estimation of bacterial load in mouse (*S. aureus* in vivo biofilm model) liver (B) and spleen (C) determined through CFU count on an agar plate. A change in CFU count after treatment was observed with respect to infected mouse tissue (Control). All data were expressed as mean ± S.D. (n = 4 mice per group). Histology of liver (D) and spleen (E) from *S. aureus* biofilm-infected BALB/c mice after treatment with RBSA-S and in combination with CiproF. Sections from the liver and spleen were collected from different experimental sets and analyzed after hematoxylin-eosin staining. In the liver different positions are denoted as, A = central vein, B = bile duct, C = lymphocytes, D = portal vein, E = hepatic artery, F = hepatocytes, G = sinusoids, and in spleen A = germinal center, B = red pulp, C = central arteriole, D = white pulp, E = trabecula.

while ciproF alone results in a colony count of 208 CFU/liver (Figure 3.8B). Whereas in the case of the spleen, we found the same trend of changes in CFU count (Figure 3.8C). Further histological analysis was performed to examine the impact of R-BSA-S at selected dosages on mouse liver (3.8D) and spleen (3.8E) tissue. Mouse liver and spleen sections

that had been paraffin-embedded and came from control and treatment sets for biofilm infection were compared. The liver of the infected mouse had a significantly dilated portal vein and hepatic artery, and the distribution of hepatocytes was irregular. Different treatment groups exhibit considerable differences in the morphology of the hepatocytes, central vein, and hepatic triad. The central vein was observed to be regular in mice treated with R-BSA-S (500 µg/Kg-body weight and 250 µg/Kg-body weight), and the morphology of the hepatic lobules was substantially restored. The central vein, hepatic lobule, liver sinusoid, and portal triads are found to be intact and healthy in the presence of R-BSA-S (500 µg/Kg-body weight) and CiproF (0.5 µg/Kg-body weight)], which demonstrated the strongest protective action. CiproF (0.5 µg/Kg-body weight) in combination with R-BSA-S (500 µg/Kg-body weight) also significantly reduces tissue damage caused by *S. aureus* biofilm infection. In the case of spleen tissue, the control and all treatment groups showed the presence of splenic nodules, a central artery, trabecular arteries, red pulp, white pulp, and a germinal center. Spleen tissues from infected mice showed dilated central veins and trabeculae, as well as a considerable proportion of red and white pulp. It was found that the central vein, trabecula, and amounts of red and white pulp were high in the tissues of *S. aureus* biofilm-infected mice. Treatment with R-BSA-S was found to restore the histological architecture of the spleen back to normal. This suggests that tissue morphology eventually returned following therapy with R-BSA-S alone or in combination with CiproF.

3.3 Conclusion

The studies mentioned above demonstrated the antimicrobial activity of the sulfonium and lauryl amine conjugated albumin protein. Both of these modifications of BSA protein provided properties of antimicrobial activity and drug-delivery capacity. Ciprofloxacin and ceftazidime antibiotics showed synergistic activity upon encapsulation into the PNPs. Membrane disruption and depolarization activity of R-BSA-S further escorted the cytosol-targeted antibiotics. Membrane disrupting activity counteracts the drug resistance activity of the drug-resistant bacterial strains and also lowers the drug resistance of the commercial antibiotics after encapsulation. In spite of having a cationic group, the sulfonium-modified protein rendered the least toxicity against red blood corpuscles. The antifouling, non-immunogenic, and biocompatible features after albumin modification were consistent. The in-vivo studies revealed that R-BSA-S and ciproF@R-BSA-S treatment reduced catheter-associated infection in the mice model. Biofilm and the number of S. *aureus* CFU in the

liver and spleen of compound-treated mice were also reduced. Therefore, R-BSA-S could be utilized to reduce the effective doses of clinically approved antibiotics and their exposure to other microbial strains. Overall, both the properties of R-BSA-S pave the way for further research on albumin-based antimicrobial agents and their antibiotic delivery aptitudes to support antibiotic stewardship.

3.4 Experimental Section

3.4.1. General information

The reagents used in this work were purchased from Merck, HImedia, Sigma-Aldrich, and used without any further filtration process. The 1-ethyl-3-(3- dimethylaminopropyl) carbodiimide (EDC), 1-hydroxybenzotriazole (HOBt), *N*,*N*-diisopropylethylamine (DIPEA), crystal violet, propidium iodide, carboxy floresceine, diacetate-succinamide ester (cFDA-SE) and bovine serum albumin (BSA) were purchased from Sigma-Aldrich. The 4-(2-hydroxyethyl)-1-piperazineethanesulfonic acid (HEPES), phosphate buffer saline buffer (PBS) components, dialysis membrane-110, and all the bacterial culture media were procured from HImedia. Antibiotic ciprofloxacin (CiproF) and ceftazidime (Cefta) and 2,3,5 Triphenyl Tetrazolium chloride were purchased from TCI. Small sulfonium and ammonium molecules were purified by thin-layer chromatography (TLC). The ^{13}C NMR and ^{1}H NMR were recorded at 600 MHz with a Brucker spectrometer to observe the chemical shift, and for this purpose, DMSO-d_6 and $CDCl_3$ were used as the internal solvent. Multiplicities of the NMR spectra have been reported as m (multiplet), d (doublet), s (singlet).

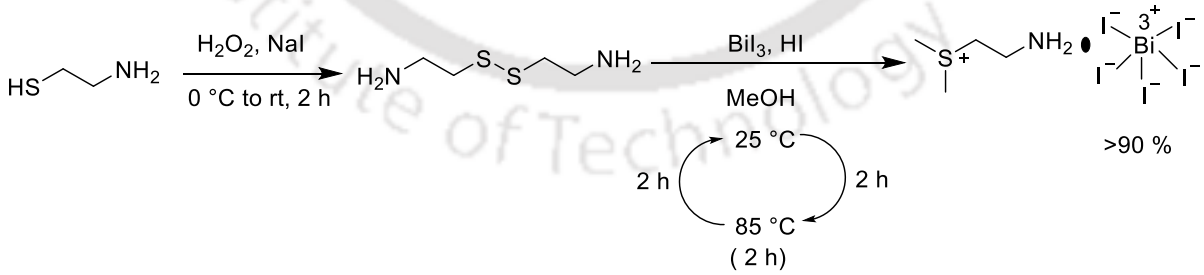

Scheme 3.1. Synthetic routes to (2-aminoethyl)dimethylsulfonium.

3.4.2 Synthesis of (2-aminoethyl)dimethylsulfonium — To a stirring solution of 2-aminoethane-1-thiol (3.89 mmol) in methanol at 0 °C was added a solution of hydrogen peroxide (3.89 mmol) and sodium iodide (10 mol %). After 10-15 minutes, the reaction

mixture was allowed to warm up to room temperature, and the stirring was continued for 2 h. After

completion of the reaction mixture, the solution was concentrated under reduced pressure and washed with diethyl ether to remove the unwanted residues and used for the next step without further purification. In the next step, to a stirring solution of the cystamine (**1a,** 3.89 mmol) and BiI_3 (7.78 mmol) in methanol were added MeOH (4 mL) and hydroiodic acid (2 mL). After 2 h, the temperature of the reaction mixture was gradually increased from 25 °C to 85 °C, and for the next 2 h was stirred at 85 °C. Finally, the temperature was gradually decreased from 85 °C to 25 °C and stirred for 12 h. Dark red crystals were collected by filtration and washed with cold ethyl acetate. The above reactions were carried out by following the literature and the characterization data are in accordance with the literature.[24]

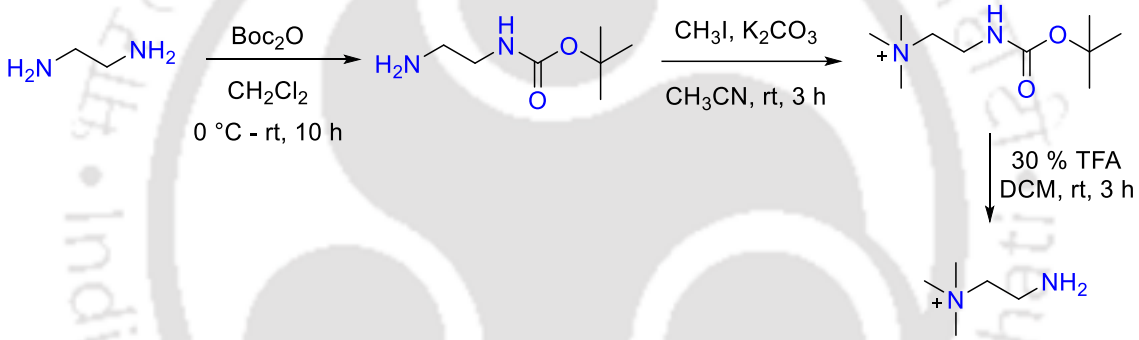

Scheme 3.2. Synthetic route to 2-amino-*N*,*N*,*N*-trimethylethan-1-aminium.

3.4.3 Synthesis of 2-amino-*N*,*N*,*N*-trimethylethan-1-aminium —To a stirring solution of ethylenediamine (2g, 2.14 mL, 32 mmol) in dichloromethane (20 mL), solution of di-tert-butyl bicarbonate (1g, 4.5 mmol) in dichloromethane (10 mL) was added dropwise at 0 ºC, and the reaction mixture was stirred for 6 h. The reaction mixture was also stirred for an additional 20 h at room temperature. Thereafter, the solvent was removed and purified with column chromatography using a methanol/dichloromethane (5 %) solvent gradient to afford tert-butyl (2-aminoethyl) carbamate.

To a stirring solution of tert-butyl (2-aminoethyl) carbamate (700 mg, 4.369 mmol) and potassium carbonate (1.509 g, 43.69 mmol) in dry acetonitrile (20 mL) was added a solution of methyl iodide (6.199g, 2.719 mL) at room temperature. The progress of the reaction was monitored by TLC. After the completion of the reaction, the residue was removed by filtration and purified by column chromatography using a methanol/dichloromethane (10

%) gradient to get a yellowish solid of 2-((tert-butoxycarbonyl)amino)-*N*,*N*,*N*-trimethylethan-1-aminium.

To a stirring solution of 2-((tert-butoxycarbonyl)amino)-*N*,*N*,*N*-trimethylethan-1-aminium (1g) in dichloromethane, a solution of TFA (10 % in dichloromethane) was added and stirred for 3 h at room temperature. After the competition of the reaction, the solvent was removed under reduced pressure. The product 2-amino-*N*,*N*,*N*-trimethylethan-1-aminium was washed with diethyl ether and dried under reduced pressure to get the brownish color solid.

The compound was characterized by HRMS (ESI), ^{1}H NMR and ^{13}C NMR analysis. **^{1}H NMR (600 MHz, DMSO-d$_6$):** δ 3.49-3.47(t, J=6 Hz, 2H), 3.25-3.22 (t, J=6 Hz,2H), 3.15 (s, 9H), 2.51 (s, 2H). **^{13}C NMR (150 MHz, DMSO d$_6$):** 63.1, 53.3, 37.4; **HRMS (ESI) *m*/*z*:** calculated for C5H15N2 $(M+H)^+$ 104.1308 found 104.1404.

3.4.4 Synthesis of (2-aminoethyl)dimethylsulfonium modified BSA nanoparticle— Aforementioned synthesized (2-aminoethyl)dimethylsulfonium was linked with the BSA-COOH group by well-known EDC/HOBT mediated acid amide coupling method. Briefly, BSA (20 mg) was stirred in DMSO (6 mL) for 6 h to unfold the tertiary structure of the protein. To activate the -COOH group of the acidic amino acid EDC/HOBT was added to the BSA in a ratio of 5 equivalent with respect to the -COOH group of BSA. To this unfolded activated BSA, DIPEA activated sulfonium molecule in DMSO was added and stirred for 72 h. After completion of the reaction, the mixture was diluted with water and freeze-dried, and the lyophilized powder was dialyzed with Mili-Q overnight by a dialysis membrane to remove the unreacted small molecule, followed by freeze dry. The sulfonium-linked BSA (BSA-S) molecule was further attached with the lauryl amine using a similar reaction procedure. After completion of the reaction, the unreacted molecule was extracted with hexane.

3.4.5 Synthesis of 2-amino-*N*,*N*,*N*-trimethylethan-1-aminium modified BSA nanoparticle— (2-Aminoethyl)dimethylsulfonium modified BSA nanoparticle was also synthesized as mentioned in the earlier section using 2-amino-*N*,*N*,*N*-trimethylethan-1-aminium**.**

3.4.6 Chemical and morphological characterization of modified BSA nanoparticles:

3.4.6.1. FTIR analysis— The BSA-S, BSA-N, lauryl amine-linked BSA-S (R-BSA-S), and lauryl amine-linked BSA-N (R-BSA-N) was analyzed by FT-IR spectroscopy.[13] A pinch of the powdered sample was placed onto the diamond-studded attenuated total reflectance (ATR) and pressed with a bar. Spectra were recorded from 4000 to 400 cm^{-1}.

3.4.6.2 Matrix-assisted laser desorption/ ionization-time of flying (MALDI-TOF) — To estimate the extent of modification of the BSA, MALDI-TOF analysis was performed (Auto flex speed, Bruker, Germany).[13] Before analysis sample was suspended in a solution of 50 % acetonitrile and 0.05 % TFA, and this was further mixed with α-Cyano-4-hydroxycinnamic acid (CHCA) dissolved in 50 % Acetonitrile and .1 % TFA. The sample was spotted onto the MALDI plate and was analyzed.

3.4.6.3 Circular Dichroism (CD) analysis— Modification of BSA could cause deformation in the secondary structure, which was further investigated by CD analysis (Jasco J-1500 spectropolarimeter) at 17 °C. For CD analysis, the sample was prepared in 10 mM phosphate buffer at pH 7.2.[13] The secondary structure was recorded between 200-260 nm wavelength. The resolution was 0.2 nm, bandwidth was kept at 1.0 nm, and the scan rate was taken at a speed of 100 nm/min. The change in spectra of α- helix and ß sheet was analyzed with respect to yang's module. The difference in the secondary structure of the modified protein was compared with the native protein.

3.4.6.4 Morphological investigation by electron microscopic analysis— After BSA modification with the addition of long-chain amine, its posited aggregation behavior was analyzed by FESEM and FETEM. The samples for FESEM and FETEM analysis were prepared in Milli-Q water.[13] For FESEM analysis, 2 µL of the aqueous solution was spotted onto the aluminum foil-covered glass plate and dried at room temperature overnight. Before analysis, the glass plate was stacked on the metal grid, and the sample was coated with gold for conductivity. The images were analyzed by Gemini 300 field-emission transmission electron microscope at 2 to 5 kV. For FETEM analysis sample preparation, 10 µM 10 µL sample was dropped onto the carbon-coated copper grid and allowed to absorb for 10 min at 37 °C, and after that remaining sample was taken off. The sample was further coated with freshly prepared 2% (in water) 10 µL of uranyl acetate solution, and the grid was

incubated at 37 °C to dry for 2 min, and the remaining solution was soaked away by tissue paper. The images were analyzed by JEOL JEM 2100 transmission electron microscope at an accelerating voltage of 200kV.

3.4.6.5 Critical aggregation concentration (CAC) measurement —Aggregation properties of the R-BSA-S were determined by pyrene-mediated fluorescence quenching.[13] Variable concentration of the compound was prepared by dispersing the R-BSA-S in 10 mM PBS buffer, pH 7.2 followed by the serial dilution. Pyrene was added to the serially diluted samples at a constant concentration (0.5 mM). Fluorescence spectra of pyrene were measured by Fluoromax-4 spectrofluorometer (λ_{ex} = 335 nm). The intensity ratio of the I_1 and I_2 was analyzed to measure the CAC value of R-BSA-S.

3.4.6.6 Hydrodynamic diameter and surface potential measurement —Hydrodynamic diameter and surface potential of the R-BSA-S were measured by Zetasizer Nano ZS90 (Malvern).[13] Sample stock was prepared in Milli-Q water as mentioned above and was aliquoted at the constant concentration in different pH to determine the isoelectric point of the BSA and R-BSA-S. All measurements were recorded in triplicate and presented as the average size. Different pH buffers were prepared by our earlier reported methods; briefly, 10 mM citrate buffer was prepared for the pH range of 3 to 6, MOPS buffer was used for pH 7, and other pH was prepared by PBS and tris(hydroxymethyl)aminomethane (Tris)-HCl.[13]

3.4.6.7Antibiotics loading and release efficiency measurement— Clinically certified commercial antibiotics were used for encapsulation to test their efficacy. The stock solution of the Cefta antibiotic was prepared in PBS buffer, pH 7.2, and CiproF was solubilized at a slightly acidic pH 6.5. A 200 µg/mL stock was mixed with 1mg R-BSA-S and stirred overnight, followed by centrifugation at 20,000 rpm for 30 min to separate the non-encapsulated antibiotic. Antibiotic encapsulated nanoparticle was again washed with Milli-Q water to wash off the free antibiotic attached to the nanoparticle. The antibiotics loading capacity was analyzed by UV spectroscopy, and the release profile was analyzed by high-pressure liquid chromatography (HPLC). At different time intervals, the sample was collected and centrifuged as earlier and analyzed by HPLC using water (with 0.1 % formic acid) and a methanol eluent system.

3.4.7 Measurements of biocidal activity

3.4.7.1 Bacterial cell susceptibility test —Bacterial cell susceptibility test against Gram-negative and Gram-positive representing bacterial strain was done using a micro broth dilution method using reported standard protocol.[7] Briefly, bacterial strains of *E. coli* (MTCC 1687), *P. aeruginosa* (MTCC-2488), *S. aureus* (MTCC 96) were procured from Microbial type culture collection (MTCC) as lyophilized powder and were cultured as per the protocol in nutrient-rich media. The drug-resistant strain of gentamicin and methicillin-resistant *S. aureus* (GR-MRSA; ATCC 33592) was procured from ATCC and cultured in brain heart infusion (BHI) media. Bacterial cells *E. coli* and *P. aeruginosa* in Luria Bertani (LB) and S. *aureus* in BHI were grown till mid-logarithmic phase at 37 °C, 180 rpm in a shaker incubator and collected by centrifugation followed by its washing in PBS twice. Modified BSA stocks and antibiotics (CiproF and Cefta) encapsulated R-BSA-S were prepared in water and serially diluted into the 96-well plates. This varied compound concentration was further mixed with the bacterial cell at a fixed colony-forming unit (CFU), i.e., 10^6 CFU/mL. The plate was incubated at 37°C for 16 to 20 h. Bacterial growth was assessed by visual observation and by recording its optical density at 600 nm using a plate reader (Biotech).

The synergistic effect was calculated by fractional inhibitory concentration (FIC) index, where an FIC value less than 0.5 predicts the synergistic effect.

$$\frac{\text{MIC of R-BSA-S loaded with antibiotic } \left(\frac{\mu g}{mL}\right)}{\text{MIC of R-BSA-S} \left(\frac{\mu g}{mL}\right)} + \frac{\text{MIC of antibiotic loaded in R-BSA-S} \left(\frac{\mu g}{mL}\right)}{\text{MIC of antibiotic} \left(\frac{\mu g}{mL}\right)} = \text{FIC Index}$$

3.4.7.2 Antibacterial activity of bovine serum treated R-BSA-S —R-BSA-S, antibiotic encapsulated nanoparticles were first treated with bovine blood serum for 30 min. As explained in the previous section, the bacterial cells were treated to test their antimicrobial efficacy.[7]

3.4.7.3 Antibiofilm activity test —Antibiofilm efficacy by R-BSA-S was tested by crystal violet staining of the biofilm biomass. *S. aureus* bacterial cells were grown and treated with the R-BSA-S as described in the aforementioned section.[7] Wells with only buffer and media was considered as negative control while wells with bacterial cells and media was

considered as positive control. This was further proceeded with aspiring the planktonic cells from the wells and washing the wells to remove any remaining free cells. Crystal violet (5% w/v) prepared in Milli-Q was added to the wells to stain the biofilm. The plate was incubated for 30 min, and then the crystal violet solution was taken out with a pipette and washed with Milli-Q. Wells were dried, and then 95% ethanol was added to the wells to solubilize the stained biomass. The absorbance of the wells was recorded at 550 nm. Biofilm biomass was compared with the wells with no R-BSA-S at all. At different R-BSA-S concentration biofilm biomass was quantified by the following equation —

$$Biofilm\ biomass\ \% = ((Ac\text{-}Ac°) * 100)/Ac^{100}$$

(Where Ac is the Absorbance at different concentration of compound, Ac° is the Absorbance of negative control sample and Ac^{100} is the absorbance of positive control).

The viability of the biofilm in the presence of R-BSA-S was assessed by 2,3,5 triphenyl tetrazolium chloride (TTC) reduction assay where instead of staining the biofilm with crystal violet fresh growth media and TTC solution was added to the well and incubated for 12 h at 37°C. The absorbance of the plate was measured at 410 nm. Biofilm viability was quantified in the same manner as biofilm biomass.

3.4.7.4 Estimation of total protein concentration from MRSA biofilm —The concentration of extractable protein is directly related to the microbial population density in the biofilm. To estimate the extractable protein from biofilm, MRSA was incubated at 37 °C for 48 hours with or without sub-MIC dosages of R-BSA-S alone and in combination with CiproF. The planktonic cells were removed following incubation, and adherent cells in the biofilm were gently washed with sterile PBS, and the attached biofilm cells were extracted by scrapping with 5 mL of 0.5 N NaOH and allowed to boil for 30 minutes to extract protein. The suspension was centrifuged at 10,000 rpm for 5 minutes, and the clear supernatant was collected. The supernatant was used to measure protein concentration by using the Bradford method.[25]

3.4.7.5 Fluorescence and FESEM microscopy for characterizing the effect of R-BSA-S on the formation of biofilm by MRSA on glass surface —To investigate the effect of R-BSA-S on biofilm formation over the glass surface, MRSA was separately inoculated in the presence and absence of chosen sub-MIC dosages of R-BSA-S alone and in combination with the CiproF. Bacteria were grown into 35 mm x 10 mm petridishes with

sterile glass coverslips, and they were then incubated for 48 hours at 37 °C. Coverslips were carefully removed from each petridish after incubation and washed with sterile PBS. For fluorescence microscopic analysis, the coverslips were dyed with acridine orange for 15 minutes in the dark condition. The coverslips were dried at room temperature, and the attached live biofilm cells on the glass surface were visualized under a fluorescence microscope (Leica DM 4000B, Germany).[25] For FESEM, the coverslips were washed with PBS followed by fixation with 2% glutaraldehyde solution for overnight at 4 °C. After fixation, coverslips were washed with sterile PBS and dried with ethanol 25%, 50%, 75%, and 100% 10 minutes for each concentration. After dried, the attached biofilm cells are visualized in FESEM (sigma-300, Carl Zeiss).[25]

3.4.7.6 Extraction and quantification of exopolysaccharide (EPS) —To investigate the effect of RBSA-S alone and in combination with CiproF on the EPS of MRSA biofilm, bacteria were grown for 48 h at 37 °C in the presence and absence of selected sub-MIC doses stated above. The biofilm suspension that had grown on the glass surface was extracted by scrapping in sterile water, and it was centrifuged at 3500 g for 20 minutes at 4 °C. The supernatant was collected in a new tube, and to extract the cell-bound EPS, the pellet was then treated with 10mM/l EDTA, vortexed for 15 minutes, and centrifuged again. After centrifugation, the obtained supernatant was mixed with the initial supernatant. Following this, the mixed supernatant was treated with 2.2 volumes of chilled absolute ethanol and incubated it at -20 °C for one hour. After incubation, the samples were re-centrifuged at 3500 g for 20 minutes at 4 °C. The pellets were dissolved in sterile water, and the EPS was measured by the phenol sulphuric-acid method.[26, 27]

3.4.7.7 Resistance test— For drug resistance study, *S. aureus* bacterial cells were cultured as mentioned in aforementioned section**.** The MIC values of R-BSA-S, cefta@R-BSA-S, and cefta were tested and the cells were incubated in presence of sub-inhibitory concentration of these compounds at 37 °C, 180 rpm. The bacterial cells were passessed over 18 days in the presence of growth media and additives (R-BSA-S, cefta@R-BSA-S, and cefta) at a concentration above which the MIC was recorded. The MIC assays were performed on alternate days to analyse the changes in the antimicrobial efficacy of the additioves over the time.

3.4.7.8 Bacterial membrane disrupting assay — Nucleic acid staining dye propidium iodide (PI) was used to quantify the loss of membrane integrity. The same protocol was followed as reported earlier.[7] Briefly, *S. aureus* bacterial cells were grown in BHI media at 37 °C, 180 rpm. At log phase cells were collected by centrifugation at 4000 rpm for 5 min, washed with PBS buffer. At 10^6 CFU/mL cells were incubated in the presence of 2x of the MIC concentration of the R-BSA-S, and as a control, cells were treated only with buffer (solvent of the compound). To compare the PI uptake ability of the drug encapsulated R-BSA-S the cefta@R-BSA-S, cipro@R-BSA-S and free antibiotics were also treated at its MIC value. Bacterial culture vials were removed at different time intervals, and cells were pelleted down by centrifugation. Compound-treated bacterial cells were resuspended in buffer and treated with PI at a final concentration of 30 µM and incubated for 30 min. Extra dye was removed by centrifugation followed by resuspension of the cells into the buffer, and just after short procrastination, fluorescence emission spectra of the samples were measured at excitation and emission wavelength of 535 and 610 nm, respectively.

3.4.7.9 Membrane depolarization assay —A change in membrane integrity of the bacterial cell follows the change in osmotic balance and membrane potential. This was analyzed in R-BSA-S treated bacterial cells by membrane depolarisation sensing dye $DiSC_3(5)$.[7] The *S. aureus* cells were cultured and harvested as mentioned in the earlier section and resuspended in 10 mM HEPES and 100 mM glucose buffer. Dye was added to the cells at a final concentration of 0.4 µM and incubated for one h at 37 °C, 180 rpm. Potassium chloride was added to the dye-added cell culture, and fluorescence spectra of the sample were measured at λ_{ex} = 620 λ_{em} = 650 nm. For comparison, valinomycin-treated bacterial cells were also analyzed.

3.4.7.10 FESEM image analysis of the bacterial cell morphology — Bacterial cells *S. aureus* and *E. coli* were cultured and grown until the exponential phase in BHI and LB media, respectively at 37 °C, 180 rpm, followed by the treatment with R-BSA-S. As a control, the only buffer was added to the bacterial culture. Cells were incubated for 3 h at 37 °C and 180 rpm, harvested by centrifugation, and washed in Mili-Q water to remove the buffer salt. Bacterial cells were mounted and fixed with 3% glutaraldehyde and washed twice afterward. Cell specimens were drop-casted onto a glass gride after dehydration with

70 % ethanol. Before analysis grid was stacked on copper stub and coated with gold, and morphology was analyzed under FESEM (sigma 300).

3.4.7.11 In-vitro cytotoxicity assay —In vitro cytotoxicity assay was performed using human peripheral blood mononuclear cells (PBMC). Briefly, 5 mL of peripheral blood was collected from healthy adult individuals in EDTA-coated vacutainer tubes. The EDTA-treated blood was diluted with 2x volume of sterile 1x phosphate buffer saline (PBS) at 20 °C. Then 2.5 mL of HiSep LSM 1077 was taken in a sterile 15 mL centrifuge tube, and 7.5 mL of diluted blood was carefully layered on HiSep LSM 1077 and centrifuged at 400 g for 30 min at 20°C. After centrifugation interface layer containing mononuclear cells was collected in a sterile new tube and washed twice with 3 volumes of 1xPBS at 160 g for 10 min at 20 °C. The supernatant was discarded, and the pellet containing PBMCs was cultured in RPMI medium-1640 with 10% FBS, supplemented with 2 mM L-glutamine, 1% penicillin/streptomycin.[28]

For the MTT assay, isolated PBMC $4x10^6$ cells/mL were seeded equally in a 96-well plate and incubated for 24 h in a 5% CO_2 incubator at 37 °C. After that, different doses of R-BSA-S alone and in combination with CiproF (0.01 µg/mL) were added and incubated for another 24 h. After incubation, MTT (1 mg/mL) was added to each well and incubated for 3 h in a 5% CO_2 incubator at 37 °C. The formazan crystals were dissolved in MTT solubilization buffer solution (50 µL of 0.04 M HCL- Isopropanol) and measured the optical density at 570 nm using a microplate reader (BIOTEK-EPOCH-2).[29] Cell viability (%) was calculated by considering the OD of the untreated set as 100%.

3.5 References

1. Briones, E.; Colino, C. I.; Lanao, J. M., Delivery systems to increase the selectivity of antibiotics in phagocytic cells. *J Control Release* **2008,** *125* (3), 210-227.
2. Canaparo, R.; Foglietta, F.; Giuntini, F.; Della Pepa, C.; Dosio, F.; Serpe, L., Recent Developments in Antibacterial Therapy: Focus on Stimuli-Responsive Drug-Delivery Systems and Therapeutic Nanoparticles. *Molecules* **2019,** *24* (10), 1991-2006.
3. Karimi, M.; Bahrami, S.; Ravari, S. B.; Zangabad, P. S.; Mirshekari, H.; Bozorgomid, M.; Shahreza, S.; Sori, M.; Hamblin, M. R., Albumin nanostructures as advanced drug delivery systems. *Expert Opinion on Drug Delivery* **2016,** *13* (11), 1609-1623.
4. Hoque, J.; Konai, M. M.; Gonuguntla, S.; Manjunath, G. B.; Samaddar, S.; Yarlagadda, V.; Haldar, J., Membrane Active Small Molecules Show Selective Broad Spectrum Antibacterial Activity with No Detectable Resistance and Eradicate Biofilms. *J Med Chem* **2015,** *58* (14), 5486-500.

5. Zhou, M.; Zheng, M.; Cai, J., Small Molecules with Membrane-Active Antibacterial Activity. *ACS Appl Mater Interfaces* **2020,** *12* (19), 21292-21299.
6. Epand, R. M.; Walker, C.; Epand, R. F.; Magarvey, N. A., Molecular mechanisms of membrane targeting antibiotics. *Biochim Biophys Acta* **2016,** *1858* (5), 980-7.
7. Patel, A.; Dey, S.; Shokeen, K.; Karpinski, T. M.; Sivaprakasam, S.; Kumar, S.; Manna, D., Sulfonium-based liposome-encapsulated antibiotics deliver a synergistic antibacterial activity. *Rsc Med Chem* **2021,** *12* (6), 1005-1015.
8. Spada, A.; Emami, J.; Tuszynski, J. A.; Lavasanifar, A., The Uniqueness of Albumin as a Carrier in Nanodrug Delivery. *Mol Pharmaceut* **2021,** *18* (5), 1862-1894.
9. Larsen, M. T.; Kuhlmann, M.; Hvam, M. L.; Howard, K. A., Albumin-based drug delivery: harnessing nature to cure disease. *Mol Cell Ther* **2016,** *4*, 3.
10. Kratz, F., Albumin as a drug carrier: Design of prodrugs, drug conjugates and nanoparticles. *J Control Release* **2008,** *132* (3), 171-183.
11. Loureiro, A.; Azoia, N. G.; Gomes, A. C.; Cavaco-Paulo, A., Albumin-Based Nanodevices as Drug Carriers. *Curr Pharm Design* **2016,** *22* (10), 1371-1390.
12. Tsai, C. Y.; Chen, Y. J.; Fu, Y. S.; Chang, L. S., Antibacterial and membrane-damaging activities of mannosylated bovine serum albumin. *Arch Biochem Biophys* **2015,** *573*, 14-22.
13. Saha, A.; Pradhan, N.; Chatterjee, S.; Singh, R. K.; Trivedi, V.; Bhattacharyya, A.; Manna, D., Fatty-Amine-Conjugated Cationic Bovine Serum Albumin Nanoparticles for Target-Specific Hydrophobic Drug Delivery. *Acs Appl Nano Mater* **2019,** *2* (6), 3671-3683.
14. Shi, Y. J.; Wang, R. T.; Chu, Y. H.; Chen, Y. J.; Tang, C. C.; Fu, Y. S.; Lee, Y. C.; Wang, L. J.; Huang, C. H.; Chang, L. S., Membrane-damaging activities of mannosylated ovalbumin are involved in its antibacterial action. *Arch Biochem Biophys* **2018,** *639*, 1-8.
15. Hazam, P. K.; Cheng, C. C.; Hsieh, C. Y.; Lin, W. C.; Hsu, P. H.; Chen, T. L.; Lee, Y. T.; Chen, J. Y., Development of Bactericidal Peptides against Multidrug-Resistant Acinetobacter baumannii with Enhanced Stability and Low Toxicity. *Int J Mol Sci* **2022,** *23* (4).
16. Oh, J.; Khan, A., Main-Chain Polysulfonium Salts: Development of Non-Ammonium Antibacterial Polymers Similar in Their Activity to Antibiotic Drugs Vancomycin and Kanamycin. *Biomacromolecules* **2021,** *22* (8), 3534-3542.
17. Bhatia, E.; Sharma, S.; Jadhav, K.; Banerjee, R., Combinatorial liposomes of berberine and curcumin inhibit biofilm formation and intracellular methicillin resistant Staphylococcus aureus infections and associated inflammation. *J Mater Chem B* **2021,** *9* (3), 864-875.
18. Goswami, S.; Thiyagarajan, D.; Samanta, S.; Das, G.; Ramesh, A., A zinc complex of a neutral pyridine-based amphiphile: a highly efficient and potentially therapeutic bactericidal material. *J Mater Chem B* **2015,** *3* (35), 7068-7078.
19. Mingeot-Leclercq, M. P.; Decout, J. L., Bacterial lipid membranes as promising targets to fight antimicrobial resistance, molecular foundations and illustration through the renewal of aminoglycoside antibiotics and emergence of amphiphilic aminoglycosides. *Medchemcomm* **2016,** *7* (4), 586-611.
20. MacNair, C. R.; Brown, E. D., Outer Membrane Disruption Overcomes Intrinsic, Acquired, and Spontaneous Antibiotic Resistance. *Mbio* **2020,** *11* (5).
21. Chamberlin, J.; Story, S.; Ranjan, N.; Chesser, G.; Arya, D. P., Gram-negative synergy and mechanism of action of alkynyl bisbenzimidazoles. *Sci Rep-Uk* **2019,** *9*.

22. Zasowski, E. J.; Rybak, J. M.; Rybak, M. J., The beta-Lactams Strike Back: Ceftazidime-Avibactam. *Pharmacotherapy* **2015,** *35* (8), 755-70.
23. Virtanen, J. A.; Cheng, K. H.; Somerharju, P., Phospholipid composition of the mammalian red cell membrane can be rationalized by a superlattice model. *P Natl Acad Sci USA* **1998,** *95* (9), 4964-4969.
24. Chai, W. X.; Wu, L. M.; Li, J. Q.; Chen, L., Silver iodobismuthates: syntheses, structures, properties, and theoretical studies of [Bi2Ag2I10 2-]n and [Bi4Ag2I16 2-]n. *Inorg Chem* **2007,** *46* (4), 1042-4.
25. Das, M. C.; Samaddar, S.; Jawed, J. J.; Ghosh, C.; Acharjee, S.; Sandhu, P.; Das, A.; Daware, A. V.; De, U. C.; Majumdar, S.; Das Gupta, S. K.; Akhter, Y.; Bhattacharjee, S., Vitexin alters Staphylococcus aureus surface hydrophobicity to obstruct biofilm formation. *Microbiol Res* **2022,** *263*, 127126.
26. Das, M. C.; Sandhu, P.; Gupta, P.; Rudrapaul, P.; De, U. C.; Tribedi, P.; Akhter, Y.; Bhattacharjee, S., Attenuation of Pseudomonas aeruginosa biofilm formation by Vitexin: A combinatorial study with azithromycin and gentamicin. *Sci Rep* **2016,** *6*, 23347.
27. Dubois, M.; Gilles, K.; Hamilton, J. K.; Rebers, P. A.; Smith, F., A colorimetric method for the determination of sugars. *Nature* **1951,** *168* (4265), 167.
28. Aimola, I.; Inuwa, H.; Nok, A.; Mamman, A.; Habila, N.; Muhammad, A.; Ndidi, U.; Ignatius, B.; Jande, P.; Oghor, R.; Afolabi-Balogun, N., Isolation of Peripheral Blood Mononuclear Cells Using Glycerol Density Gradient. *Exp Hematol* **2013,** *41* (8), S66-S66.
29. Sardar, D.; Neogi, S. K.; Bandyopadhyay, S.; Satpati, B.; Ahir, M.; Adhikary, A.; Jain, R.; Gopinath, C. S.; Bala, T., Multifaceted core-shell nanoparticles: superparamagnetism and biocompatibility. *New J Chem* **2015,** *39* (11), 8513-8521.

CHAPTER 4

SULFONIUM-CROSS-LINKED HYALURONIC ACID-BASED SELF-HEALING HYDROGEL: STIMULI-RESPONSIVE DRUG CARRIER WITH INHERENT ANTIBACTERIAL ACTIVITY TO COUNTERACT ANTIBIOTIC-RESISTANT BACTERIA

4.1 Background objective of the present work

Of late, hydrogels have engrossed widespread consideration for thwarting bacterial infections, especially as wound dressings for promoting wound healing because of biocompatibility and high water-retention capacity. The antimicrobial hydrogel can prevent the loss of body fluids and microbial infection, which could hasten wound healing.[14] Several antimicrobial hydrogels have been developed by introducing various antibacterial mechanisms, including contact killing and stimuli-responsive antibiotic release.[14, 15] Hydrogels with quaternary ammonium moieties have attracted special attention due to their ability to disrupt cell membrane integrity and deactivate bacterial enzymes.[16, 17] However, developing broad-spectrum antibacterial hydrogel with antibiotics encapsulation efficacy and specific recognition for bacteria remains challenging. Here, we report the development of a sulfonium-containing linker to generate a hyaluronic acid (HA)-based cross-linked biopolymer. We presumed that the sulfonium-containing HA-based cross-linked polymer (HA-SS-HA) could suppress the toxicity of cationic sulfonium while harboring the biocompatible and other inherent properties of the polymer. In earlier reports, we demonstrated that the sulfonium and pyridine-containing liposomes and nano-aggregates displayed antimicrobial activity against Gram-negative and Gram-positive bacterial cells.[10-12] Recently, HA-based hydrogel played a significant role in tissue engineering and wound management.[18, 19] HA-based hydrogel is more beneficial than other materials due to its inherent wound healing property. HA, a polysaccharide-based glycosaminoglycan and a ligand for CD44, which after the interaction, promotes the epithelial cell migration followed by an accelerated wound healing process. The presence of infection in wounds can significantly impede the natural healing process. Extensive research has demonstrated that biofilms are found in more than 80% of infected wounds. Thus, there is a pressing need to develop biopolymers that possess not only wound healing properties but also exhibit antimicrobial and biofilm inhibitory activities.[1, 2] By effectively exploring the synthesis of such biopolymers, we can potentially address the treatment of wound-associated infections and enhance the overall healing process.

Inspired by the success of sulfonium-based amphiphiles, we synthesized (pyridine-2,6-diylbis(methylene))bis((2-aminoethyl)(methyl)sulfonium) as a linker molecule with two sulfonium and one pyridine group that can be conjugated from both sides with –COOH group of the HA. Cross-linking of HA with this pyridine-containing sulfonium linker (HA-

SS-HA) provided antimicrobial activity and riveted it with the porous structure to trap the antibiotics. The HA-SS-HA showed moderate antibacterial activity; however, the antibiotics encapsulated HA-SS-HA (antibiotics@HA-SS-HA) showed excellent antibacterial activity against antibiotic-susceptible and antibiotic-resistant bacterial strains. HA is sensitive to the hyaluronidase enzyme, which is also secreted by bacterial cells in its extracellular space. Hence, we used hyaluronidase as stimuli to regulate the release of antibiotics from the antibiotics@HA-SS-HA in a controlled manner. Coating of this gel onto fabrics showed a Band-Aid-like use of HA-SS-HA and antibiotics@HA-SS-HA.

4.2 Results and Discussion

4.2.1 Synthesis of sulfonium linker and cross-linked hydrogel

HA of high molecular weight (around 2.94 MDa) was extracted from *Streptococcus zooepidemicus* as described in the literature.[22] To fabricate the cross-linked HA polymer, the linker molecule (pyridine-2,6-diylbis(methylene))bis((2-aminoethyl)(methyl)sulfonium) (Compound B) was synthesized from 2,6-bis(bromomethyl)pyridine. Condensation of tert-butyl (2-(methylthio)ethyl)carbamate with 2,6-bis(bromomethyl)pyridine resulted in the desired (pyridine-2,6-diylbis(methylene))bis((2-aminoethyl)(methyl)sulfonium). Finally, the sulfonium-containing linker molecule was used to cross-link HA via the amide coupling method was performed in PBS buffer using DMTMM as the coupling reagent (Figure 4.1). The amide coupling between HA and

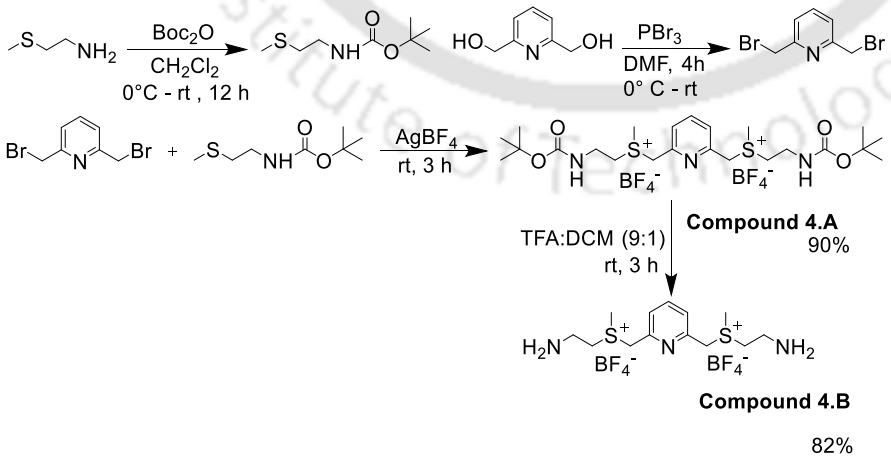

Figure 4.1 Synthetic routes to sulfonium-containing linker.

linker molecule resulted in the formation of immovable cross-linked gel under the reaction conditions (Figure 4.2A). After purification, the dried polymer was characterized by FTIR and NMR. The FTIR spectrum of HA-SS-HA gel showed a characteristic C=C and C=N stretching peak at 1459 and around 1500 $cm^{-1,}$ respectively, suggesting a pyridine-containing sulfonium linker. In addition, the aromatic and aliphatic C-N stretches near 1100-1200 cm^{-1} were also present in cross-linked HA-SS-HA akin to the sulfonium linker molecule (Figure 4.2B).[23] In the case of ^{1}H NMR studies compared to only HA, the HA-SS-HA showed the aromatic ring (pyridine) installation in HA due to sulfonium conjugation (Figure 4.2C). Further, dynamic light scattering (DLS) measurements revealed a significant change in the hydrodynamic diameter (d_H) of the HA-SS-HA (3982 nm) compared to that of HA (1091 nm) (Figure 2D). An increase in HA-SS-HA size corresponds to the cross-linking of the HA with the sulfonium-containing linker molecule.

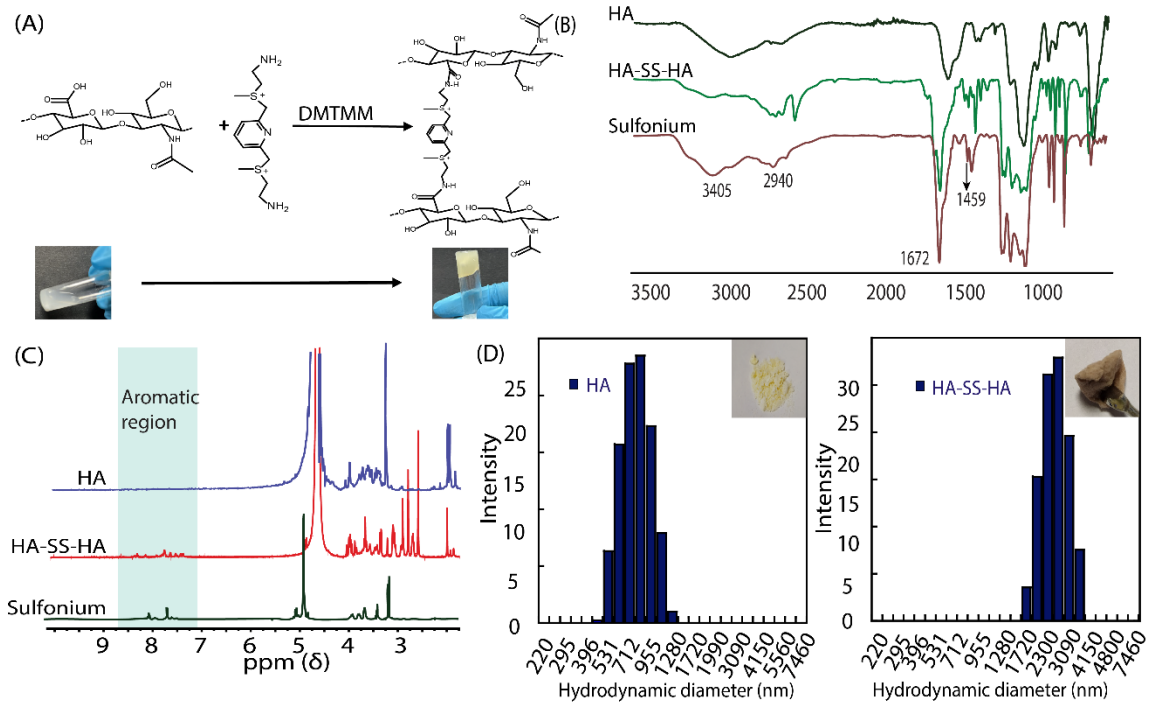

Figure 4.2 Synthetic route to HA-SS-HA biopolymer (A). FTIR spectra of HA, HA-SS-HA, and compound B (B). ^{1}H NMR spectra of HA, HA-SS-HA, and compound B (C). Average hydrodynamic diameter (nm) of HA and HA-SS-HA biopolymer (D).

4.2.2 Physical and morphological characterization

The dry cross-linked HA-SS-HA polymer had a porous structure, which inspired us to investigate its gelation property. The swelling property of the lyophilized material was

analyzed by immersing the fixed amount of dried HA-SS-HA in PBS buffer at pH-7.4. At different time intervals, the weight of the gel was measured after removing the surface water, and it was observed that within an hour gel had maximum water adsorption, its weight got enhanced up to 10 times, and the gel reached an equilibrium state after around 3 h (Figure 4.3A). These findings suggest the swelling properties of the HA-SS-HA gel. Instant swelling of the gel is helpful for its antimicrobial activity, as it can entrap more small molecules or antibiotics or instantly absorb the wound exudates when applied.

The rheological properties of the hydrogel were recorded to analyze the viscoelastic property of the HA-SS-HA gel. In this regard, the angular frequency sweep experiment was executed at a static strain of 0.1 % for the hydrogel. The storage module (G′) was observed to be higher than the loss module (G″), up to around 80 rad/s. G′ and G″ were independent of the angular frequency within the range of 1 to 80 rad/s, indicating the stability of the gel (Figure 4.3B). Followed by this experiment, a strain sweep experiment was executed, revealing that G′ was higher than the G″ up to 10 % strain, representing the gel akin property of the HA-SS-HA (Figure 4.3C). The self-healing activity of the gel was analyzed by cutting it into two pieces, and one part was stained with methylene blue dye to differentiate them from each other and allowed to reform. It showed that after 3 minutes, two pieces of the gel were healed (Figure 4.3D). This efficient self-healing property of the gel could be due to the dynamic non-covalent interaction, such as hydrogen bonding among the hydroxyl groups of HA molecules and electrostatic interactions of the cationic sulfonium moiety with the anionic carboxylic acid groups of HA. Additionally, the HA-SS-HA hydrogel showed adhesive properties (Figure 4.3E). The good adhesive and self-healing properties would give an advantage to the HA-SS-HA hydrogel for preventing foreign invasion and dressing wounds.

The morphology of the cross-linked HA-SS-HA was analyzed by its FESEM analysis. The analysis of the microscopic images showed the formation of microfiber and porous structure of HA-SS-HA in comparison to that of HA. FESEM images after the hyaluronidase treatments revealed that the enzyme digested the fibrous structure of the HA-SS-HA material (Figure 4.3F).

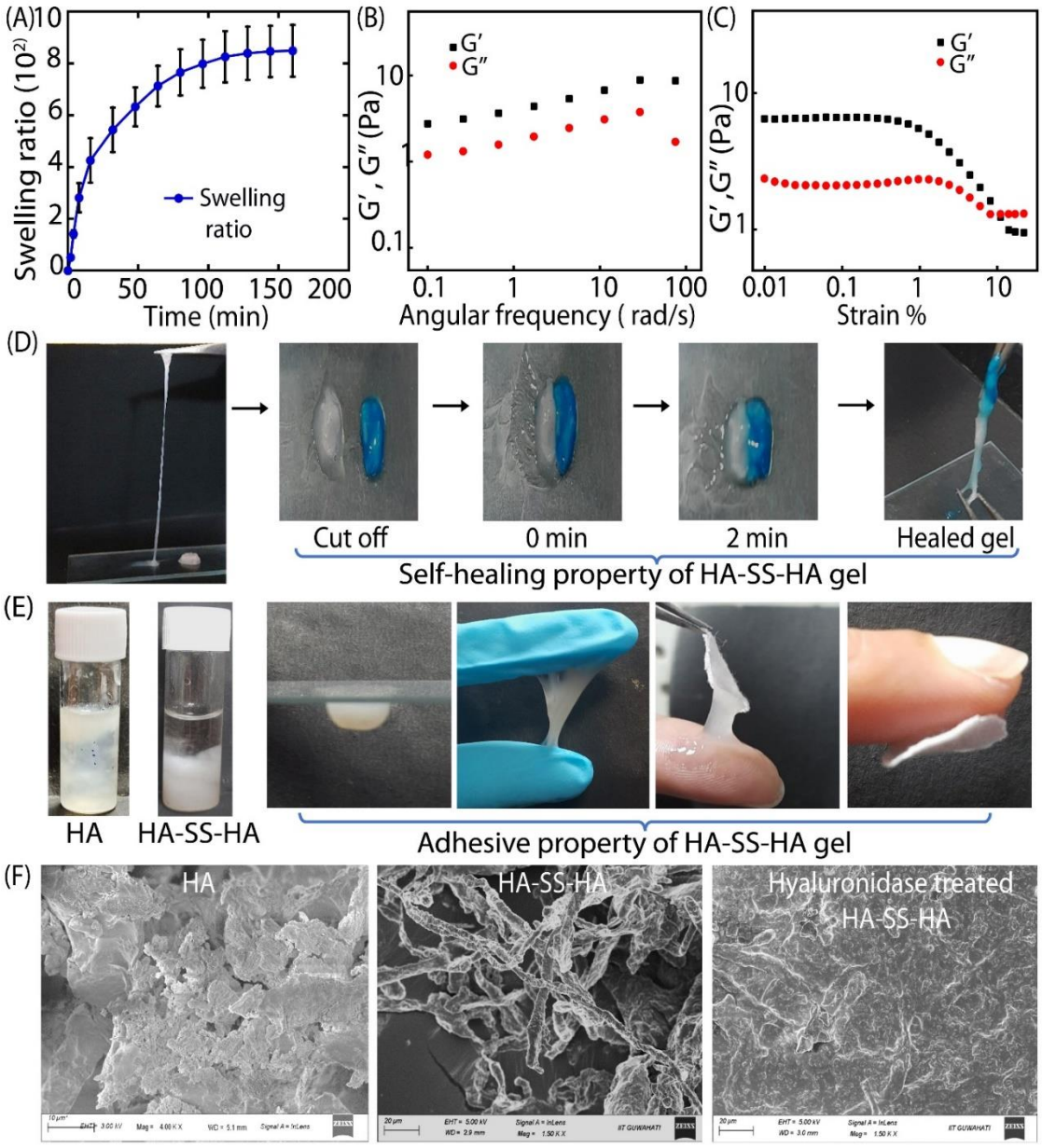

Figure 4.3 Water uptake-dependent swelling property of HA-SS-HA hydrogel (A). Dynamic storage moduli (G') and Loss moduli (G") of HA-SS-HA hydrogel at a variable angular frequency (B) and strain (C). Representative images demonstrating the elastic and self-healing properties of the HA-SS-HA hydrogel (D). Representative images demonstrate the adhesive property of HA-SS-HA hydrogel (E). Morphological analysis of HA, HA-SS-HA, and Hyaluronidase treated HA-SS-HA (F).

4.2.3 Antimicrobial activity of the modified hyaluronic acid

As per our earlier investigations, sulfonium and pyridinium-containing HA-SS-HA hydrogel are presumed to have antimicrobial activity.[13-15] Hence, we tested the antibacterial

efficacy of the HA-SS-HA hydrogel against both Gram-negative and Gram-positive bacterial cells. The Gram-positive bacteria such as *S. aureus*, GR-MRSA, vancomycin-sensitive *Enterococci sp.* (VSE), and vancomycin-resistant *Enterococci* (VRE1, VRE4, and VRE5) and Gram-negative bacteria such as *Escherichia coli* (*E. coli*) and *Pseudomonas aeruginosa* (*P. aeruginosa*) were used for antibacterial studies. Hydrogel at different concentrations was incubated with bacterial cells (10^6 CFU/mL) for 12-16 h, and then bacterial growth was monitored. The HA-SS-HA hydrogel showed antibacterial activities with minimum inhibitory concentration (MIC values) of 31.25, 125, 31.25, 31.25, 31.25, and 31.25 μg/mL against *S. aureus*, GR-MRSA, VSE, VRE1, VRE4, and VRE5, respectively (Table 1). Additionally, the HA-SS-HA hydrogel also showed antibacterial activities with MIC values of 62.5 and 31.25 μg/mL against *E. coli* and *P. aeruginosa*. The calculated MIC values suggested moderate antibacterial activities of the HA-SS-HA gel against the tested bacterial strains. However, only HA did not show any significant antibacterial activities under similar experimental conditions. Additionally, the antimicrobial activity of HA-SS-HA was also monitored at different time intervals. The time-killing assay was performed against *S. aureus* bacterial cells at a 2 x MIC value. Bacterial cells (10^6 CFU/mL) treated with HA-SS-HA (at 2 x MIC value) were harvested for 0, 2, 4, and 8 h and cultured on agar-containing media plates. The agar plate showed biocidal activity that started even after 2 h of incubation, and after four h of incubation, most of the bacterial cells were killed (Figure 4.4A).

4.2.4 Antibiotic encapsulation and release efficacy of the modified hyaluronic acid

The use of HA in antibiotics delivery applications inspired us to investigate the antimicrobial activities of the antibiotics-encapsulated HA-SS-HA gel.[24-27] In this regard, different classes of antibiotics, such as β-lactam (amoxicillin), polyketide (tetracycline), and arsenal (vancomycin) antibiotics, were entrapped within the hydrogel. The antibiotic encapsulation efficacy of the hydrogel was investigated from the loading and release profiles of the respective antibiotics. The spectrophotometric method revealed that the antibiotic loading efficacy was around 48% for HA-SS-HA gel. Here, we monitored the representative antibiotic release profile of vancomycin-encapsulated HA-SS-HA (van@HA-SS-HA). The time-dependent vancomycin-release profile was monitored by measuring the change in fluorescence intensity in the presence of PBS buffer, hyaluronidase enzyme, and the *S. aureus* cell lysate (Figure 4.4B).[28] The outcome of the vancomycin-

release study revealed a burst release profile in the presence of hyaluronidase enzyme and the *S. aureus* cell lysate in comparison to that of only buffer, suggesting that the degradation of HA polymer by hyaluronidase enzyme and the *S. aureus* cell lysate promote the fast release of vancomycin from the complex. The hyaluronidase enzyme cleaves the β-1,4 or β-1,3-glycosidic bond of HA to disaccharides.[29] Bacterial cells such as *S. aureus*, a common pathogen residing in wounded skin, secret hyaluronidase in extracellular space and help the bacterium spread in host tissues. Hence, we used this enzyme as stimuli for releasing more antibiotics at infected sites.

The antibiotics encapsulated HA-SS-HA (antibiotics@HA-SS-HA) were also used to investigate their antibacterial activities (Table 1). The antibacterial studies showed that the antibiotics@HA-SS-HA significantly affected the activity of the tested antibiotics, in particular those against the antibiotic-resistant bacterial strains. It is astonishing to note that the growth of VRE, which was found to be ineffective in the presence of even >125 μg/mL, restored its activity with van@HA-SS-HA. Additionally, the activity of amoxicillin@HA-SS-HA and Tet@HA-SS-HA against other antibiotic-resistant bacterial strains MRSA also showed the restoration of the activity of the respective antibiotics. The superior activity of antibiotics@HA-SS-HA over the only antibiotics could be due to the destabilization of bacterial membrane integrity, which is primarily responsible for developing resistance towards the antibiotics via various pathways, including efflux transporters and reduction in porins.[13-14, 30] While the vancomycin did not show significant activity, the van@HA-SS-HA was active, against the *E. coli* and *P. aeruginosa* (Table 1), suggesting that encapsulation of vancomycin within HA-SS-HA hydrogel is necessary for antimicrobial activity against Gram-negative bacteria. Hence, van@HA-SS-HA displayed similar activity against tested Gram-positive and Gram-negative bacterial strains. Therefore, at higher concentrations, sulfonium-containing HA-SS-HA acts as an antimicrobial agent. In comparison, it has adjuvant-like features at lower concentrations to escort the activity of other commercial antibiotics.[4-6]

Table 4.1 In vitro activities of the HA-SS-HA and antibiotics encapsulated HA-SS-HA hydrogels against various bacterial strains.

	Minimum Inhibitory Concentration (MIC) μg/mL

Bacterial strains	HA	HA-SS-HA	Van	Amox	Tet	Van@HA-SS-HA	Amox@HA-SS-HA	Tet@HA-SS-HA
S. aureus	>250	31.21 ± 7.52	1.56 ± 0.78	2.54 ± 0.62	1.86 ± 0.61	1.11 ± 0.20	0.22 ± 0.06	0.91 ± 0.21
GR-MRSA	>250	125 ± 15	3.92 ± 0.91	20 ± 5	168 ± 42	2.00 ± 0.41	3.71 ± 0.92	1.82 ± 0.45
VSE	>250	31.25 ± 7.51	3.12 ± 0.72	1.92 ± 0.51	3.92 ± 0.91	2.33 ± 0.45	0.45 ± 0.11	1.82 ± 0.45
VRE1	>250	31.25 ± 7.51	>125	31.25 ± 7.53	15.62 ± 3.02	1.51 ± 0.41	7.51 ± 1.81	0.91 ± 0.21
VRE4	>250	31.25 ± 7.51	>125	31.25 ± 7.52	15.62 ± 3.01	2.52 ± 1.21	3.72 ± 0.92	1.82 ± 0.45
VRE5	>250	31.25 ± 7.51	>125	62.52 ± 15	15.62 ± 3.05	1.92 ± 0.51	3.71 ± 0.91	7.52 ± 1.81
E. coli	>250	62.52 ± 15.01	125 ± 15	4.51 ± 1.12	3.77 ± 0.92	3.52 ± 0.87	0.94 ± 0.23	1.89 ± 0.46
P. aeruginosa	>250	31.21 ± 7.53	125 ± 15	3.37 ± 0.92	6.67 ± 1.61	3.52 ± 0.87	1.92 ± 0.42	3.91 ± 0.91

Van = vancomycin; Amox = amoxicillin; Tet = tetracycline. The MIC values were calculated using the weight of the HA-SS-HA polymer. VRE1, VRE4, and VRE5 are different clinical isolates. For antibiotic@HA-SS-HA, the MIC values were calculated based on the encapsulated concentration of antibiotics. All measurements were performed in triplicate.

4.2.5 Antibiofilm activity

The antimicrobial activity of these compounds or substances is leveraged by their antibiofilm activity. Hence, the antibiofilm activity of the HA-SS-HA was also investigated. In this regard, *S. aureus* biofilm was grown on a coverslip for four days and treated with HA-SS-HA for 12 h. A coverslip with treated and untreated biofilm was stained with acridine orange. The analysis of the fluorescence microscopic images was further scrutinized with Image-J software, which revealed that the HA-SS-HA treatment was

efficient enough to degrade the robust biofilm (Figure 4.4C). Recent studies also showed that carbohydrate-derived molecules have antibiofilm activities.[31]

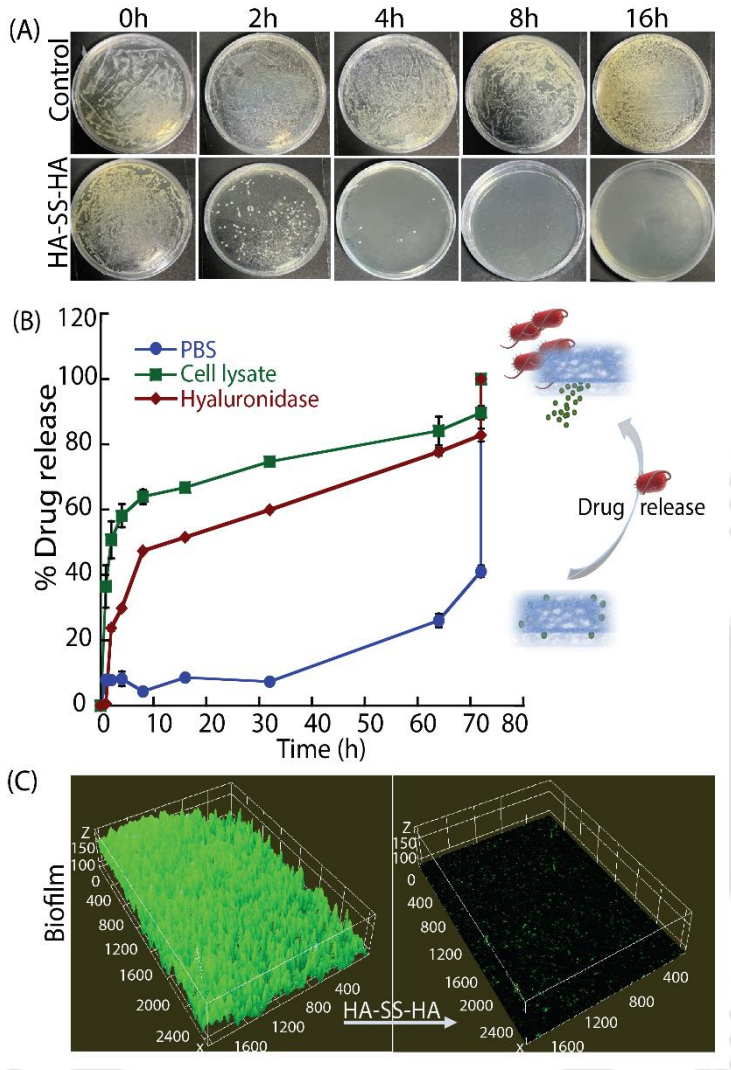

Figure 4.4 Bacterial killing kinetics of HA-SS-HA hydrogel (A). The drug release profile of Van@HA-SS-HA at different time intervals in the presence of bacterial cell lysate and hyaluronidase enzyme (B). Biofilm eradication activity of HA-SS-HA hydrogel (C).

4.2.6 Mechanistic studies

Earlier studies validated that sulfonium and pyridinium-containing molecules promote bacterial membrane-disrupting activity because of the electrostatic interaction of these cationic moieties with the negatively charged lipopolysaccharide or teichoic acid present on the bacterial membrane surface.[13-14, 30, 32-33] Hence, the HA-SS-HA treated bacterial cells were stained with dual staining agents, *i.e.,* propidium iodide and cFDA-SE, which stains

the membrane integrity compromised dead cells and esterase active live cells, respectively. Higher intensity of PI and lower intensity of cFDA-SE in HA-SS-HA gel-treated cells suggested the formation of membrane-compromised *S. aureus* cells; conversely, lower intensity of PI and higher intensity of cFDA-SE exhibited a high number of live cells in control, or untreated bacterial cells (Figure 4.5A).[13-14, 30, 32] The dual staining study was followed by morphological analysis of *E. coli* and *S. aureus* cells. Bacterial cells under the scanning electron microscope showed a distinct shape and surface of the typical cocci and rod-like architecture. The HA-SS-HA gel-treated *E. coli* cells lost their uniform cell identity and clustered around. The *S. aureus* cells lost their cocci chain and osmotic pressure-assisted surface morphology (Figure 4.5B). Hence, the distorted morphology and higher fluorescence intensity of propidium iodide (PI) stained S. aureus bacterial cells proved the membrane-disrupting activity of HA-SS-HA gel. We hypothesized that the membrane-disrupting activity of HA-SS-HA gel could assist vancomycin, amoxicillin, and other antibiotics in rejuvenating its activity against VRE, MRSA, and other antibiotic-resistant bacterial strains.[10]

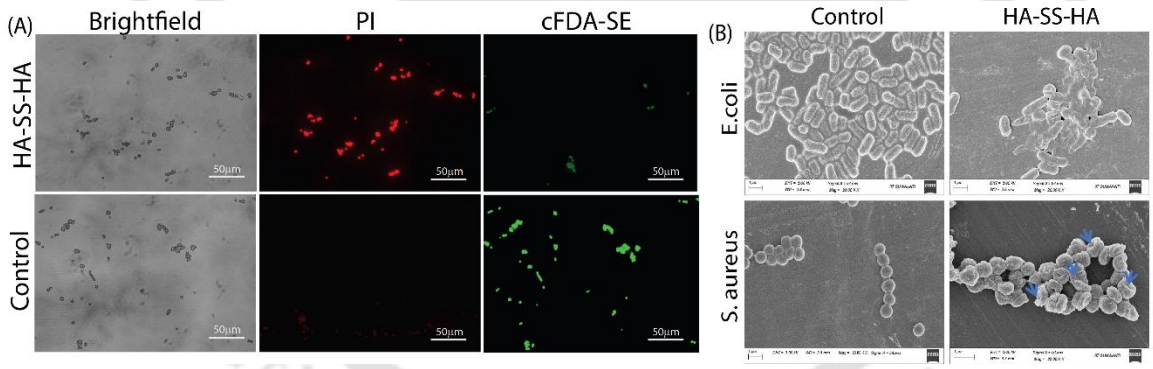

Figure 4.5 Representative live dead (cFDA-SE and PI stained) cell images of control and HA-SS-HA treated *S. aureus* cells shows membrane-directed antimicrobial activity (A). Morphological analysis of HA-SS-HA treated *E. coli* and *S. aureus* cells by FESEM (B).

4.2.7 Resistance study

Recent studies revealed that the presence of vancomycin in the extracellular environment induces the expression of vancomycin resistance vanHAX gene, a van operon cluster of the gene.[34] The expression of vanHAX causes the target site modification in the presence of vancomycin antibiotic. Therefore, we investigated whether the encapsulation of vancomycin within the HA-SS-HA gel reduces the resistance capability of the VSE cells.

Our studies showed that HA-SS-HA hydrogel had a consistent MIC value, while only vancomycin showed an enhancement of MIC value (2-fold after 24 days and 8-fold after 32 days). In comparison, the van@HA-SS-HA-treated bacterial cells showed very low or negligible resistance even after 32 days (Figure 4.6). The outcome of the resistance study suggested that the membrane-disrupting activity and multidimensional binding sites of polymeric HA-SS-HA gel could efficiently counteract the resistance mechanism of the bacterial cells.[30, 32] Additionally, the antibacterial studies showed a similar activity of van@HA-SS-HA gel against the vancomycin-resistant *Enterococcus spp.* (VRE) and vancomycin-sensitive *Enterococcus spp*. (VSE) bacterial strain, suggesting its ability to counteract the vancomycin-resistance mechanism of VRE cells (Table 1).

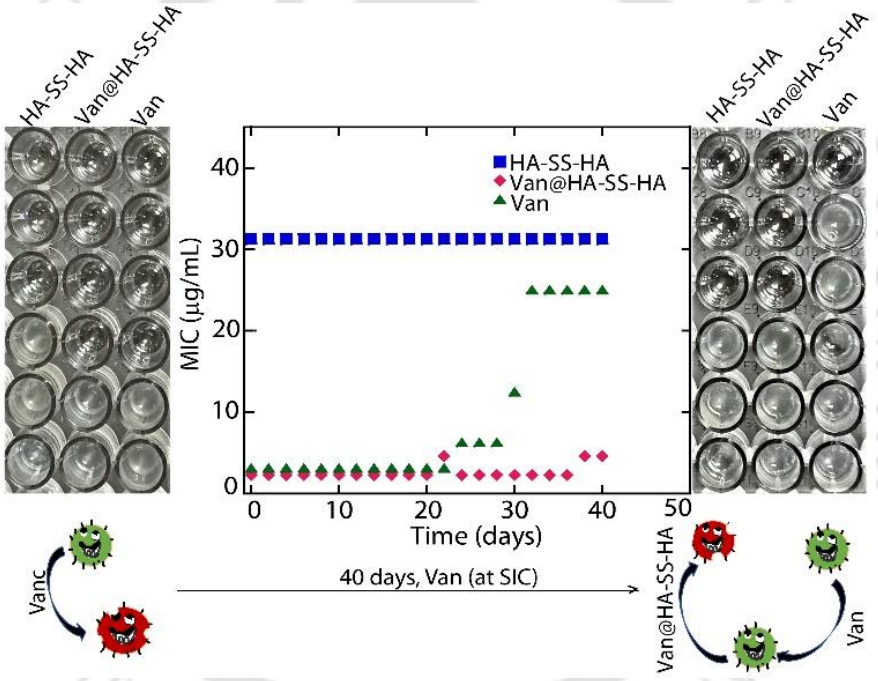

Figure 4.6 Resistance study of the HA-SS-HA, Van@HA-SS-HA, and Van. Representative plate images depict the changes in the growth pattern at o and after 40 days. The plot demonstrates the changes in MIC values within 0-40 days. SIC = Sub-inhibitory concentration.

4.2.8 Cytotoxicity Assay

The cytotoxicity of the HA-SS-HA gel on PBMC cells was evaluated using the MTT assay. After 24 hours of incubation, the viability of the cells was assessed at different concentrations of HA-SS-HA. The results indicated that more than 80% of the cells remained viable up to a concentration of 100 µg/mL of HA-SS-HA (Figure 4.7) and even

at 200 µg/mL more than 70 % cells were viable and gel can be considered biocompatible for potential applications.

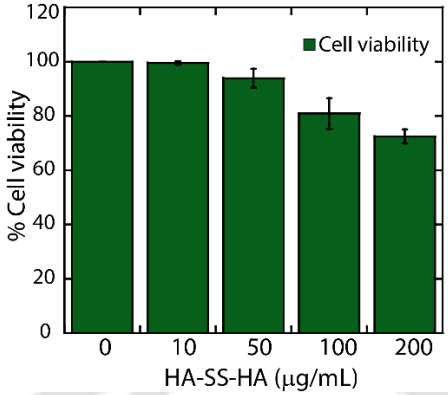

Figure 4.7 In vitro cytotoxicity assessment of HA-SS-HA hydrogel. The figure depicts the viability of Peripheral Blood Mononuclear Cells (PBMCs) after a 24-hour incubation with HA-SS-HA gel at varying concentrations. The data presented in the figure represent the mean values with standard deviation (SD) indicated and the experiment was performed in triplicates.

4.2.9 In vivo studies

4.2.9 .1 *In vivo* Wound Healing activity

The wound healing efficacy of the HA-SS-HA gel was evaluated in a BALB/c mice model. In the treated group, wounds were treated with the HA-SS-HA gel twice (on day 1 and day 7 post incision), without the use of any secondary dressing. (Figure 4.8B). The wound diameter was measured at multiple time points (day 1, 3, 7, and 12) in both the treated and control groups. At day 1 after the incision, the wound diameter was comparable between the control group (5.9 ± 0.05 mm) and the treated group (5.9 ± 0.11 mm while by day 3 the treated group exhibited a 7% reduction in wound area, with a diameter of 3.8 ± 0.2 mm, while the control group had a diameter of 4 ± 0.36 mm (*$p < 0.05$). Significant progress in wound closure was observed in the treated group at day 7 after treatment, with a significantly reduced wound diameter of 1.6 ± 0.15 mm (**$p < 0.005$), corresponding to a 45% closure compared to the untreated control group (3 ± 0.5 mm). By day 12 post-incision, the treated group exhibited further advancement in wound closure, as indicated by a diameter of 0.5 mm, representing a 61% closure compared to the control group (1.3 ± 0.4 mm) (**$p < 0.005$These findings emphasize the remarkable wound healing benefits of the

HA-SS-HA treatment, as evidenced by accelerated closure rates at different time points compared to the untreated control group.

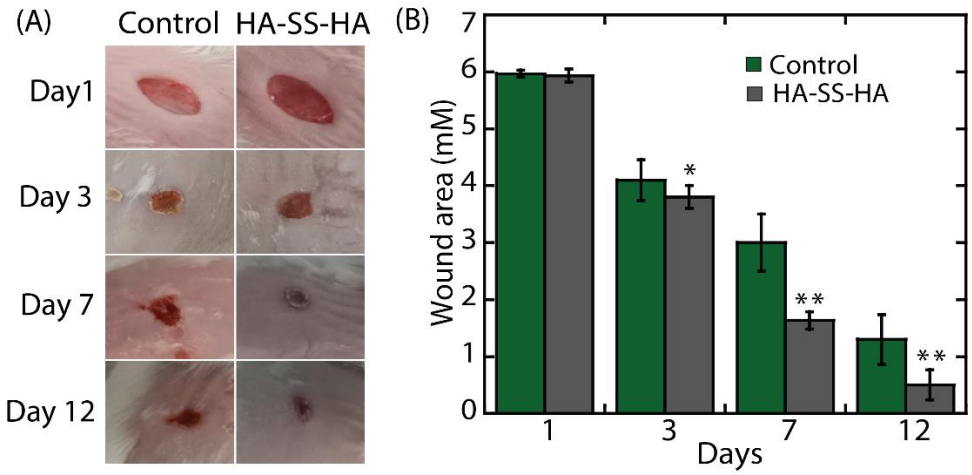

Figure 4.8 Promotion of wound healing in a BALB/c mouse model by HA-SS-HA hydrogel. (A) Representative images showcasing the progressive closure of wounds at day 1, day 3, day 7, day 12, and day 14. (B) Graphical representation illustrating the comparison of wound closure areas (in mm) between the HA-SS-HA treated group and the untreated control group at the specified time points. Standard deviations are provided to indicate the variability of three experiments.

4.2.9.2 Histological evaluations

Histological analysis was performed to assess the wound healing potential of HA-SS-HA hydrogel in a murine model by staining the wound sections on the 1st, 3rd, and 7th day post-treatment. Histomorphological findings play a crucial role in evaluating the effectiveness of compounds during the wound healing process. The healing process of wounds involves three main phases: hemostasis, inflammation, and tissue regeneration. The presence of certain facultative bacteria can significantly accelerate inflammation and impede the healing process. The intensity of the inflammatory response is directly proportional to the bacterial load in the tissue. The extent of newly formed epithelium, the increase in granulated tissue thickness, and the decrease in inflammatory cell count were considered as indicators of the healing process. Hematoxylin and eosin staining of wound sections on the 1st, 3rd, and 7th day post-treatment were performed to evaluate epithelial regeneration and tissue formation. As illustrated in Figure 9, both the treated and untreated groups of animals exhibited a ruptured epidermal (E) layer in the early stage of wound creation (day-

1). In the untreated control wounds, the presence of epithelial necrosis (N) and less organized granulation (G) tissue was observed. Conversely, on day-3 the HA-SS-HA treated animals displayed the proliferation of the epidermal layer along with well-organized granulation tissue (G) containing numerous blood vessels (B) (Figure 4.9). By day 7 of the healing process, complete regeneration of the epidermis was observed in the HA-SS-HA treated group. In contrast, the untreated group of animals still exhibited a poorly arranged dermis, immature granulation tissue with a high cell count, and a significant presence of inflammatory infiltrate. This was in stark contrast to the wounds treated with HA-SS-HA gel, where well-organized granulation tissue with abundant blood vessels were noticed. These histological findings demonstrate that the HA-SS-HA gel treatment promotes epithelial regeneration, the development of well-organized granulation tissue, and a reduction in inflammatory response, highlighting its potential for enhancing the wound healing process.

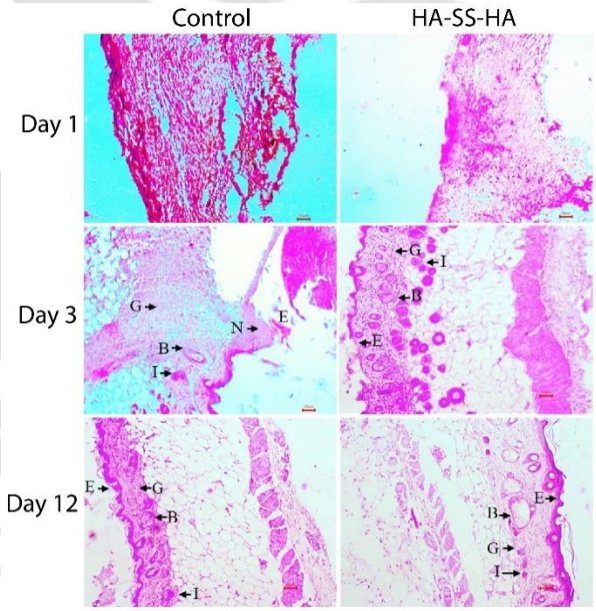

Figure 4.9 Histological analysis of wounds using H&E staining after treatment with HA-SS-HA gel and comparison to untreated control tissue at various time points: day 1, day 3, and day 7. Key histological features identified include E (epidermal layer), G (granulation tissue), B (blood vessels), N (epithelial necrosis), and I (inflammatory cell infiltration).

4.2.10 Application

The aforementioned characteristics of the gel, including swelling behavior, elasticity, adhesive nature, and efficient antimicrobial activity against antibiotic-sensitive and antibiotic-resistant bacterial strains, gave us a glimpse of its usability to counteract pathogenic bacterial infection. Hence, we tried examining one such application by coating the gel onto fabric to render its Band-Aid-like features. Excess wound exudates may cause maceration and delay of healing followed by pathogenic infection. Hence, due to their swelling behavior, coated fabrics can be used for wound dressing with antimicrobial activity and high soaking capability. The soaking ability of the gel may further render it faster antibiotic release due to the hyaluronidase enzyme secreted by the tissue and bacterial cells around the wound. We coated the HA-SS-HA (5 mg/mL) and van@HA-SS-HA (2.5 mg/mL HA-SS-HA, 1.25 mg/mL vancomycin) and vancomycin (5 mg/mL) gel onto the fabric and tested the antimicrobial efficacy of the HA-SS-HA and against antibiotic-sensitive (VSE) and antibiotic-resistant (VRE) bacterial strains by zone inhibition assay. We observed that all three wet-coated fabrics containing HA-SS-HA, vancomycin@HA-SS-HA, and vancomycin showed radial zone inhibition of 8.0, 9.0, and 5.0 mm against VSE, and the radial zone inhibition was 6.0, 8.0, 0.00 mm against VRE, respectively (Figure 4.10). It can be noted from this data that here, akin to the earlier antimicrobial activity, VRE failed to reveal any inhibitory activity against antibiotic-resistant bacterial strains, while van@HA-SS-HA effectively inhibited the growth of bacteria.

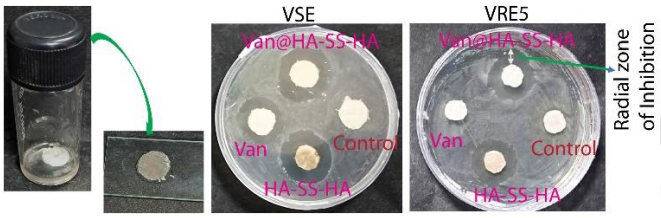

Figure 4.10 Plate images to reveal the antimicrobial efficacy of the Van, Van@HA-SS-HA, and HA-SS-HA against VSE and VRE by zone inhibition method.

Commercial antibiotics such as vancomycin, amoxicillin, and tetracycline served as life-saving antibiotics over the years until the reports of resistance. This observation suggests that antibiotics are insufficient to address the antimicrobial resistance crisis. Meanwhile, recent interest in developing membrane-active vancomycin or beta-lactam antibiotics has grown due to their ability to overcome inherited and non-inherited resistance. However,

their synthetic methods are cumbersome, and large-scale production is challenging. Clinical approval of these synthetic antibiotic analogs is also time-consuming and economically unviable. Therefore, a holistic approach of developing a common platform that would act as a carrier or adjuvant for commercially available antibiotics would be imperative. Antimicrobial adjuvants or carriers could be considered part of an interconnected web of tactics that ensures the strategic use of antibiotics. We have shown that the development of suitable adjuvants or carriers to these commercial antibiotics could resensitize these antibiotics against antibiotic-resistant bacterial strains. The presence of cationic moiety within such adjuvants or carriers promotes interactions with the negatively charged bacterial membrane to agitate the membrane integrity, resulting in a broad-spectrum activity against Gram-positive, Gram-negative, and antibiotic-resistant bacteria. The antibiotic@HA-SS-HA showed remarkable improvement in antibacterial efficacy in a mouse thigh infection model compared to vancomycin against MRSA. Overall, we demonstrated that antibiotic adjuvants or carriers such as HA-SS-HA in combination with antibiotics are important for fostering a future in which bacterial infections are treated with better efficacy. These observations also expand a new dimension in understanding the mechanism of such membrane-active antibiotic adjuvants or carriers.

4.3 Summary

Several bacterial strains, including *E. coli*, MRSA, *P. aeruginosa*, and VRE, have been resistant to the available antimicrobial agents. We developed sulfonium-containing HA-based cross-linked hydrogel (HA-SS-HA) to combat these antibiotic-resistant bacterial strains. Conjugation of (pyridine-2,6-diylbis(methylene))bis((2-aminoethyl)(methyl)sulfonium) with HA provided the hydrogel with inherent antibacterial properties, and its cross-linking makes it a suitable carrier for commercial antibiotics. The viscous, adhesive, and self-healing properties of the HA-SS-HA gel make it suitable for topical use. Membrane subverting activity of HA-SS-HA resensitized the antibiotic-resistant strain VRE against vancomycin at a concentration lower than its MIC value. The hydrogel also had the robust capability to breach the biofilm. The HA-SS-HA gel demonstrated remarkable biocompatibility significant acceleration of wound closure compared to the untreated control group which was further supported by the positive histological changes. HA-SS-HA gel at lower concentrations formed a film on the fabric. After swelling, it can diffuse through the wounds and inhibit the infection, and this property

was demonstrated by a zone inhibition experiment against *S. aureus* by the fabric coated with a gel. Overall, the conjugation of sulfonium molecule provides the membrane destabilizing activity to the HA, while the same provides the faster wound healing properties and biocompatible nature to the sulfonium-containing gel. These modifications and development of antimicrobial agents pave the way for further biocompatible antibiotic adjuvants and carriers in a cost-effective manner to counteract the resistance and promote antibiotic stewardship.

4.4 Experimental section

4.4.1 Synthesis of tert-butyl (2-(methylthio)ethyl)carbamate — To a stirring solution of 2-(methylthio)ethan-1-amine (100 mg, 1.096 mmol) in dichloromethane (5 mL), a solution of di-tert-butyl dicarbonate (240 mg, 1.096 mmol) in dichloromethane (3 mL) was added dropwise at 0° C, and the reaction mixture was stirred for 30 min. The reaction mixture was also stirred at room temperature for an additional 12 h. After that, the solvent was removed under reduced pressure and purification with column chromatography using a methanol/dichloromethane (0-5 %) solvent gradient afforded the target compound, tert-butyl (2-(methylthio)ethyl)carbamate. The compound was characterized by ^{1}H NMR and ^{13}C NMR analysis. ^{1}H NMR (600 MHz, $CDCl_3$): δ_{ppm} 1.43 (s, 9H), 2.10 (s,3H), 2.60-2.62 (t, 2H), 3.31-3.32 (d, 2H), 5 (s, 1H). ^{13}C NMR (600 MHz, $CDCl_3$): δ_{ppm} 15.03, 34.20, 39.05, 79.34, 155.80.

4.4.2 Synthesis of 2,6-bis(bromomethyl)pyridine — To a stirring solution of pyridine-2,6-diyldimethanol (100 mg, 0.718 mmol) in DMF (5 mL), PBr_3 (0.164 mL, 1.72 mmol) was added dropwise at 0° C, and the reaction mixture was stirred for 20 min. The reaction mixture was also stirred at room temperature for an additional 4 h. The resulting residue was dissolved in H_2O and extracted with EtOAc (4×50 mL). The combined organic layers were dried over anhydrous Na_2SO_4. The solvent was removed under reduced pressure to afford 2,6-bis(bromomethyl)pyridine, which was used without further purification. The compound was characterized by ^{1}H NMR and ^{13}C NMR analysis. ^{1}H NMR (600 MHz, $CDCl_3$): δ_{ppm} 4.56(s, 4H), 7.40-7.41 (d, 2H), 7.72-7.75 (t, 1H). ^{13}C NMR (600 MHz, $CDCl_3$): δ_{ppm} 33.45, 122.83, 138.15, 156.76.

4.4.3 Synthesis of (pyridine-2,6-diylbis(methylene))bis((2-((tert-butoxycarbonyl)amino)ethyl)(methyl)sulfonium) (compound A) — To the stirring

solution of 2,6-bis(bromomethyl)pyridine (100 mg, 0.377 mmol) and tert-butyl (2-(methylthio)ethyl)carbamate (191.28 mg, 0.830 mmol) in 10 mL of dry acetonitrile was added AgBF4 (147 mg, 0.377 mmol). The resulting mixture was stirred at room temperature for 4 hours under N_2 atmosphere. The progress of the reaction was monitored by TLC. After completion of the reaction, the solvent was removed under reduced pressure, and the resulting mixture was filtered off using a celite pad to remove excess silver salt. After that, the solvent was removed and purified with column chromatography using a methanol/dichloromethane (5 % - 10%) solvent gradient to afford the (pyridine-2,6-diylbis(methylene))bis((2-((tert-butoxycarbonyl)amino)ethyl)(methyl)sulfonium) (compound A). The compound was characterized by ^{1}H NMR and ^{13}C NMR analysis. ^{1}H NMR (600 MHz, $MeOD_4$): δ_{ppm} 1.46 (s, 18H), 1.94 (s, 4H), 3.05 (s, 6H), 3.33 (t, 4H), 3.61-3.67 (m, 4H), 7.66-7.67 (d, 2H), 8.03-8.05 (t, 1H). ^{13}C NMR (600 MHz, $MeOD_4$): δ_{ppm} 22.45, 27.29, 29.33, 43.87, 79.73, 125.19, 139.54, 149.82, 157.32.

4.4.4 Synthesis of (pyridine-2,6-diylbis(methylene))bis((2-aminoethyl)(methyl)sulfonium) (compound B) — Compound A (100 mg) was stirred with TFA (5 mL, 30% in dichloromethane) for 2 hours at room temperature. The progress of the reaction was monitored by TLC. After the completion of the reaction, the solvent was removed under reduced pressure. The reaction mixture was washed with dichloromethane and n-pentane and dried under reduced pressure. The compound was characterized by ^{1}H NMR and ^{13}C NMR analysis. ^{1}H NMR (400 MHz, $MeOD_4$) δ_{ppm} 3.06 (brs, 6H), 3.55-3.58 (br, 4H), 3.64-3.69 (m, 4H), 3.70-3.84 (m, 4H), 4.93-5.03 (m, 4H), 7.63-7.65(d, 2H),7.99-8.03(t, 1H); ^{13}C NMR (400 MHz, $MeOD_4$) δ_{ppm} 22.52-22.76, 34.22, 38.39-38.43, 63.96, 124.87-125.00, 139.64, 149.31.

4.4.5 Cross-linked Hyaluronic acid gel preparation — The hyaluronic acid gel was cross-linked with pyridine-2,6-diylbis(methylene))bis((2-aminoethyl)(methyl)sulfonium molecules in an aqueous medium via amide coupling method in the presence of the coupling reagent 4-(4,6-dimethoxy-1,3,5-triazin-2-yl)-4-methylmorpholinium tetrafluoroborate (DMTMM). The 50 mg of HA and 1:1 equivalent of DMTMM (30 mg) were stirred in water until they dissolved completely. Sulfonium compound dissolved in methanol at 1:2 equivalents were added to the gel solution dropwise and allowed to stir until cross-linking occurred and the gel's movement was immobile. The gel product was

dialyzed against adequate water to remove the reagent and unreacted molecules, followed by its lyophilization. The obtained product was encoded as HA-SS-HA.

4.4.6 Characterization of HA-SS-HA — The chemical and physical characterization of the HA-SS-HA was performed by FTIR, NMR, DLS-Zeta, and FESEM. To confirm the chemical modification of HA polymer, the NMR and FTIR studies were performed using the freeze-dried HA-SS-HA. For FTIR dried 1 mg sample was placed on the attenuated total reflectance (ATR), and % transmittance spectra were observed from 4000-400 cm^{-1}. NMR spectra were recorded by dissolving the 5 mg of the dried sample into D_2O at 25°C by Bruker 600 NMR. The hydrodynamic diameter and surface potential of the polymer were analyzed by a Zetasizer Nano ZS90 (Malvern). Dried HA and HA-SS-HA sample solutions were prepared in Mili-Q water. This stock sample was diluted in buffer at physiological pH, and its hydrodynamic diameter was measured in a 3 mL cuvette, followed by the zeta potential measurement in a 1 mL Zeta cuvette.

4.4.7 Rheological study — Anton par MCR 102 rheometer instrument equipped with a 20 mm parallel plate measurement system was used to analyze the viscoelastic property of the hydrogel at 25°C. HA-SS-HA gel was prepared at 5 mg/mL concentration in PBS buffer at physiological pH. A strain sweep test was executed at a constant oscillatory frequency of 1 rad/s while varying the strain from 0.01 to 100%. Further, to analyze the mechanical strength of the gel, the frequency sweep experiment was performed at a static strain of 0.1% by varying the frequency from 1 to 100 rad/s. From this experiment, the storage module (G′) and loss moduli (G″) were analyzed to measure the gelation quality of the HA-SS-HA gel.

4.4.8 Swelling behavior and self-healing activity — Swelling behavior of the HA-SS-HA was performed by taking a fixed amount of freeze-dried compound followed by its dry weight (WD) measurement. PBS buffer was added to the sample and incubated at room temperature. The sample was taken out at different time intervals, and the extra water was soaked away before its weight (WT) was measured. The swelling ratio was determined using the following formula.

$$\%\,\text{Swelling} = \frac{WT - WD}{WD} * 100$$

The swollen gel was cut into two parts, and one part was stained with methylene blue dye to differentiate it from the other part, allowed to come into contact, and left for 3 minutes to examine the self-healing activity of the gel.

4.4.9 FESEM of HA-SS-HA — Morphological analysis of the cross-linked HA-SS-HA was analyzed by FESEM images. The dried sample was glued onto double-sided carbon tape, which was further stacked onto the copper grid. Before the analysis, the sample was coated with gold, and images were analyzed and captured at 2 to 5 kV by Zeiss, Sigma 300.

4.4.10 Antibiotic encapsulation within the cross-linked hydrogel — Dried HA-SS-HA was mixed with PBS buffer containing vancomycin at 1 mg/mL concentration and stirred for 4 h. Unbounded antibiotics were removed by centrifugation, and the amount of encapsulated antibiotic was assessed by spectroscopic measurement of the supernatant and total concentration of the antibiotic added before entrapment. Antibiotic release behavior was analyzed in the presence of *S. aureus* cell lysate, glutathione, hyaluronidase, and only buffer. After the entrapment of the antibiotic at different time intervals, the sample was collected and centrifuged at 10,000 rpm for 5 min. The supernatant was collected, and its fluorescence spectra were measured at an excitation wavelength of 280 nm and emission wavelength of 310 nm to assess the released concentration of the vancomycin.

4.4.11 Antimicrobial activity of the hydrogel — The hyaluronic hydrogel was examined for its antimicrobial activity against Gram-negative (E. *coli;* MTCC 1687 and P. *aeruginosa;* MTCC 2488) and Gram-positive (*S. aureus*; MTCC 96, gentamycin resistance methicillin resistance *S. aureus*), clinical isolates of VSE and VRE1, VRE4, VRE5 strains (a generous gift from Prof. Gopal Nath, Institute of Medical Science, Banaras Hindu University, (IMS-BHU) Varanasi India). The Glycerol stock of the bacterial strains was cultured in Luria Bertani (LB) media until the mid-logarithmic phase at 37ºC and 180 rpm and harvested by centrifugation re-suspended in PBS. HA-SS-HA gel stock was prepared in PBS and diluted at various concentrations in a 96-well plate. Only PBS-treated bacterial culture was used as a control. Bacterial cells at 10^6 CFU/mL were added to the gel solution and incubated for 12 to 16 h at 37ºC.

4.4.12 Antibiofilm activity — *S. aureus* bacterial cell was cultured until the mid-logarithmic phase and transferred in a 12 mm Petri plate containing a thin glass cover slip. Robust biofilm was allowed to grow for 4 days on the cover slip. Incubation was followed

by washing with PBS buffer to remove the planktonic cells, and the cover slip was further treated with HA-SS-HA gel and incubated for 12 to 16 h. The gel was washed with buffer, and the cover slip was immersed in 0.2% w/v acridine orange and incubated for 10 min. A biofilm containing a cover slip was analyzed under a fluorescence microscope (Nikon Eclipse Ts2R).

4.4.13 Time kill assay — *S. aureus* bacterial strain was cultured and harvested at 37ºC and 180 rpm and treated with the HA-SS-HA followed by incubation at 37ºC. At various time intervals (0, 2, 4, 8, and 16 h), 20 µL of the bacterial culture was collected and plated onto the LB agar media containing a Petri plate after 10 times dilution in broth media. The plate was incubated for 16 h at 37ºC.

4.4.14 Live dead cell imaging of the bacterial cells — *S. aureus* cell was cultured and treated with HA-SS-HA at 2X MIC value and incubated for 4 h. Bacterial cells without treatment were taken as a control. Followed by the incubation, bacterial cells were washed with PBS and stained with live cell (CFDA-SE) and dying cell (PI) staining dye and incubated for 30 min under dark conditions. Cells were further washed with buffer by centrifugation to remove the superfluous dye. Cells were fixed with 2.5 % glutaraldehyde solution and drop-casted onto a glass slide before analysis, and images were captured under a fluorescence microscope (Nikon Eclipse Ts2R).

4.4.15 Morphological analysis of the hydrogel-treated bacterial cells — Morphological analysis of the HA-SS-HA was performed against *S. aureus* and *E. coli* cells. Towards this approach, both types of cells were cultured and treated as in the aforementioned section. Treated and untreated cells were washed with buffer by centrifugation, followed by Milli-Q water. Cells were fixed with 2.5% glutaraldehyde, drop-casted onto aluminum foil, wrapped onto the glass grid, and allowed to dry under laminar airflow. The sample was further stacked onto the copper grid and gold coated before analysis under the microscope (Zeiss, Sigma 300).

4.4.16 Antibiotic resistance experiments— The ability to counteract the resistance mechanism of the HA-SS-HA, Van@HA-SS-HA, and vancomycin against VSE was tested for 40 days. The VSE strain was cultured, as stated in the earlier section. Separately, VSE was cultured in the presence of subinhibitory concentration (SIC) of HA-SS-HA, Van@HA-SS-HA, and vancomycin. Till 40 days, cell passaging was performed, and MIC

of these 3 bacterial cultures was analyzed on alternate days by the micro-broth dilution method.

4.4.17 Cytotoxicity Assay — The cytotoxicity of HA-SS-HA gel was assessed using the MTT assay. Peripheral blood mononuclear cells (PBMCs) were isolated by density gradient centrifugation using Hisep (centrifuge at 1000g for 30 minutes). The isolated PBMCs were then seeded at a concentration of 3 × 105 cells/ml in a 96-well microtitre plate, which contained Roswell Park Memorial Institute medium (RPMI) supplemented with 10% heat-inactivated fetal bovine serum (FBS) and 1% penicillin/streptomycin. To evaluate cytotoxic effects, various concentrations of HA-SS-HA hydrogel (0, 10, 50, 100, and 200 µg/ml) were incubated with the cells for 24 hours at 37°C with 5% CO2 (Da Silva J, 2019 Jun). Subsequently, the medium was replaced with fresh DMEM (without Phenol Red) containing 1 mg/mL MTT (Himedia, India). The cells were then incubated for 3 hours, and untransformed MTT was removed. Next, 50 µL of 0.04M HCl isopropanolic solution was added to each well. After 15 minutes of incubation at room temperature, absorbance was measured using an automatic plate reader (Synergy H1 Hybrid Reader, Biotek, Winooski, VT) at a background wavelength of 690 nm and a test wavelength of 650 nm. The viability of the cells after treatment was calculated using the following equation:

$$cell\ viability\ (\%) = \frac{Sample(OD630nm)}{UntreatedControl(OD630nm)} * 100$$

4.4.18 *In vivo* wound healing —The wound healing effect of HA-SS-HA was assessed using an *in vivo* BALB/c mouse model. All animal experiments were conducted under aseptic conditions and in accordance with the guidelines established by the Institutional Animal Ethical Committee (IAEC) with ethical approval number TU/IAEC/2022/1/2-12. Mice, aged 6-8 weeks and weighing approximately 20 g, were randomly divided into two groups: the control group and the HA-SS-HA gel-treated group, with six mice in each group. The mice were anesthetized with a ketamine-xylazine cocktail by intraperitoneal injection before the experiment, and the hair on their backside was carefully shaved. Circular wounds were created using a 6 mm puncher and surgical scissors. In the treatment group, the wounds were covered with HA-SS-HA gel, while the control group treated with saline solution topically. The wound area was documented through photographs on days 1, 3, 7, 12, and 14 to monitor the progression of wound healing[1].

4.4.19 Histological Analysis — On days 1, 3, and 12, mice from both the groups were euthanized using the cervical dislocation method for tissue collection. Skin specimens were carefully obtained from the widest area of the wound tissue, including the surrounding normal skin margin. These specimens were then fixed in a 4% paraformaldehyde solution for 24 hours. Subsequently, paraffin blocks were prepared from the fixed specimens, and 3µm thick sections were sliced from these blocks. To enable histological examination, Hematoxylin and Eosin (H&E) staining was performed on the sections (Fasiku VO, 2021).

4.4.20 Coating of the gel onto fabric and its zone inhibition experiment — HA-SS-HA and antibiotics@HA-SS-HA gel at a concentration of 10 mg/mL was coated onto fabric. The fabric pieces were immersed in the gel for 1 min and dried at room temperature. A zone inhibition experiment against *S. aureus* analyzed the antimicrobial efficacy of the HA-SS-HA coated fabric**.** Bacterial cells were cultured, as in the aforementioned section. At 10^8 CFU/mL, the cells were plated on a BHI agar plate. A small piece of coated and uncoated fabrics was placed on the agar plate with bacterial cells and incubated at 37ºC for 16 to 20 h.

4.5 References

(1) Willyard, C. The Drug-Resistant Bacteria That Pose the Greatest Health Threats. *Nature* **2017,** *543* (543), 15, DOI: org/10.1038/nature.2017.21550.

(2) Jones, K. E.; Patel, N. G.; Levy, M. A.; Storeygard, A.; Balk, D.; Gittleman, J. L.; Daszak, P. Global Trends in Emerging Infectious Diseases. *Nature* **2008,** *451* (7181), 990-U4, DOI: 10.1038/nature06536.

(3) Costerton, J. W.; Stewart, P. S.; Greenberg, E. P. Bacterial Biofilms: A Common Cause of Persistent Infections. *Science* **1999,** *284* (5418), 1318-1322, DOI: DOI 10.1126/science.284.5418.1318.

(4) Melander, R. J.; Melander, C. The Challenge of Overcoming Antibiotic Resistance: An Adjuvant Approach? *ACS Infect Dis* **2017,** *3* (8), 559-563, DOI: 10.1021/acsinfecdis.7b00071.

(5) Berndsen, R.; Cunningham, T.; Kaelin, L.; Callender, M.; Boldog, W. D.; Viering, B.; King, A.; Labban, N.; Pollock, J. A.; Miller, H. B.; Blackledge, M. S. Identification and

Evaluation of Brominated Carbazoles as a Novel Antibiotic Adjuvant Scaffold in Mrsa. *Acs Med Chem Lett* **2022,** *13* (3), 483-491, DOI: 10.1021/acsmedchemlett.1c00680.

(6) Wei, M.; Wu, J. H.; Sun, H.; Zhang, B.; Hu, X.; Wang, Q. Y.; Li, B. W.; Xu, L. L.; Ma, T.; Gao, J. Q.; Li, F. Y.; Ling, D. S. An Enzymatic Antibiotic Adjuvant Modulates the Infectious Microenvironment to Overcome Antimicrobial Resistance of Pathogens. *Small* **2022**, DOI: 10.1002/smll.202205471.

(7) Bush, K.; Bradford, P. A. Beta-Lactams and Beta-Lactamase Inhibitors: An Overview. *Cold Spring Harb Perspect Med* **2016,** *6* (8), DOI: 10.1101/cshperspect.a025247.

(8) Tooke, C. L.; Hinchliffe, P.; Bragginton, E. C.; Colenso, C. K.; Hirvonen, V. H. A.; Takebayashi, Y.; Spencer, J. Beta-Lactamases and Beta-Lactamase Inhibitors in the 21st Century. *J Mol Biol* **2019,** *431* (18), 3472-3500, DOI: 10.1016/j.jmb.2019.04.002.

(9) Wu, Z. C.; Boger, D. L. Maxamycins: Durable Antibiotics Derived by Rational Redesign of Vancomycin. *Acc Chem Res* **2020,** *53* (11), 2587-2599, DOI: 10.1021/acs.accounts.0c00569.

(10) Guan, D. L.; Chen, F. F.; Qiu, Y. G.; Jiang, B. F.; Gong, L. K.; Law, L. F.; Huang, W. Sulfonium, an Underestimated Moiety for Structural Modification, Alters the Antibacterial Profile of Vancomycin against Multidrug-Resistant Bacteria. *Angew Chem Int Edit* **2019,** *58* (20), 6678-6682, DOI: 10.1002/anie.201902210.

(11) Yarlagadda, V.; Sarkar, P.; Samaddar, S.; Haldar, J. A Vancomycin Derivative with a Pyrophosphate-Binding Group: A Strategy to Combat Vancomycin-Resistant Bacteria. *Angew Chem Int Ed Engl* **2016,** *55* (27), 7836-40, DOI: 10.1002/anie.201601621.

(12) Sarkar, P.; Samaddar, S.; Ammanathan, V.; Yarlagadda, V.; Ghosh, C.; Shukla, M.; Kaul, G.; Manjithaya, R.; Chopra, S.; Haldar, J. Vancomycin Derivative Inactivates Carbapenem-Resistant Acinetobacter Baumannii and Induces Autophagy. *Acs Chem Biol* **2020,** *15* (4), 884-889, DOI: 10.1021/acschembio.0c00091.

(13) Patel, A.; Paul, S.; Akhtar, N.; Das, S.; Kar, S.; Bhattacharjee, S.; Manna, D. Onium- and Alkyl Amine-Decorated Protein Nanoparticles as Antimicrobial Agents and Carriers of Antibiotics to Promote Synergistic Antibacterial and Antibiofilm Activities. *Acs Appl Nano Mater* **2022,** *5* (11), 16602-16611, DOI: 10.1021/acsanm.2c03665.

(14) Patel, A.; Dey, S.; Shokeen, K.; Karpinski, T. M.; Sivaprakasam, S.; Kumar, S.; Manna, D. Sulfonium-Based Liposome-Encapsulated Antibiotics Deliver a Synergistic Antibacterial Activity. *Rsc Med Chem* **2021,** *12* (6), 1005-1015, DOI: 10.1039/d1md00091h.

(15) Dey, S.; Patel, A.; Raina, K.; Pradhan, N.; Biswas, O.; Thummer, R.; Manna, D. A Stimuli-Responsive Anticancer Drug Delivery System with Inherent Antibacterial Activities. *Chem Commun* **2020,** *56* (11), 1661-1664, DOI: 10.1039/c9cc08834b.

(16) Wang, X.; Wang, G. X.; Zhao, J. H.; Zhu, Z. Y.; Rao, J. Y. Main-Chain Sulfonium-Containing Homopolymers with Negligible Hemolytic Toxicity for Eradication of Bacterial and Fungal Biofilms. *Acs Macro Lett* **2021,** *10* (12), 1643-1649, DOI: 10.1021/acsmacrolett.1c00698.

(17) Zhao, J.; Zhu, Z.; Rao, J. The development of Cationic Sulfonium-Based Gels with Inherent Antibacterial, Excellent Antibiofilm, and Tunable Swelling Properties. *European Polymer Journal* **2022,** *179*, 111551, DOI: doi.org/10.1016/j.eurpolymj.2022.111551.

(18) Zhao, X.; Wu, H.; Guo, B. L.; Dong, R. N.; Qiu, Y. S.; Ma, P. X. Antibacterial Anti-Oxidant Electroactive Injectable Hydrogel as Self-Healing Wound Dressing with Hemostasis and Adhesiveness for Cutaneous Wound Healing. *Biomaterials* **2017,** *122*, 34-47, DOI: 10.1016/j.biomaterials.2017.01.011.

(19) Chen, M. M.; Tian, J.; Liu, Y.; Cao, H.; Li, R. Y.; Wang, J. H.; Wu, J. L.; Zhang, Q. Q. Dynamic Covalent Constructed Self-Healing Hydrogel for Sequential Delivery of Antibacterial Agent and Growth Factor in Wound Healing. *Chem Eng J* **2019,** *373*, 413-424, DOI: 10.1016/j.cej.2019.05.043.

(20) Sautrot-Ba, P.; Jockusch, S.; Nguyen, T. T. T.; Grande, D.; Chiapionne, A.; Abbad-Andaloussi, S.; Pan, M. B.; Meallet-Renault, R.; Versace, D. L. Photoinduced Synthesis of Antibacterial Hydrogel from an Aqueous Photoinitiating System. *European Polymer Journal* **2020,** *138*, DOI: ARTN 109936 10.1016/j.eurpolymj.2020.109936.

(21) Du, H.; Zha, G. Y.; Gao, L. L.; Wang, H.; Li, X. D.; Shen, Z. Q.; Zhu, W. P. Fully Biodegradable Antibacterial Hydrogels Via Thiol-Ene "Click" Chemistry. *Polym Chem-Uk* **2014,** *5* (13), 4002-4008, DOI: 10.1039/c4py00030g.

(22) Mohan, N.; Pavan, S. S.; Jayakumar, A.; Rathinavelu, S.; Sivaprakasam, S. Real-Time Metabolic Heat-Based Specific Growth Rate Soft Sensor for Monitoring and Control of High Molecular Weight Hyaluronic Acid Production by Streptococcus Zooepidemicus. *Appl Microbiol Biot* **2022,** *106* (3), 1079-1095, DOI: 10.1007/s00253-022-11760-1.

(23) Mavronasou, K.; Zamboulis, A.; Klonos, P.; Kyritsis, A.; Bikiaris, D. N.; Papadakis, R.; Deligkiozi, I. Poly(Vinyl Pyridine) and Its Quaternized Derivatives: Understanding Their Solvation and Solid State Properties. *Polymers-Basel* **2022,** *14* (4), DOI: ARTN 804 10.3390/polym14040804.

(24) Alipoor, R.; Ayan, M.; Hamblin, M. R.; Ranjbar, R.; Rashki, S. Hyaluronic Acid-Based Nanomaterials as a New Approach to the Treatment and Prevention of Bacterial Infections. *Front Bioeng Biotech* **2022,** *10*, DOI: ARTN 913912 10.3389/fbioe.2022.913912.

(25) Zamboni, F.; Wong, C. K.; Collins, M. N. The Hyaluronic Acid Association with Bacterial, Fungal and Viral Infections: Can Hyaluronic Acid Be Used as an Antimicrobial Polymer for Biomedical and Pharmaceutical Applications? *Bioact Mater* **2023,** *19*, 458-473, DOI: 10.1016/j.bioactmat.2022.04.023.

(26) Zhang, Z.; Suner, S. S.; Blake, D. A.; Ayyala, R. S.; Sahiner, N. Antimicrobial Activity and Biocompatibility of Slow-Release Hyaluronic Acid-Antibiotic Conjugated Particles. *Int J Pharmaceut* **2020,** *576*, DOI: ARTN 119024 10.1016/j.ijpharm.2020.119024.

(27) Boot, W.; Schmid, T.; D'Este, M.; Guillaume, O.; Foster, A.; Decosterd, L.; Richards, R. G.; Eglin, D.; Zeiter, S.; Moriarty, T. F. A Hyaluronic Acid Hydrogel Loaded with Gentamicin and Vancomycin Successfully Eradicates Chronic Methicillin-Resistant Staphylococcus Aureus Orthopedic Infection in a Sheep Model. *Antimicrob Agents Ch* **2021,** *65* (4), DOI: ARTN e01840-20 10.1128/AAC.01840-20.

(28) Zarkan, A.; Macklyne, H. R.; Truman, A. W.; Hesketh, A. R.; Hong, H. J. The Frontline Antibiotic Vancomycin Induces a Zinc Starvation Response in Bacteria by Binding to Zn(Ii). *Sci Rep-Uk* **2016,** *6*, DOI: ARTN 19602 10.1038/srep19602.

(29) Zins, J. E.; Grow, J. N. Commentary On: Endovascular Hyaluronidase Application through Superselective Angiography to Rescue Blindness Caused by Hyaluronic Acid Injection Comment. *Aesthet Surg J* **2021,** *41* (3), 356-357, DOI: 10.1093/asj/sjaa278.

(30) Hoque, J.; Konai, M. M.; Gonuguntla, S.; Manjunath, G. B.; Samaddar, S.; Yarlagadda, V.; Haldar, J. Membrane Active Small Molecules Show Selective Broad Spectrum Antibacterial Activity with No Detectable Resistance and Eradicate Biofilms. *J Med Chem* **2015,** *58* (14), 5486-5500, DOI: 10.1021/acs.jmedchem.5b00443.

(31) Singh, K.; Kulkarni, S. S. Small Carbohydrate Derivatives as Potent Antibiofilm Agents. *J Med Chem* **2022,** *65* (13), 8525-8549, DOI: 10.1021/acs.jmedchem.1c01039.

(32) Zhou, M.; Zheng, M. M.; Cai, J. F. Small Molecules with Membrane-Active Antibacterial Activity. *Acs Appl Mater Inter* **2020,** *12* (19), 21292-21299, DOI: 10.1021/acsami.9b20161.

(33) Sousa, M. C. New Antibiotics Target the Outer Membrane of Bacteria. *Nature* **2019,** *576* (7787), 389-390, DOI: 10.1038/d41586-019-03730-x.

(34) Yushchuk, O.; Binda, E.; Marinelli, F. Glycopeptide Antibiotic Resistance Genes: Distribution and Function in the Producer Actinomycetes. *Front Microbiol* **2020,** *11*, DOI: ARTN 1173 10.3389/fmicb.2020.01173.

Thesis conclusion

Thesis commences with (**Chapter 1**) laconic information about the role of antibiotic and its development. It explains the requirement to develop new antimicrobial drug due to drug resistant superbugs. Here we concluded that due to simple and smart genetic machinery of bacterial cell they can adopt themselves in harsh environment and can cop up with the antibiotics too. Hence development of new antibacterial agent is highly required and for this we concluded that drug with membrane directed activity can withstand the drug resistance strategy of the bacterial cell. Cationic amphiphilic molecules (eg. Sulfonium) are supposed to meet these criteria because they can provide electrostatic interaction with the negatively charged bacterial membrane as well as they can form nanoaggregate to encapsulate the drug and enhance their activity. Research work about sulfonium compounds enunciates that it is the rising epitome of potent antimicrobial agents to combat the resistance mechanism of the bacterial strains. In our study we ensured that in spite of having membrane directed activity sulfonium containing molecules are less toxic compare to its ammonium counterpart. Mammalian cell is already adapted for sulfonium molecules as it has sulfonium metabolites. Biopolymers used in the compound have additional In our prior study (**Chapter 2**) bactericidal amphiphilic **2.7a** compound was proved to be effective against drug sensitive and drug resistant bacterial strains with lower MIC value and antibiofilm activity. It had the tendency to form liposomes which can be used to encapsulate the other drug molecules approved by the drug encapsulation and release behavior study followed by its synergistic antibacterial activity test. This finding suggests that sulfonium amphiphilic compounds have the buoyancy to become a perspective antimicrobial agent to treat the drug resistant infections. The liposome forming aptitude acclaims that it can be used as aerosol agent for the patients suffering from lung infections including pneumonia, cystic fibrosis, bronchitis, asthma etc. With a purpose to make sulfonium compound more biocompatible and efficient drug carrier we conjugated long hydrocarbon chain and small sulfonium molecule to a biopolymer namely albumin that is a natural drug transporter in blood (**Chapter 3**). This was successfully used to encapsulate clinically proven antibiotics with synergistic efficacy. Membrane directed bactericidal activity of the R-BSA-S had the ability to counteract the resistance mechanism of the bacterial strains. Compound was tested under in vivo condition for its antimicrobial activity in mice model where it had number of bacterial colony reduction. Furthermore, similar sulfonium linker molecule was

designed and used to cross link a polysaccharide molecule with inherent wound healing property (**Chapter 4**). Fibrous and porous polymer was utilized to incorporate vancomycin antibiotic to rejuvenate its activity against VRE bacterial strains. With wound healing property it was applied on to fabrics to prepare Band-Aid like material for wound dressing and it was tested for its antimicrobial activity against drug resistant bacterial strains.

Future Prospects

Antimicrobial drug resistance has become one of the major global health issues and parallel to this hospital is running out of effective antibiotics to fight back the infectious diseases caused by bacteria pushing us back to the pre antibiotic era. This situation demands the developments of time and cost-effective strategy to tackle the antibacterial drug resistance. All these research work presented in this report elaborated the development of both membranes targeted antimicrobial agent and drug carrier molecule in one chemical composite. Henceforth one sulfonium drug carrier with inherent antibacterial activity which can rejuvenate the activity of many antibiotics with synergistic activity could be the suitable agent for future use. The membrane directed bactericidal activity of the sulfonium studded compound also showed the ability to counteract the resistance mechanism of the bacterial strains suggesting that the drug-carrier composite could be used for longer period of time without developing the resistance. All these developed compounds being had the potency against drug resistant and drug sensitive bacterial strains which paves the way for further research as they have the potency to provide new hope against infectious superbugs.

Sulfonium-based liposome-encapsulated antibiotics deliver a synergistic antibacterial activity

A. Patel, S. Dey, K. Shokeen, T. M. Karpiński, S. Sivaprakasam, S. Kumar and D. Manna, *RSC Med. Chem.*, 2021, **12**, 1005
DOI: 10.1039/D1MD00091H

Onium- and Alkyl Amine-Decorated Protein Nanoparticles as Antimicrobial Agents and Carriers of Antibiotics to Promote Synergistic Antibacterial and Antibiofilm Activities

Author: Anjali Patel, Suman Paul, Nasim Akhtar, et al

Publication: ACS Applied Nano Materials

Publisher: American Chemical Society

Date: Nov 1, 2022

PERMISSION/LICENSE IS GRANTED FOR YOUR ORDER AT NO CHARGE

This type of permission/license, instead of the standard Terms and Conditions, is sent to you because no fee is being charged for your order. Please note the following:

- Permission is granted for your request in both print and electronic formats, and translations.
- If figures and/or tables were requested, they may be adapted or used in part.
- Please print this page for your records and send a copy of it to your publisher/graduate school.
- Appropriate credit for the requested material should be given as follows: "Reprinted (adapted) with permission from {COMPLETE REFERENCE CITATION}. Copyright {YEAR} American Chemical Society." Insert appropriate information in place of the capitalized words.
- One-time permission is granted only for the use specified in your RightsLink request. No additional uses are granted (such as derivative works or other editions). For any uses, please submit a new request.

If credit is given to another source for the material you requested from RightsLink, permission must be obtained from that source.

Publications from Thesis

1. **Patel, A.;** Paul, S.; Akhtar, N.; Das, S.; Kar, S.; Bhattacharjee, S.; Manna, D. J. A. A. N. M., Onium-and Alkyl Amine-Decorated Protein Nanoparticles as Antimicrobial Agents and Carriers of Antibiotics to Promote Synergistic Antibacterial and Antibiofilm Activities. *ACS Appl. Nano Mater.* **2022**, *5* (11), 16602-16611.

2. Patel, A.; Dey, S.; Shokeen, K.; Karpiński, T. M.; Sivaprakasam, S.; Kumar, S.; Manna, D. J. R. M. C., Sulfonium-based liposome-encapsulated antibiotics deliver a synergistic antibacterial activity. *RSC med. chem.* **2021**, *12* (6), 1005-1015.

Other publications

1. Prusty, B. M., Karn, R., **Patel, A**., Mazumder, P., Kumar, S., Manna, D. Stimuli-responsive assembly and disassembly of anionic suprasomes with tunable antibacterial activity *ChemComm*, **2023**, Just Accepted

2. Dey, S.+; **Patel, A**.+; Haloi, N.; Srimayee, S.; Paul, S.; Barik, G. K.; Akhtar, N.; Shaw, D.; Hazarika, G.; Prusty, B. M. J. J. o. M. C., Quinoline Thiourea-Based Zinc Ionophores with Antibacterial Activity. *J. Med. Chem.* **2023**. (+ Equal contribution)

3. Dey, S.; Chatterjee, S.; **Patel, A.**; Pradhan, N.; Srivastava, D.; Patra, N.; Bhattacharyya, A.; Manna, D. J. C. C., Photoresponsive transformation from spherical to nanotubular assemblies: anticancer drug delivery using macrocyclic cationic gemini amphiphiles. *ChemComm* **2021**, *57* (38), 4646-4649.

4. Dey, S.; Sen, P.; **Patel, A.**; Prusty, B. M.; Ghosh, S. S.; Manna, D. J. O.; Chemistry, B., A photo-responsive fluorescent amphiphile for target-specific and image-guided drug delivery applications. *Org. Biomol. Chem.* **2022**, *20* (39), 7803-7813.

5. Dey, S.; Das, S.; **Patel, A.;** Raj, K. V.; Vanka, K.; Manna, D. J. J. o. M. C. A., Antimicrobial two-dimensional covalent organic nanosheets (2D-CONs) for the fast and highly efficient capture and recovery of phosphate ions from water. *J. Mater. Chem.* **2022**, *10* (9), 4585-4593.

6. Das, S.; Biswas, O.; Akhtar, N.; **Patel, A.**; Manna, D. J. O.; Chemistry, B., Multi-stimuli controlled release of a transmembrane chloride ion carrier from a sulfonium-linked procarrier. *Org. Biomol. Chem.* **2020**, *18* (45), 9246-9252.

9. Dey, S.; **Patel, A.**; Raina, K.; Pradhan, N.; Biswas, O.; Thummer, R. P.; Manna, D. J. C. C., A stimuli-responsive anticancer drug delivery system with inherent antibacterial activities. *ChemComm* **2020**, *56* (11), 1661-1664.